Bulletin 686

The Citrate Process for Flue Gas Desulfurization

By W. I. Nissen, L. Crocker, L. L. Oden, and others

UNITED STATES DEPARTMENT OF THE INTERIOR
BUREAU OF MINES

Bulletin 686

The Citrate Process for Flue Gas Desulfurization

By W. I. Nissen, L. Crocker, L. L. Oden, and others

UNITED STATES DEPARTMENT OF THE INTERIOR
Donald Paul Hodel, Secretary

BUREAU OF MINES
Robert C. Horton, Director

As the Nation's principal conservation agency, the Department of the Interior has responsibility for most of our nationally owned public lands and natural resources. This includes fostering the wisest use of our land and water resources, protecting our fish and wildlife, preserving the environment and cultural values of our national parks and historical places, and providing for the enjoyment of life through outdoor recreation. The Department assesses our energy and mineral resources and works to assure that their development is in the best interests of all our people. The Department also has a major responsibility for American Indian reservation communities and for people who live in island territories under U.S. administration.

Library of Congress Cataloging in Publication Data

Main entry under title:
The Citrate process for flue gas desulfurization.

(Bulletin; 686)

Bibliography: p. 69

Supt. of Docs. no: I 28.3:686

1. Flue gases—Desulphurization. 2. Citric acid. 3. Chemistry, Analytic. I. Nissen, W. I. (William I.) II. Series: Bulletin (United States. Bureau of Mines); 686.

TD885.5.S8C53 1985 628.5'32 85-600312

For sale by the Superintendent of Documents, U.S. Government Printing Office
Washington, DC 20402

CONTENTS

	Page
Abstract	1
Introduction	2
Chapter 1.—Process description and chemistry, by W. I. Nissen and L. Crocker	3
Background	3
Process description	3
SO_2 absorption with H_2S regeneration	3
SO_2 absorption with steam stripping	4
Process chemistry	4
SO_2 absorption with H_2S regeneration	4
SO_2 absorption with steam stripping	5
H_2S generation	6
Summary	6
Chapter 2.—Laboratory investigations, by W. I. Nissen, L. Crocker, D. A. Martin, and R. H. Lien	7
Background	7
Pioneering tests	7
SO_2 absorption	8
Distribution curves	8
Continuous test unit	8
Sulfur precipitation and solution regeneration	10
Separation of sulfur from regenerated solution	12
H_2S generation	14
Bench-scale investigations	14
CH_4, sulfur, and steam tests	14
Other reducing-gas tests	16
Catalyst tests	16
Continuous test unit	16
Steam stripping	16
Bench-scale investigations	17
Batch tests	17
Atmospheric and reduced pressure	17
Elevated pressure	19
Continuous tests	19
Buffer solution evaluation	19
Stripping tower height	19
Simulated industrial gas	20
SO_4^{2-} formation	20
Continuous test unit	20
Atmospheric pressure tests	20
Optimum solution flow rates	20
Optimum citric acid concentrations	21
Distribution curves	22
Mass transfer rates	23
Elevated-pressure tests	23
SO_4^{2-} formation and removal	23
SO_4^{2-} formation	23
SO_4^{2-} removal	24
Citrate decomposition	24
Summary	25
Chapter 3.—Pilot plant investigations, by W. I. Nissen, L. Crocker, and D. A. Martin	26
Background	26
San Manuel pilot plant	26
Gas cleaning and cooling	26
SO_2 absorption	26
Solution regeneration and sulfur precipitation	26
Sulfur separation and solution recovery	26
Instrumentation and control	27
Test results	27
Bunker Hill pilot plant	29
Design and construction	29
Pilot plant description and operation	29
Gas cooling and cleaning	29
SO_2 absorption	32
SO_2 absorption results	33
SO_2 absorption rates	34
Solution regeneration	34
Sulfur separation and solution recovery	35
Sulfur melting and solution recovery	36
Solution makeup	37
Chemical usage—inventories	37
H_2S generation	38
Safety	40
Personnel requirements	40
Corrosion testing	41
Summary	41
Chapter 4.—Demonstration plant, by W. I. Nissen and L. Crocker	42
Background	42
George F. Weaton Power Station	42
Citrate process demonstration plant	43
Gas cleaning and cooling	43
SO_2 absorption	43
Solution regeneration and sulfur precipitation	46
Sulfur recovery	46
SO_4^{2-} removal	46
H_2S generation	47
Safety	47
Operator training	47
H_2S monitors	47
Engineered safety features	48
Personnel requirements	48
Summary	48
Chapter 5.—Corrosion tests and analyses in support of the citrate process, by L. L. Oden and G. Asai	49
Corrosion in H_2S generator of Bunker Hill pilot plant	49
Background	49
Observations	49
Summary	51
Demonstration plant at George F. Weaton Power Station	51
Background	51
Laboratory corrosion tests simulating in-plant conditions	51
Sulfur vapor and sulfur vapor containing steam	51
Materials and specimen preparation	51
Apparatus	53
Analytical methods	53
Results and discussion	53
Iron- and nickel-base alloys	53
Vapor-aluminum-diffused iron-base alloys	54
Reactive and refractory metals	54
Refractory nonmetals and miscellaneous materials	55

CONTENTS—Continued

	Page
H_2S-CO_2-steam simulating the H_2S generator	56
Apparatus and experimental procedures	56
Results and discussion	57
Ferritic iron-base alloys	57
Austenitic iron-base alloys and miscellaneous alloys	58
Reactive metals	58
Aluminum alloys	58
Citrate solutions simulating SO_2 absorption and solution regeneration	59
Materials, sample preparation, and test conditions	60
Stagnant rich citrate solution at 120° F	60
Iron- and nickel-base alloys, titanium, and zirconium	60
Effect of chloride concentration	62
Aluminum alloys 5052 and 5086 and high-silicon iron alloy Durichlor 51	62
Recirculating rich citrate solution at 120° F	62
Stagnant lean citrate solution at 260° F and 4 atm	63
Recirculating lean citrate solution at 260° F and 4 atm	63
Discussion of results	64
In-plant corrosion testing and analysis	65
Conclusions	67
References	68

ILLUSTRATIONS

		Page
1.	Generalized citrate process flowsheet	3
2.	Generalized modified citrate process flowsheet	4
3.	Effect of SO_2 loading on solution pH	5
4.	Effect of initial pH on SO_2 absorption in 0.5*M* citrate solution at 113° F	9
5.	Effect of gas concentration and citrate concentration on SO_2 absorption	9
6.	Effect of gas concentration and citrate solution temperature on SO_2 absorption at 640 mm Hg absolute pressure	10
7.	Laboratory continuous test unit	11
8.	Continuous test unit sulfur precipitation and separation assembly	12
9.	Sulfur flotation demonstration	13
10.	Continuous test unit sulfur flotation cell	13
11.	Continuous test unit sulfur melter and settler	13
12.	Bench-scale apparatus for preparation of H_2S	14
13.	Laboratory catalytic H_2S generator	15
14.	Effect of temperature on CH_4, sulfur, and steam reaction	15
15.	Effect of space velocity on CH_4, sulfur, and steam reaction at 1,220° F	16
16.	H_2S generator section of continuous test unit	17
17.	Laboratory absorber-stripper system	18
18.	Batch test pressurized stripper	18
19.	Effect of pH and pressure on steam efficiency	18
20.	Effect of stripper height on steam efficiency	20
21.	Continuous test unit atmospheric pressure stripping	21
22.	Continuous test unit pressurized steam stripping	21
23.	SO_2 distribution curves, using various citrate solution concentrations at pH 4.7	22
24.	SO_2 distribution curves at solution boiling points	23
25.	Effect of stripper pressure on steam consumption	24
26.	San Manuel pilot plant flowsheet	27
27.	Pilot plant at San Manuel	28
28.	Bunker Hill pilot plant flowsheet	30
29.	Overview of Bunker Hill pilot plant from west	31
30.	Overview of Bunker Hill pilot plant from southeast	31
31.	Gas cooling and cleaning section (Bunker Hill pilot plant)	32
32.	Citrate solution clarification filters (Bunker Hill pilot plant)	32
33.	Solution regeneration reactors (Bunker Hill pilot plant)	35
34.	Sulfur flotation cell and storage bin (Bunker Hill pilot plant)	36
35.	Sulfur melter and sulfur molds (Bunker Hill pilot plant)	37
36.	Solid sulfur product (Bunker Hill pilot plant)	37
37.	H_2S generator (Bunker Hill pilot plant)	38
38.	Flowsheet for H_2S generator at Bunker Hill pilot plant	39
39.	Control panel (Bunker Hill pilot plant)	41
40.	George F. Weaton Power Station	42
41.	Powerplant stack gas SO_2 scrubbing—citrate process flowsheet	44
42.	Citrate process demonstration plant	45
43.	Schematic diagram of demonstration plant H_2S generator	47
44.	Apparatus for laboratory corrosion tests in dry and wet sulfur vapor	53
45.	Crushing strength of castable refractory cements after exposure to air, dry sulfur vapor, steam, and wet sulfur vapor for 30 days at 1,450° F	56
46.	Apparatus for laboratory corrosion tests in H_2S-CO_2-steam	56
47.	Schematic drawing of system for corrosion tests in recirculating lean citrate solution at 260° F and 4 atm	64

TABLES

		Page
1.	Absorbents screened for SO_2 solubility	7
2.	SO_2 removal efficiencies using pure organic absorbents	7
3.	SO_2 removal efficiencies using aqueous absorbents	8
4.	Results of tests in 20-ft^3/min continuous test unit	10
5.	Summary of results of H_2S generation tests using various reductants	16
6.	Effect of catalyst type on production of H_2S by reaction of CH_4, sulfur, and steam in a 1-in single-stage tube reactor	17
7.	Typical results for H_2S generator section of continuous test unit	17
8.	Effect of stripper pressure on steam consumption	19
9.	Effect of citric acid concentration on steam efficiency and SO_2 absorption	19
10.	Effect of citrate solution pH on steam efficiency and SO_2 absorption	19
11.	Steam requirements for 90-pct SO_2 removal from waste gases	20
12.	Effect of $S_2O_3^{2-}$ on SO_4^{2-} formation in steam stripping	20
13.	Effect of SO_2 gas concentration on solution flow rate and steam efficiency	21
14.	Effect of citric acid concentration on SO_2 absorption and steam efficiency	22
15.	Mass transfer rates (K_Ga, K_La) for steam-stripping continuous test unit	23
16.	Oxidation of SO_2 to SO_4^{2-} during SO_2 removal from various feed gases using the citrate system	23
17.	Crystallization of $Na_2SO_4 \cdot 10H_2O$ from citrate solutions	24
18.	Citric acid decomposition during sulfur melting in autoclave	25
19.	Effect of stripper temperature on citrate decomposition and absorption capacity during steam stripping	25
20.	SO_2 removal results for San Manuel pilot plant	29
21.	Effect of citrate solution concentration, absorption temperature, and solution and gas flow rates on SO_2 removal efficiency at Bunker Hill pilot plant	33
22.	Comparison of SO_2 removal efficiency from feed gases containing about 0.1 versus about 0.5 vol pct SO_2	33
23.	Effect of excess H_2S on SO_2 removal efficiency and pH of regenerated solution	34
24.	Overall mass transfer coefficient (K_Ga) for SO_2 absorption at Bunker Hill pilot plant	34
25.	Regeneration data for SO_2-loaded citrate solutions at Bunker Hill pilot plant	35
26.	Bunker Hill pilot plant sulfur product analysis	38
27.	Bunker Hill pilot plant H_2S generation results using natural gas reductant	39
28.	H_2S generation results using C_3H_8, CH_3OH, and CO reductants	40
29.	Summary of results of preliminary operation of the citrate process demonstration plant	45
30.	Description of corrosion specimens obtained from Bunker Hill pilot plant H_2S generator	50
31.	Nominal composition of alloys evaluated in laboratory and in-plant corrosion tests	52
32.	Corrosion rates of iron- and nickel-base alloys in dry and wet sulfur vapor at 1,150° to 1,450° F	54
33.	Corrosion rates of vapor-aluminum-diffused iron-base alloys in dry and wet sulfur vapor at 1,150° to 1,450° F	55
34.	Corrosion rates of reactive and refractory metals in dry and wet sulfur vapor at 1,150° to 1,450° F	55
35.	Corrosion rates of ferritic iron-base alloys in H_2S-CO_2-steam	57
36.	Corrosion rates of austenitic iron-base alloys, nickel- and cobalt-base alloys, and reactive metals in H_2S-CO_2-steam	59
37.	Corrosion rates of aluminum alloys in H_2S-16 pct CO_2-16 pct steam	59
38.	Nominal composition of citrate solutions	60
39.	Corrosion rates of unwelded coupons, welded coupons, and annealed weldments in stagnant rich citrate solution at 120° F	61
40.	Comparison of corrosion results for unwelded and welded iron- and nickel-base alloys in recirculating rich citrate solution at 120° F	63
41.	Corrosion rates of alloys in stagnant lean citrate solution at 260° F and 4 atm	64
42.	Performance ranking of materials in laboratory corrosion tests in citrate solutions	65
43.	Corrosion rates of alloys in prescrubber at George F. Weaton citrate process demonstration plant	66
44.	Corrosion rates of alloys in absorber at George F. Weaton citrate process demonstration plant	66
45.	Corrosion rates of alloys in decanter and sulfur flotation tank at George F. Weaton citrate process demonstration plant	67
46.	Performance ranking of materials tested at George F. Weaton citrate process demonstration plant	67

UNIT OF MEASURE ABBREVIATIONS USED IN THIS REPORT

atm	atmosphere, standard
Btu	British thermal unit
Btu/h	British thermal unit per hour
°C	degree Celsius
cm^3/min	cubic centimeter per minute
°F	degree Fahrenheit
ft	foot
ft^2	square foot
ft^3	cubic foot
ft/min	foot per minute
ft^3/min	cubic foot per minute
$ft^3/(min \cdot ft^2)$	cubic foot per minute per square foot
g	gram
gal	gallon
gal/min	gallon per minute
$gal/(min \cdot ft^2)$	gallon per minute per square foot
g/L	gram per liter
g/min	gram per minute
h	hour
hp	horsepower
in	inch
in H_2O	inch of water (pressure)
in/min	inch per minute
in/yr	inch per year
kV	kilovolt
L	liter
L/min	liter per minute
lb	pound
lb/d	pound per day
lb/h	pound per hour
lb/(h·gal)	pound per hour per gallon
lbf/in^2	pound (force) per square inch
$lbf/in^2(ga)$	pound (force) per square inch, gauge
lb mol/h	pound-mole per hour
lt/d	long ton per day
mA	milliampere
mg	milligram
mg/ft^3	milligram per cubic foot
mil/yr	mil per year
min	minute
mL	milliliter
mL/min	milliliter per minute
mm	millimeter
mm Hg	millimeter of mercury (atmospheric pressure)
mol	mole
MW	megawatt
nA	nanoampere
pct	percent
pH	hydrogen ion concentration
ppm	part per million
ppmv	part per million by volume
r/min	revolution per minute
s	second
st	short ton
st/d	short ton per day
std ft^3	standard cubic foot
std ft^3/min	standard cubic foot per minute
vol pct	volume percent
W	watt
yr	year

THE CITRATE PROCESS FOR FLUE GAS DESULFURIZATION

By W. I. Nissen,[1] L. Crocker,[2] L. L. Oden,[3] and others[4]

ABSTRACT

As part of its program to provide technology for reducing undesirable environmental impacts of mineral processing operations, the Bureau of Mines developed the citrate process for desulfurizing industrial stack gases that contain from 0.1 to 2 vol pct SO_2. In this regenerable flue gas desulfurization (FGD) process, SO_2 is absorbed from cleaned and cooled industrial flue gas with a citric acid-sodium citrate solution. The absorbed SO_2 is subsequently reacted with H_2S to precipitate marketable elemental sulfur and regenerate the solution for recycle.

Laboratory investigations of process parameters provided information for designing larger scale continuous operations. Information gathered from operation of two pilot plants, one at a copper smelter and one at a lead smelter, confirmed the laboratory results. Data were obtained for design and construction of a commercial-sized demonstration plant at the George F. Weaton Power Station, Monaca, PA. A preliminary operation of the plant was demonstrated, under a cost-sharing Bureau-industry contract. This bulletin describes the citrate process and gives results of the laboratory, pilot plant, and demonstration plant studies, as well as corrosion investigations.

[1]Staff engineer, Salt Lake City Research Center, Bureau of Mines, Salt Lake City, UT.
[2]Staff engineer, Salt Lake City Research Center, (retired).
[3]Research chemist (group supervisor), Albany Research Center, Bureau of Mines, Albany, OR.
[4]Others are identified at the start of chapters they prepared.

INTRODUCTION

During the past 20 yr, this Nation's principal concern with controlling SO_2 emissions has focused on flue gases from fossil-fuel-burning powerplants. Electric powerplants and steam-generating plants account for about 85 pct of the estimated 20 to 25 million st of SO_2 emissions per year (*23*).[5] The remaining 15 pct of the total SO_2 emissions is from other industrial processes that, in some cases, produce stack gases that are more concentrated and more visible than those from powerplants, thus causing local pollution problems. Historically, copper, lead, and zinc smelters have been known SO_2 pollution sources that frequently fall into this category.

Air quality standards for SO_2 limit the amount of emission or refer to the ambient air concentration. To meet these standards, powerplants burn low-sulfur fuel or remove SO_2 from the flue gases resulting from burning high-sulfur fuel. Smelters make H_2SO_4 from strong SO_2 gases, increase dispersion of weak SO_2 gases with tall stacks, and reduce production. However, stricter air quality standards in some areas require additional control measures. During the short term, FGD may be the only solution.

Research has been conducted in this country and abroad for nearly 50 yr to develop FGD technology. Of the many processes investigated, five FGD systems have received the most attention for commercial application. These processes are (1) wet lime or limestone scrubbing, (2) double alkali scrubbing, (3) MgO scrubbing, (4) catalytic oxidation, and (5) sodium-base scrubbing. The first two processes are nonregenerable and produce a throwaway sludge. In the remaining three processes, the SO_2 absorbent is regenerated, and marketable H_2SO_4 or elemental sulfur is produced. The following paragraphs briefly describe the chemistry of these FGD processes.

Reacting SO_2 with lime or limestone slurries in scrubbing towers to form a calcium sulfate-sulfite sludge is the most thoroughly studied of all FGD systems. Lime or limestone scrubbing removes particulate matter as well as SO_2, and capital costs are low compared with those of other processes.

The double alkali process uses a clear sodium or ammonium alkaline liquor to absorb the SO_2, and the resulting solution is treated outside the scrubber with either limestone or lime to regenerate the absorbent solution and produce a throwaway sludge of calcium sulfate and sulfite.

MgO FGD comprises reaction of SO_2 with a magnesia slurry, followed by thickening, centrifuging, and calcining the resulting magnesium sulfite and sulfate with added carbon to regenerate the MgO and evolve SO_2 for conversion to H_2SO_4.

In the catalytic oxidation process, SO_2-bearing flue gas is thoroughly cleaned of dust in hot precipitators and then is passed over a catalyst to convert the SO_2 to SO_3, which combines with moisture to form an 80-pct H_2SO_4 as the end product.

One of the best known sodium-base FGD regenerable system is the Wellman-Lord sodium sulfite-bisulfite process. In the Wellman-Lord process, sodium sulfite-bisulfite solution absorbs SO_2 from stack gas and converts sulfite to bisulfite. The loaded liquor is processed in a steam-heated evaporator-crystallizer to recover strong SO_2 and regenerate sodium sulfite for recycling. The SO_2 can be used to make H_2SO_4 or can be reduced to elemental sulfur using natural gas or coal.

In 1968, the Bureau of Mines started research on FGD at the Salt Lake City Research Center, giving particular emphasis to control of SO_2 emissions from nonferrous smelters. This research was conducted in an effort to minimize the undesirable environmental impacts of mineral processing operations.

The Bureau's FGD process evolved as a result of research on recovering sulfur from H_2S. Investigators searched for a technique that would be more manageable on a laboratory scale than the Claus process for reacting H_2S with SO_2. (The Claus process reacts H_2S with SO_2 at temperatures above 500° F to form sulfur and steam. The sulfur is separated from the steam using a sulfur condenser and a sulfur scrubber.) Initial experiments confirmed that H_2S and SO_2 can be readily reacted in many organic liquids to recover sulfur. Furthermore, the ease and completeness of the reaction suggested that the technique might be applicable for removing SO_2 from a dilute powerplant gas or smelter gas.

After a year of screening many possible reagent combinations of inorganic and organic solutions, investigators established that an aqueous solution of citric acid and sodium citrate was an effective absorbent for SO_2. Among the desirable characteristics affecting the choice of citrate were its good chemical stability, low vapor pressure, and adequate pH buffering capacity, and the high purity and desirable physical character of the precipitated sulfur.

Active Bureau research on the citrate process ceased in September 1982. This bulletin is intended to consolidate the data reported in previous publications and to present data on work not reported elsewhere. Chapter 1 describes the process and the chemistry; chapter 2, laboratory investigations; chapter 3, pilot plant investigations; chapter 4, the full-scale demonstration plant; and chapter 5, the results of corrosion studies.

[5]Italicized numbers in parentheses refer to items in the list of references at the end of the bulletin.

CHAPTER 1.—PROCESS DESCRIPTION AND CHEMISTRY

By W. I. Nissen and L. Crocker

BACKGROUND

Original research on the citrate process involved absorption of SO_2 in a buffered solution of citric acid, followed by reaction of the SO_2 with H_2S to regenerate the solution and form elemental sulfur. Later research modified the citrate process so that the SO_2-loaded solution was regenerated by countercurrent contact with steam in packed towers to strip a strong-SO_2 gas, which may be liquefied, oxidized for acid production, or reduced for sulfur production.

PROCESS DESCRIPTION

SO_2 Absorption With H_2S Regeneration

Basically, the original citrate process consists of the following steps (fig. 1):

1. Water scrubs H_2SO_4 mist and solid particulates from SO_2-bearing gas while cooling the gas to between 113° and 149° F.
2. A citric acid, sodium citrate, and sodium thiosulfate ($Na_2S_2O_3$) solution adjusted to pH 4.5 absorbs the SO_2 from the cleaned and cooled gas. Other organic acids such as glycolic acid may be substituted for citric acid.
3. Citrate solution loaded with SO_2 reacts with H_2S at about 131° to 149° F to precipitate elemental sulfur and regenerate the solution for recycle.
4. When a slipstream of recycled citrate solution is cooled, sulfate (SO_4^{2-}), which results from the oxidation of SO_2, crystallizes as Glauber's salt ($Na_2SO_4 \cdot 10H_2O$). The $Na_2SO_4 \cdot 10H_2O$ is filtered and washed to recover citrate solution.
5. Sulfur flotation and melting separate the sulfur product from the regenerated citrate solution, and the latter is recycled to absorb more SO_2.
6. If not otherwise available, the required H_2S is provided by an H_2S generator, which reacts two-thirds of the recovered sulfur with natural gas (CH_4) and steam.

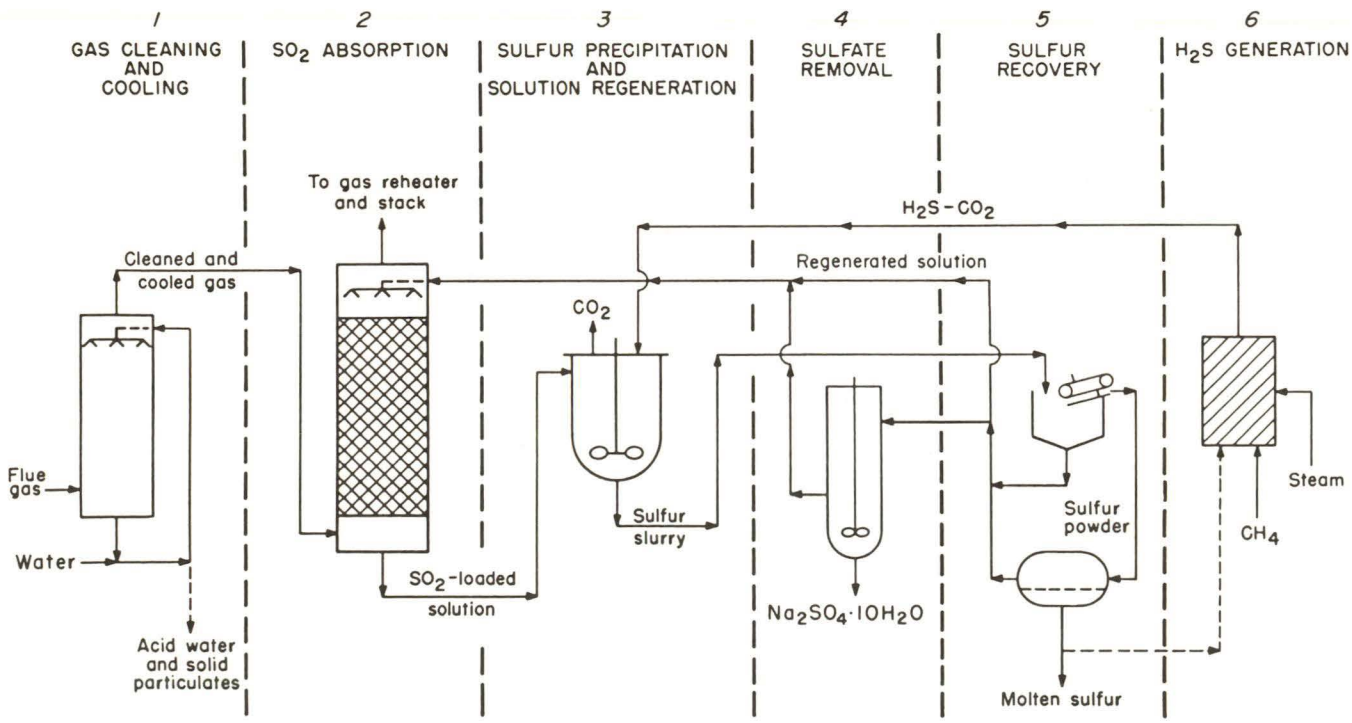


Figure 1.—Generalized citrate process flowsheet.

SO_2 Absorption With Steam Stripping

The modified citrate process (*34-36*) differs from the original process concept in that the SO_2-loaded citrate solution is regenerated with steam instead of H_2S. Steam is passed through a stripping tower to recover SO_2 gas, which can be made into H_2SO_4. Regeneration by steam stripping is not economic for use on gases containing less than 1 pct SO_2. However, the modified process may have application in nonferrous smelting FGD.

The modified citrate process consists of the steps shown in figure 2:

1. A citric acid and sodium citrate solution adjusted to pH 4.75 absorbs SO_2 from a cooled and cleaned (H_2SO_4 mist- and particulate-free) gas.

2. When the SO_2-loaded citrate solution is heated to boiling, the generated steam strips the SO_2 from the solution and regenerates the solution for recycle.

Further processing of the wet SO_2-steam mixture can produce dry SO_2, H_2SO_4, or sulfur. Like the H_2S regeneration process, the steam stripping process requires a SO_4^{2-} removal step.

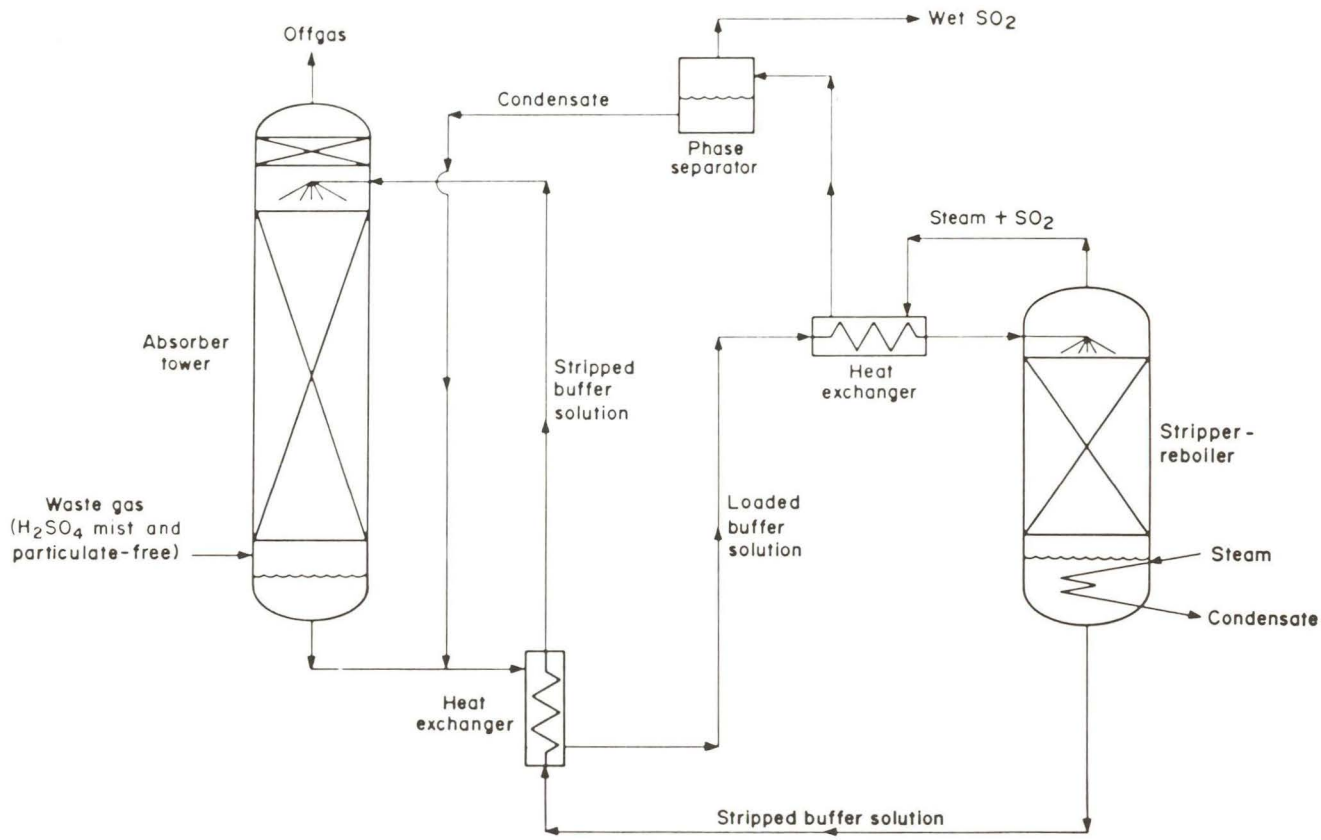


Figure 2.—Generalized modified citrate process flowsheet.

PROCESS CHEMISTRY

The chemistry of the original citrate process, comprising regeneration by H_2S, and the modified process consisting of steam stripping is briefly described in this section. The Bureau of Mines (*47*) and Pfizer, Inc. (*30*), have reported more detailed information on the chemistry of the citrate process.

SO_2 Absorption With H_2S Regeneration

The SO_2 absorption-solution regeneration steps of the original citrate process include the following chemical reactions:

1. Absorption of SO_2 in a buffered citric acid solution.
2. Reaction of the dissolved SO_2 with H_2S to produce sulfur.
3. Crystallization of $Na_2SO_4 \cdot 10H_2O$.

SO_2 is absorbed from a stack gas with water as shown by reaction 1:

$$SO_2 + H_2O \rightleftharpoons H^+ + HSO_3^- \quad (1)$$

Sodium citrate ($NaOOCCH_2$-$HOCCOOH$-CH_2COOH), the salt of a weak acid, dissolved in the sulfite (HSO_3^-) solution, reacts accordingly:

$$H^+ + HSO_3^- + Na^+ + \text{citrate}^- \rightleftharpoons Na^+ + HSO_3^- + \text{citric acid.} \quad (2)$$

The hydrogen ion produced by absorption of SO_2 in reaction 1 combines with a citrate ion in reaction 2, to form citric acid ($HOOCCH_2$-$HOCCOOH$-CH_2COOH). Hydrogen ion is buffered by the presence of citrate ion, allowing the solution to be loaded higher in SO_2 than would otherwise be possible. The pH variation for different loadings of SO_2 is shown in figure 3 for several different citrate concentrations. The 1.0*M* citrate (192 g/L citric acid) clearly shows a greater buffering action than do the lower concentrations.

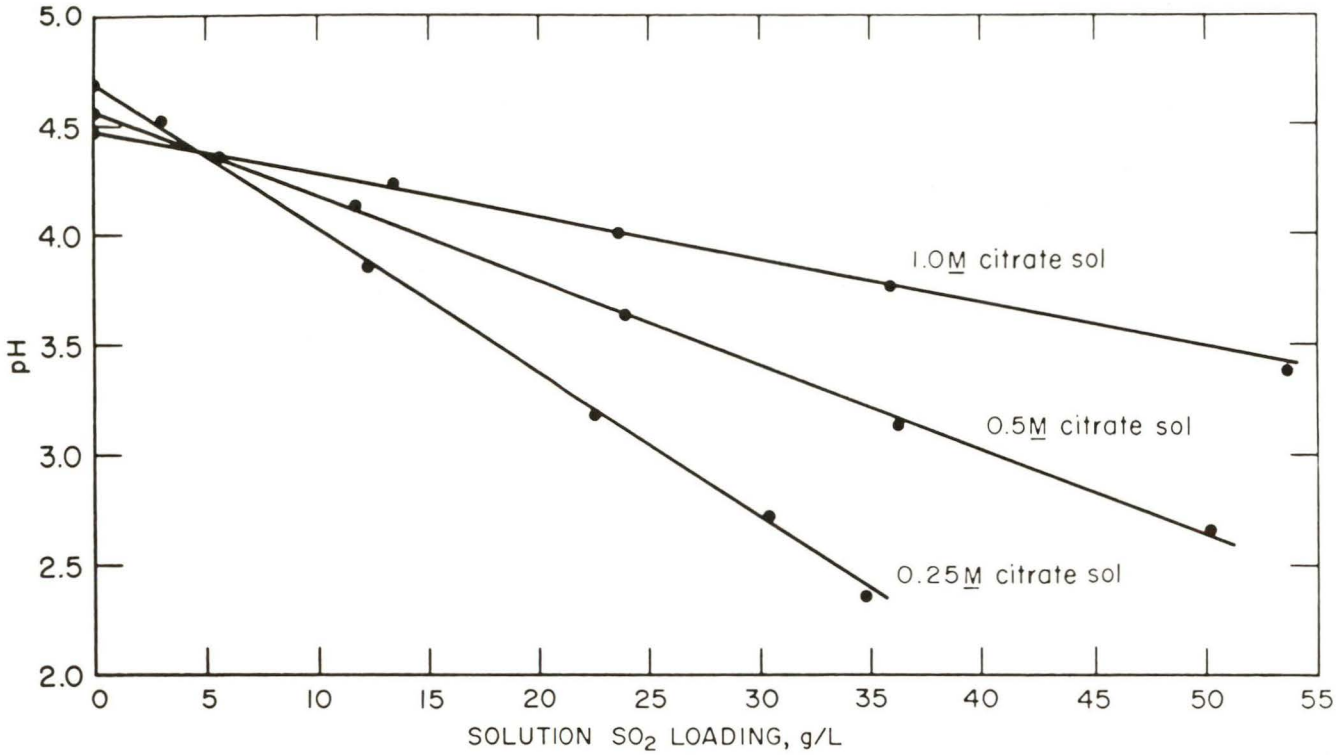


Figure 3.—Effect of SO_2 loading on solution pH.

The strength of citrate solution to be used depends on the SO_2 concentration of the gas to be scrubbed as well as the temperature of the gas, the gas flow rate, and the absorbent flow rate. Adjustment of the solution citric acid-to-base ratio achieves the desired starting pH.

While SO_2 absorbs, the solution pH decreases as illustrated in figure 3. When the HSO_3^- is reduced to sulfur with H_2S in the sulfur precipitation-solution regeneration step, the solution pH returns to the starting value. Thus, pH is one indicator of the degree of regeneration. In 1846, H. W. F. Wackenroder reported the chemical changes that occur when SO_2 and H_2S are combined in water (*59*). The stoichiometry of the regeneration reaction is usually expressed as follows:

$$2H_2S + HSO_3^- + H^+ \rightarrow 3S + 3H_2O. \quad (3)$$

Reaction 3 shows that hydrogen ion is consumed, thus bringing the pH of the solution back to its original value. This should occur if the solution is completely regenerated. Other reactions can and do occur if there is a deficiency of H_2S or if the pH of the solution gets too high or too low. This reaction does not proceed to sulfur above pH 6. Low pH favors reaction 3. However, below pH 3, the sulfur tends to be colloidal.

In the process, thiosulfate ($S_2O_3^{2-}$) is probably formed by

$$HSO_3^- + S \rightarrow S_2O_3^{2-} + H^+, \quad (4)$$

and polythionates ($S_nO_6^{2-}$, with n = 3) form by the following reaction:

$$4HSO_3^- + S_2O_3^{2-} + 2H^+ \rightarrow 2S_3O_6^{2-} + 3H_2O. \quad (5)$$

$S_2O_3^{2-}$ decomposes to sulfur and SO_4^{2-} according to reaction 6:

$$3S_2O_3^{2-} + 2H^+ \rightleftharpoons 4S + 2SO_4^{2-} + H_2O. \quad (6)$$

This reaction occurs principally in the sulfur melting step where heat increases the decomposition. Other sources of SO_4^{2-} include the oxidation of HSO_3^- according to reaction 7:

$$HSO_3^- + 1/2\ O_2 \rightarrow SO_4^{2-} + H^+, \quad (7)$$

and the absorption of SO_3 as follows:

$$SO_3 + H_2O \rightarrow SO_4^{2-} + 2H^+. \quad (8)$$

Reactions 6, 7, and 8 contribute to the buildup of SO_4^{2-} ion and hydrogen ion in the absorbent solution. Subsequent additions of base neutralize the acid.

Finally, crystallization of $Na_2SO_4 \cdot 10H_2O$ from a bleed stream of regenerated absorbent removes the buildup of SO_4^{2-} from the system.

SO_2 Absorption With Steam Stripping

The principal reactions taking place in the modified citrate process are the reversible reactions 1 and 2. This process uses the reverse of the absorption step in the stripping step. Two effects reverse the absorption process:

1. Heating the solution increases the hydrogen ion concentration by ionizing more citric acid.
2. Diluting the SO_2 over the solution with steam shifts the equilibrium between the SO_2 in the solution and SO_2 in the gas, causing the SO_2 to desorb.

These effects shift the equilibrium of reaction 1 to the left and create the necessary driving force to transfer SO_2 from the solution to the vapor. The modified citrate process does not produce $S_2O_3^{2-}$ since there is no H_2S in the system. The addition of $S_2O_3^{2-}$ was considered for inhibiting the oxidation of SO_2 to SO_3, but decomposition of $S_2O_3^{2-}$ during the stripping step outweighed the benefits that might be derived from the $S_2O_3^{2-}$ addition. Therefore, the absorbent in the modified citrate process does not contain $S_2O_3^{2-}$. Sources of SO_4^{2-} in the modified citrate process include oxidation of HSO_3^- (reaction 7) and absorption of SO_3 (reaction 8). Again, crystallization of a SO_4^{2-} salt from a bleed stream of regenerated absorbent removes the buildup of SO_4^{2-} from the process. Lien reports additional details of the chemistry of the modified citrate process (*34-36*).

H_2S Generation

The H_2S for reaction 3 may be produced by one of several different processes. Commercial H_2S comes from oil and natural gas refining and carbon disulfide (CS_2) production. On an industrial scale the reaction of hydrogen, usually from reformed CH_4, with sulfur produces H_2S (*19*) as follows:

$$H_2 + S \rightarrow H_2S. \quad (9)$$

An alternative procedure bypasses CH_4 reforming, and H_2S is produced by direct reaction of CH_4 with sulfur and steam (*3, 12, 52*) as shown in reaction 10:

$$CH_4 + 4S + 2H_2O \rightarrow CO_2 + 4H_2S. \quad (10)$$

This approach is a modification of the commercial process for producing CS_2, in which sulfur reacts with CH_4 (*17, 20, 53-56*) accordingly.

$$CH_4 + 4S \rightarrow CS_2 + 2H_2S. \quad (11)$$

By adding steam as shown in reaction 10, the CS_2 hydrolyzes to $CO_2 + H_2S$ as follows:

$$CS_2 + 2H_2O \rightarrow CO_2 + 2H_2S. \quad (12)$$

Investigations by the Bureau (*12*) show that other H_2S generation processes using reductants such as CO, C_2H_6 (ethane), and CH_3OH (methanol) may have merit according to the following reactions:

$$CO + S + H_2O \rightarrow H_2S + CO_2. \quad (13)$$

$$C_2H_6 + 7S + 4H_2O \rightarrow 7H_2S + 2CO_2. \quad (14)$$

$$CH_3OH + 3S + H_2O \rightarrow 3H_2S + CO_2. \quad (15)$$

SUMMARY

The heart of the citrate process is the absorption of SO_2 from a clean and cool flue gas in a buffered solution of citric acid. In this process, water reacts with SO_2 to form hydrogen ion and HSO_3^-, while the sodium citrate reacts to form citric acid, maintain the pH, and allow increased SO_2 absorption.

Citrate solution loaded with SO_2 may be regenerated in the following two ways:

1. Reaction of the loaded SO_2 with H_2S to form elemental sulfur.
2. Stripping of the loaded SO_2 with steam to produce a concentrated SO_2 gas.

In the citrate process, some SO_2 oxidizes to form SO_4^{2-} that may be removed by cooling the regenerated solution and crystallizing $Na_2SO_4 \cdot 10H_2O$.

If not otherwise available, H_2S may be produced on-site by reacting elemental sulfur with reducing gases such as H_2, CO, CH_4, C_2H_6, or CH_3OH.

CHAPTER 2.—LABORATORY INVESTIGATIONS

By W. I. Nissen, L. Crocker, D. A. Martin,[1] and R. H. Lien[2]

BACKGROUND

In 1968, the Bureau initiated a research program on FGD, with particular emphasis on control of SO_2 emissions from nonferrous smelters. Pioneering research and a literature survey indicated that FGD might be achieved effectively by the absorption of SO_2 in a suitable solution, followed by reaction of SO_2 with H_2S to precipitate sulfur and regenerate the solution for recycle. Initially, high-boiling organic liquids were tested for SO_2 absorption and the sulfur-forming reaction as proposed in the patent literature (*24, 57*). The relative low SO_2 absorption capacity and the high cost of pure organics led to the consideration of aqueous solutions as also proposed in the literature (*1, 4, 29, 32*).

After a year of screening many reagent combinations, investigators found that an aqueous solution of citric acid and sodium citrate was an effective absorbent for SO_2. Such a solution was proposed for absorption by Keller in his 1956 patent (*29*), and the Bureau's conclusions appeared to agree with his patent. Among the desirable factors affecting the choice of an SO_2 absorbent were good chemical stability, low vapor pressure, adequate pH buffering capacity, high water solubility, high SO_2 loading capacity, and the ability to be regenerated easily and completely with H_2S gas to produce a sulfur with high purity and desirable physical characteristics.

The initial laboratory bench-scale and continuous test investigations (*18, 51-52*) confirmed the feasibility of removing SO_2 from stack gas by absorption in a citrate solution and subsequent reduction of SO_2 to elemental sulfur in the same solution by reaction with H_2S. Enactment of the Federal Clean Air Act of 1970 encouraged the Bureau to consider the citrate process for removal of sulfur from a variety of stack gases, including those from nonferrous smelters, oil- and coal-burning electric and steam-generating plants, and oil and gas refineries. Laboratory investigations during the project studied H_2S generation (*12*), steam-stripping regeneration (*34-36*), citrate process chemistry (*6, 40-41*), sulfur separation, SO_2 absorption, H_2S regeneration, and sulfur flotation.

PIONEERING TESTS

Laboratory investigations to develop a system for wet absorption of SO_2 from dilute stack gas began with a thorough screening of a number of organic and aqueous absorbents. Table 1 lists the absorbents tested for SO_2 solubility.

Subsequent investigations with the preferred organics and dilute SO_2-air mixtures simulating smelter stack gas showed a high SO_2-removal efficiency and excellent sulfur recovery. Table 2 summarizes results obtained with the more promising organic absorbents, using a 2-in-diam absorber packed with 2 ft of 3/8-in glass Raschig rings. However, these tests also revealed an excessive loss of the high-boiling organic liquid when scrubbing the dilute SO_2 gas. For example, the tributyl phosphate tests showed that over 12 lb were lost per short ton of sulfur produced when scrubbing a gas containing 2 vol pct SO_2 at 125° F. Therefore, investigations turned to the use of inorganic and mixed organic and inorganic aqueous absorbents.

Table 1.—Absorbents screened for SO_2 solubility

Organic absorbents:	Aqueous absorbents:
Butyl phthalate	Citric acid-sodium hydroxide
Dimathy heptanone	Diglycol amine
Dimethyl aniline	Gluconic acid-sodium hydroxide
Dioctylphthalate	Glycerine
Diphenyl cresyl phosphate	Levulinic acid-sodium hydroxide
Dow Corning 55 silicone	Maleic acid-sodium hydroxide
Dow Corning 710 silicone	Malic acid-sodium hydroxide
Ethylene glycol	Monethanolamine
Flerol TOF	Sodium acetate
GE SF 96 silicone	Sodium acetate-acetic acid
GE 1093 silicone	Sodium borate
Isodecanol	Sodium citrate
Kerosene	Sodium citrate-diglycol amine
Monsanto Therminal 66	Sodium citrate-monoethanolamine
Monsanto Therminal 77	Sodium citrate-sulfaline
O-toliudine	Sodium citrate-triethylene glycol
Stauffer 3664A polyolester	Sodium hydroxide
Tetraethylene glycol	Sodium sulfite
Tributoxy ethyl phosphate	Sodium tartrate
Tributyl phosphate (TBP)	Sodium tetrathionate
Tricresyl phosphate	Sodium thiosulfate
Triethylene glycol	Triethanolamine
Triphenyl phosphate	Trisodium phosphate
Triphenyl phosphite	Trisodium phosphate-phosphoric acid
Xylidine	
2,6,8-trimethyl nonanone	
10 pct diphenylnaphthalamine in TBP	
10 pct triethylene glycol in TBP	

Table 2.—SO_2 removal efficiencies[1] using pure organic absorbents

Absorbent	Absorbent flow rate, gal/(min·ft²)	Gas flow rate, ft³/(min·ft²)	SO_2 removal efficiency, pct
Tributoxy ethyl phosphate .	1.2	64	81
Tributyl phosphate	1.8	33	95
Tricresyl phosphate	1.2	16	90

[1]From 2 vol pct SO_2 gas at room temperature.

[1]Metallurgist (retired).
[2]Chemical engineer.
Salt Lake City Research Center.

Table 3.—SO_2 removal efficiencies[1] using aqueous absorbents

Absorbent	Scrubbing temperature, °F	Initial solution acidity, pH	Absorbent flow rate, gal/(min·ft²)	Gas flow rate, ft³/(min·ft²)	SO_2 removal efficiency, pct
2.5*M* acetate	95	4.0	0.6	40	99
1.0*M* citrate	95	3.5	1.2	32	95
0.5*M* citrate	122	4.5	1.9	48	96
1.0*M* phosphate	113	4.5	4.2	48	93
0.5*M* sulfo succinate	122	4.5	1.9	48	94

[1]From 2 vol pct SO_2 gas.

Table 3 presents the results of tests with the most promising aqueous absorbents. These results were obtained using a 2-in-diam absorber packed with 2 ft of 3/8-in glass Raschig rings. An acetate solution absorbed SO_2 very efficiently, and H_2S regenerated the solution and produced a high-quality sulfur. However, the high vapor pressure of acetic acid (248° F boiling point) contributed to excessive reagent losses. In contrast, the phosphate solution did not appear to be as efficient an absorbent. Tests using the sulfosuccinate solution revealed that the SO_2 oxidized at a higher rate than that experienced when using a citrate solution. The tests with the citrate solutions showed that high SO_2 removal efficiencies could be obtained with different solution strengths, solution pH's, and scrubbing temperatures. Furthermore, reagent losses were low because of the low vapor pressure of citric acid.

By the preceding brief account, investigators concluded that studies of a process using an aqueous citrate absorbent should be expanded.

SO_2 ABSORPTION

During most of the early work, investigators tested an absorbent composed of 1*M* citric acid and 1.5*M* NaOH, which had an initial pH of 4.1. Later work determined that the citrate absorbent should contain a higher caustic-to-citric acid ratio. However, increased oxidation of SO_2 and regeneration limitations restrict the maximum operable pH to 5. As stated in chapter 1, the formation of collodial sulfur limits the minimum operable pH to 3.

Although not added to the starting solution in the early work, $S_2O_3^{2-}$ was present in the cycling absorbent. Later experiments included $S_2O_3^{2-}$ in starting solution. Once investigators established the general limits for good SO_2 absorption, they set out to determine optimum conditions and develop a process. While the citrate process was being developed, exploratory tests using a hydroxyacetic acid (glycolic acid) solution showed the same desirable results that led investigators to select citric acid. Other publications (*13, 34-36*) give results of more detailed investigations using hydroxyacetic acid.

Distribution Curves

The preparation of steady-state distribution curves involved a dynamic method. SO_2 was bubbled through a fritted-glass tube into the citrate absorbent in a stirred vessel. On the stirred vessel outlet, a reflux condenser prevented evaporation losses. When the feed gas and offgas SO_2 concentration equalized, the investigator considered the distribution of SO_2 to be at equilibrium and analyzed both the solution and the gas for SO_2. Nitrogen was used as the SO_2 diluent to avoid the effects of oxidation on absorption.

Figures 4, 5, and 6 show the steady-state distribution curves for SO_2-citrate absorbents. Data points on the curves represent the analysis of SO_2 in a dry gas for the atmospheric pressure (about 640 mm Hg).

Figure 4 shows the effect of SO_2 gas concentration and absorbent pH on the equilibrium loading of 0.5*M* citrate and 0.2*M* $S_2O_3^{2-}$ solution at 113° F. A molar ratio of NaOH to citric acid of 2 in the absorbent yielded a pH of 4.6. As stated earlier, a 1.5 ratio resulted in a pH of 4.1.

Figure 5 shows the effect of SO_2 gas concentration and absorbent concentration on the equilibrium loading of citrate solution with a molar ratio of NaOH-to-citric acid of 2 and containing 0.25*M* $S_2O_3^{2-}$.

Figure 6 shows the effect of SO_2 gas concentration and absorption temperature on the equilibrium loading of 0.5*M* citrate and 0.18*M* $S_2O_3^{2-}$ solution with a molar ratio of NaOH-to-citric acid of 2.

These equilibrium loading results show that SO_2 absorption increased with increased SO_2 concentration in the gas, increased pH and citric acid concentration of the absorbent, and decreased temperature.

To minimize reagent requirements, investigators selected the lowest citrate concentration compatible with the SO_2 content of the gas. The preferred operating temperature had to represent tradeoffs between higher SO_2 loading in the absorbent at lower temperature, the cost of cooling, and the efficiency of regenerating and sulfur recovery. During much of the subsequent research, investigators made up fresh absorbent having an NaOH-to-citric acid molar ratio of 2 and an 0.2*M* to 0.3*M* $Na_2S_2O_3$ concentration.

Continuous Test Unit

An effective means of aqueous absorption of SO_2 from a cool and clean gas is by countercurrent contact in a packed absorption tower. Figure 7 is a photograph of one of the continuous test units (CTU) used in the laboratory to study the citrate process. The right side of the photograph shows a 4-in-diam by 12-ft-tall packed absorption tower (3). The packing in this tower consisted of 1/2-in ceramic saddles. Other parts of the CTU will be described later. In this CTU, over 95 pct of the SO_2 was absorbed using the citrate process over a wide range of gas compositions, temperatures, solution pH's, and citrate concentrations, as long as the solution SO_2 loading did not exceed about 65 pct of the equilibrium loading. Results shown in table 4 from the CTU tests of from 80- to 120-h duration on 20 ft³/min of feed gas at 113° F illustrate the excellent absorption of the citrate process. In these continuous tests, 0.5*M* citrate was used and the regenerated solution pH ranged from 4.1 to 4.5. After a few cycles, the pH of the solution, which was initially 4.6, stabilized at about 4.2—provided no appreciable H_2SO_4 mist or entrained cooling liquor was present in the gas stream, an efficient sulfur precipitation system was maintained, and a slight excess of H_2S was used in regeneration.

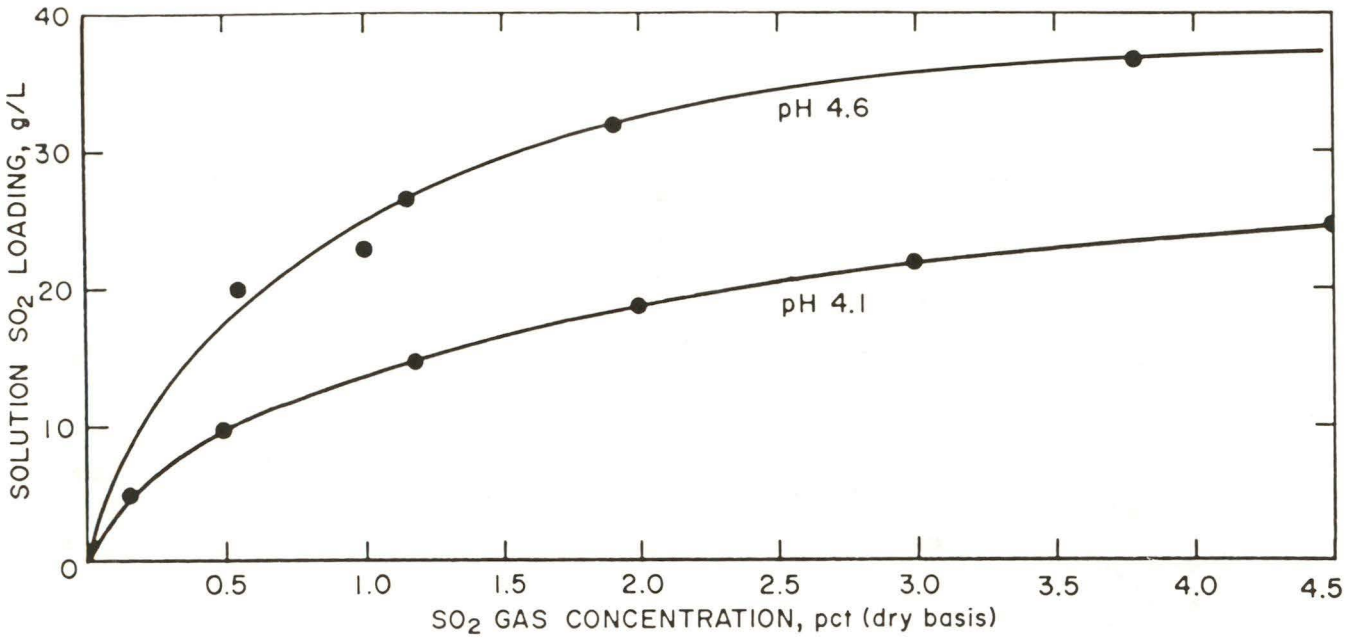


Figure 4.—Effect of initial pH on SO_2 absorption in 0.5*M* citrate solution at 113° F.

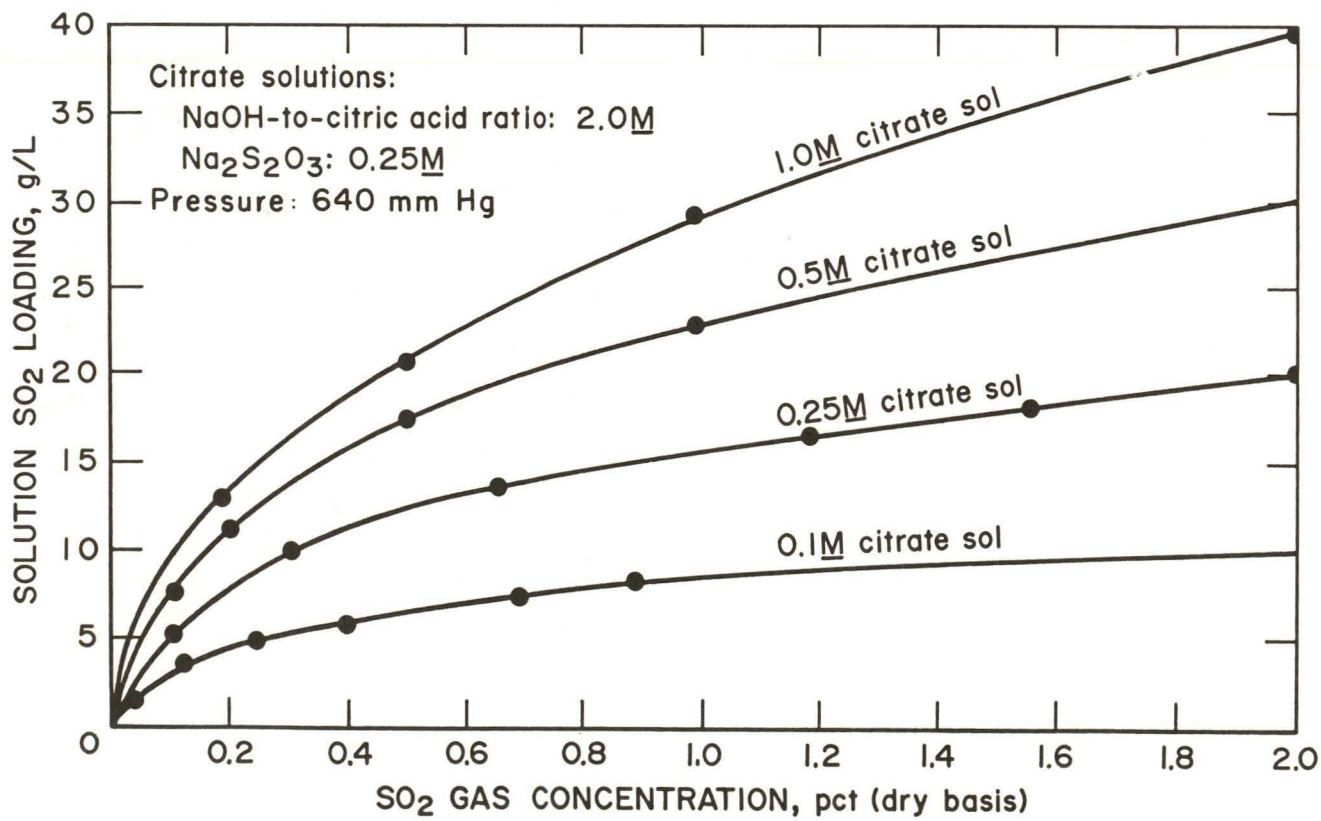


Figure 5.—Effect of gas concentration and citrate concentration on SO_2 absorption.

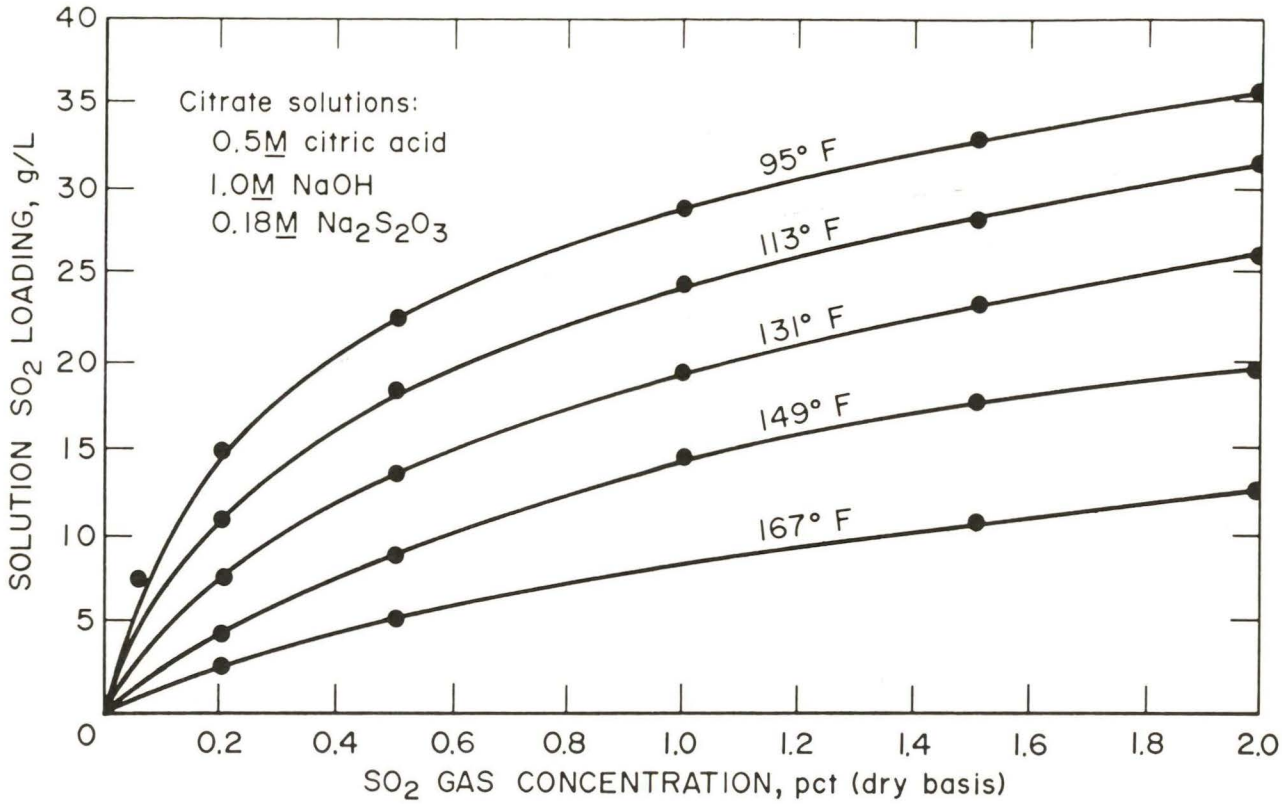


Figure 6.—Effect of gas concentration and citrate solution temperature on SO_2 absorption at 640 mm Hg absolute pressure.

SULFUR PRECIPITATION AND SOLUTION REGENERATION

An efficient sulfur precipitation system consisted of one or more closed, stirred reactor vessels in which SO_2-loaded citrate solution reacted with H_2S gas. In the reactors, the agitator must vigorously mix the solution and gas, which was introduced below the impeller in a ratio of 2 moles of H_2S per mole of SO_2. H_2S and SO_2 react exothermically and liberate 1,580 Btu per pound of SO_2. Batch test results show that about a 1-min reaction time was required when pure H_2S was used to regenerate, and temperatures between 122° and 158° F were found best for flocculating the sulfur and improving sulfur solution separation. In continuous systems, a reaction time of from 10 to 20 min and a temperature of from 140° to 158° F appeared desirable for complete regeneration. Also, the 140° to 158° F temperature aided the flocculation of the colloidal sulfur that formed initially during the regeneration.

In a continuous system using pure H_2S, investigators established that H_2S reacted efficiently with SO_2 in a closed, single-stage vessel. The H_2S addition was controlled by adding the gas at a rate sufficient to maintain a slight positive pressure of H_2S above the solution. This system reacted and dissolved all the H_2S because the reactor was not vented. Because the solubility of H_2S was low after all the SO_2 had been reacted, the citrate solution dissolved only a small amount of H_2S. The regenerated solution containing dissolved H_2S and solid sulfur flowed from the reactor through a liquid seal leg. Solution containing dissolved H_2S is a toxic hazard that must be reacted in a closed, stirred tank with a SO_2-loaded citrate solution.

Reaction of the SO_2-loaded citrate solution with dilute H_2S also proceeded rapidly. However, because inert gases such as CO_2 accompanied H_2S, the regeneration system required a series of reactors with countercurrent flow of H_2S gas and SO_2-loaded solution. An H_2S-CO_2 reactant gas, such as would be produced from the reaction of sulfur, CH_4, and steam, flowed from under the impeller of the last reactor upward countercurrent to the gravity flow of SO_2-loaded solution. The H_2S contained in the gas vented from the first reactor in the series, was incinerated to SO_2, and then scrubbed in the absorption tower. In the CTU, a series of three 5-L reactors regenerated SO_2-loaded solution using 80 pct H_2S gas. Figure 8 shows the CTU sulfur precipitation assembly. The 6-in-diam reactors contained three 5/8-in-wide vertical baffles. Agitation was accomplished using 2-1/2-in-diam impellers having four 5/8-in-high flat blades. In these reactors, an agitator speed of 1,400 r/min was necessary for rapid sulfur precipitation and regeneration of the solution.

The three-stage countercurrent flow configuration efficiently consumed the H_2S. Even so, from 1 to 3 pct excess H_2S over the stochiometric requirement was necessary in this configuration to maintain the optimum pH and achieve complete regeneration. As a matter of interest, a cocurrent flow of H_2S and SO_2-loaded solution to facilitate gas and slurry flow used at least 5 pct excess H_2S to achieve complete regeneration.

Table 4.—Results of tests in 20-ft³/min continuous test unit

SO_2 in feed gas, vol pct	Absorbent SO_2 loading, g/L	SO_2 in offgas, ppmv	SO_2 removal efficiency, pct
0.3	5.8	121	95.9
0.5	10	42	99.2
1.0	7.2	83	99.2

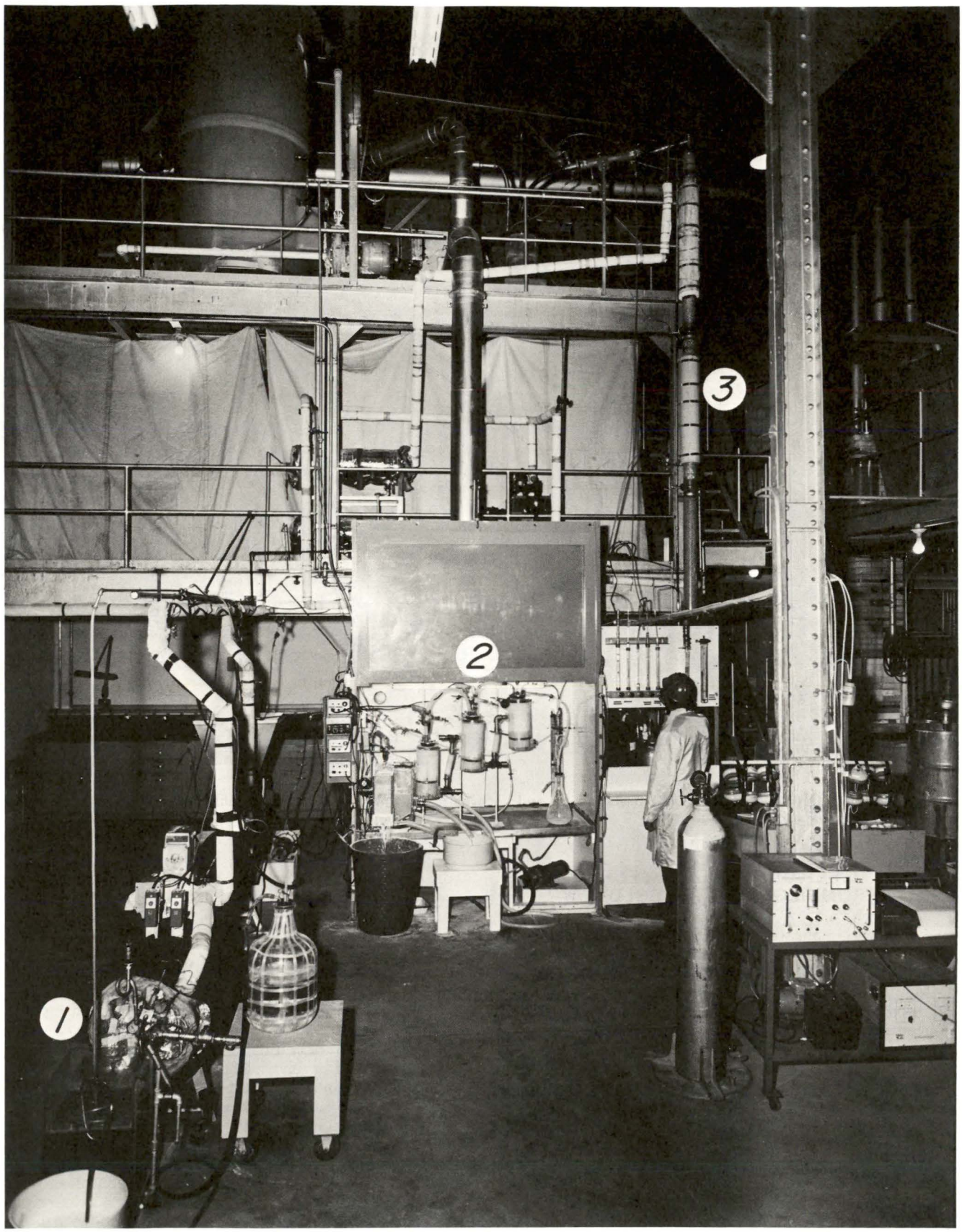


Figure 7.—Laboratory continuous test unit. *1*, Sulfur melter; *2*, sulfur precipitation—solution regeneration and sulfur flotation equipment; *3*, SO_2 absorption tower.



Figure 8.—Continuous test unit sulfur precipitation and separation assembly. *1*, Flotation machine; *2*, third reactor; *3*, second reactor; *4*, first reactor.

SEPARATION OF SULFUR FROM REGENERATED SOLUTION

Sulfur was separated from the bulk of the regenerated citrate solution by alternative liquid-solid separation procedures such as filtration, thickening, hydrocycloning, centrifuging, and flotation. The final recovery of entrained solution and sulfur product was obtained by melting of concentrated slurry or sulfur cake. A pressurized settler was used to melt the sulfur at about 275° F and a pressure of 35 lbf/in^2(ga). Molten sulfur settled and was withdrawn from the bottom of the settler. Hot citrate solution was withdrawn from the top of the settler through a control valve and then cooled in a heat exchanger or quenched with cool citrate solution.

Sulfur slurry filtered rapidly under vacuum, but the cake cracked and dried to only about 20 pct solids. Thickening of a sulfur slurry containing 1 to 3 pct solids resulted in a product containing less than 10 pct solids. Two-stage hydrocycloning of a 1-pct-solids sulfur slurry resulted in a final underflow containing from 12 to 15 pct solids. Batch or continuous centrifuging of thickened sulfur slurries produced cakes containing up to 60 pct solids. Cakes containing 60 pct solids must be reslurried in order to be pumped into a melting vessel, and centrifuging is an energy-intensive method for bulk citrate solution-sulfur separation.

Investigators found a flotation procedure to hold the most promise for an efficient, economic method for the bulk citrate solution-sulfur separation. In batch testing of the flotation procedure, the addition of 2 pct or less kerosene or oil by weight of sulfur followed by brief agitation of the slurry resulted in separation of the sulfur from the citrate solution. Without the addition of air, the sulfur floated rapidly to the surface in the form of an apparently dry powder that could be readily removed by suction or skimming. The powder contained 40 to 80 pct solids depending upon the amount of hydrocarbon added, the temperature of the slurry, and the degree and duration of agitation. Flotation of sulfur from the slurry resulted in a clear citrate solution acceptable for recycle. Figure 9 shows a typical sulfur slurry from the sulfur precipitation and solution regeneration reaction before and after flotation with kerosene.

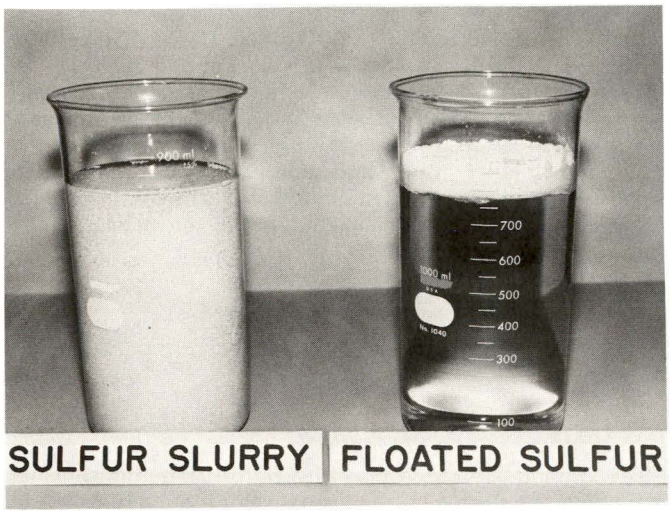


Figure 9.—Sulfur flotation demonstration.

In the CTU, the flotation procedure consisted of (1) the addition of 2 to 3 pct kerosene by weight of sulfur, (2) agitation of the slurry, (3) flotation of the sulfur from the regenerated citrate solution, and (4) skimming of the sulfur powder in the apparatus shown in figure 10. Normally in 24 h of operation, this flotation machine produced 80 lb of sulfur powder containing 50 pct solids.

The system shown in figure 11 melted sulfur powder and separated molten sulfur from residual citrate solution. The sulfur powder was pumped from the feed hopper (1) with a Moyno[3] pump (2) through a steam-jacketed sulfur melter

[3]Reference to specific products does not imply endorsement by the Bureau of Mines.

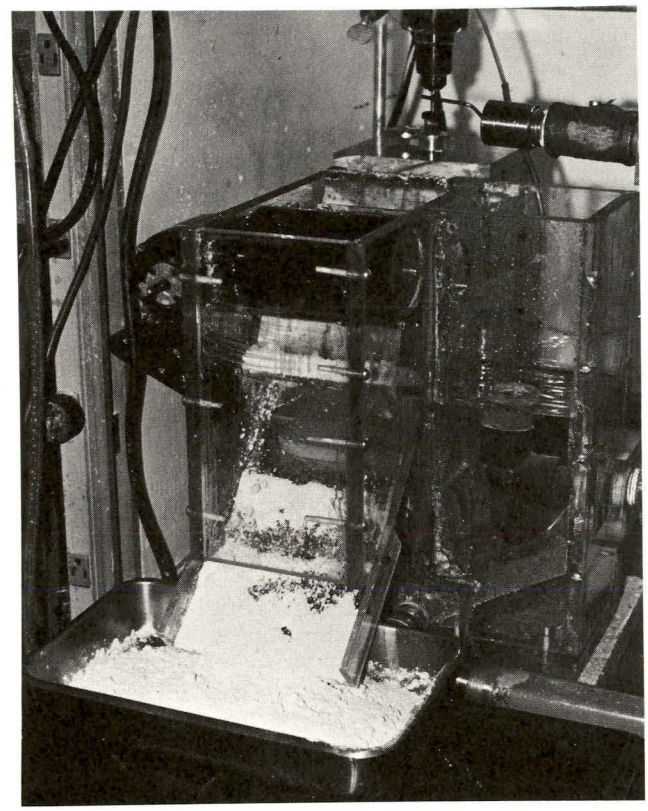


Figure 10.—Continuous test unit sulfur flotation cell.

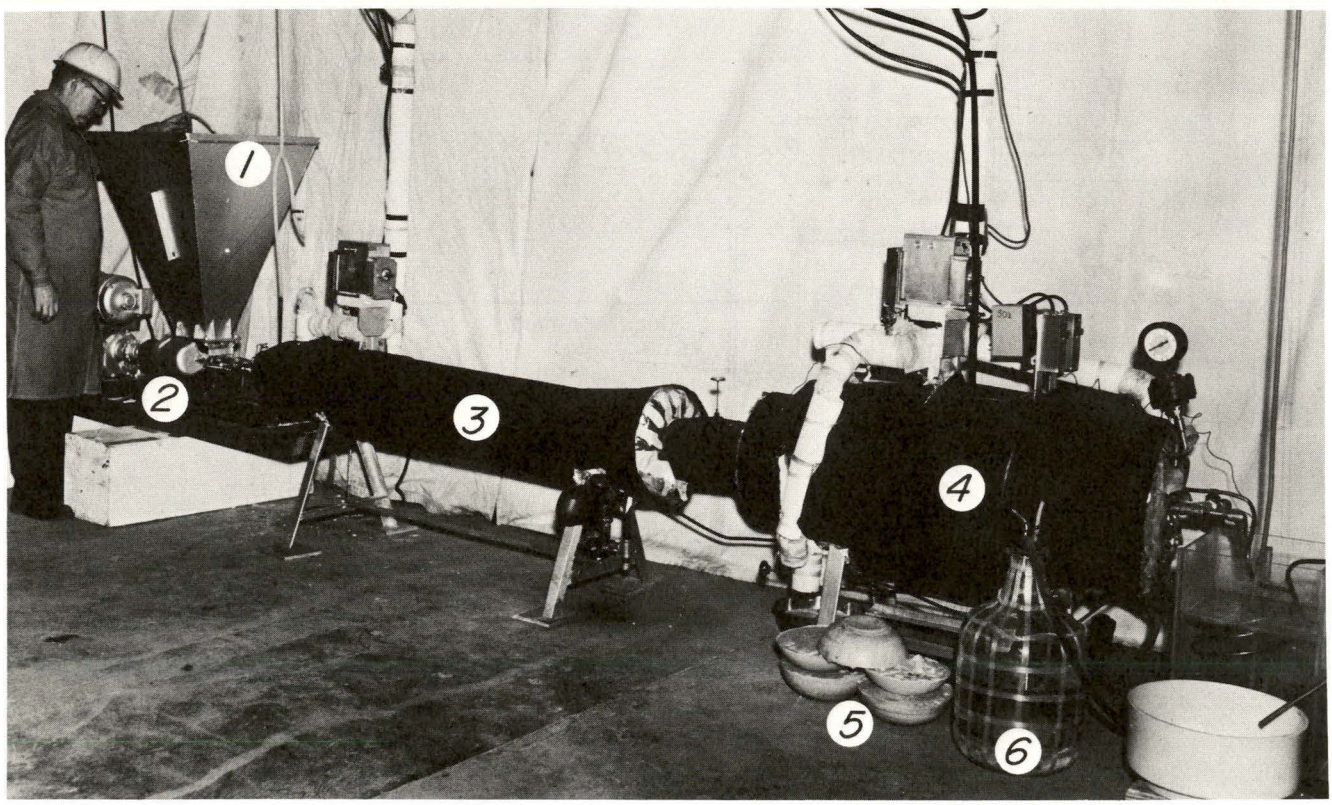


Figure 11.—Continuous test unit sulfur melter and settler. *1*, Powder sulfur feed hopper; *2*, Moyno pump; *3*, sulfur melter; *4*, sulfur settler; *5*, sulfur cake; *6*, citrate solution.

(3). The molten sulfur separated from and settled below the citrate solution in the sulfur settler (4). Molten sulfur flowed through a control valve on the bottom left of the settler and solidified in molds (5). Citrate solution with hydrocarbon floating on the surface inside the settler was withdrawn through a control valve on top right end of the settler. This solution (6) was cooled to prevent flash evaporation of water and was filtered before recycling.

H_2S GENERATION

Laboratory studies on the preparation of H_2S for precipitating sulfur from SO_2-loaded solution included reactions of the following: CH_4, sulfur, and steam; CS_2 and steam; CO, sulfur, and steam; hydrogen and sulfur; C_2H_6, sulfur, and steam; CH_3OH, sulfur, and steam; base metal sulfides or copper matte with acids or steam; and chalcopyrite concentrate, carbon, and lime to produce CaS for conversion to H_2S.

For reactions of chalcopyrite or copper matte with steam, conversion efficiencies of sulfur to H_2S ranged from 25 pct to 60 pct. The roast of chalcopyrite with lime at 1,202° F, followed by carbonation of the resulting CaS in water, gave a conversion efficiency of 40 pct. When chalcopyrite was reacted with H_2SO_4 and HCl, conversion efficiencies of 75 and 95 pct, respectively, were obtained. However, reactions with copper sulfides to produce H_2S are site-specific. Therefore, because of the general application of the citrate process, emphasis was placed on generating H_2S in situ using product sulfur and a suitable reductant.

Commercially, sulfur vapor and CH_4 react over an activated alumina catalyst at 1,292° F to form CS_2. The reaction, equation 11 shown in chapter 1, converts half the sulfur to CS_2 and half to H_2S:

$$CH_4 + 4S \rightarrow CS_2 + 2H_2S. \quad (11)$$

In the presence of steam, CS_2 hydrolyzes to produce CO_2 and H_2S:

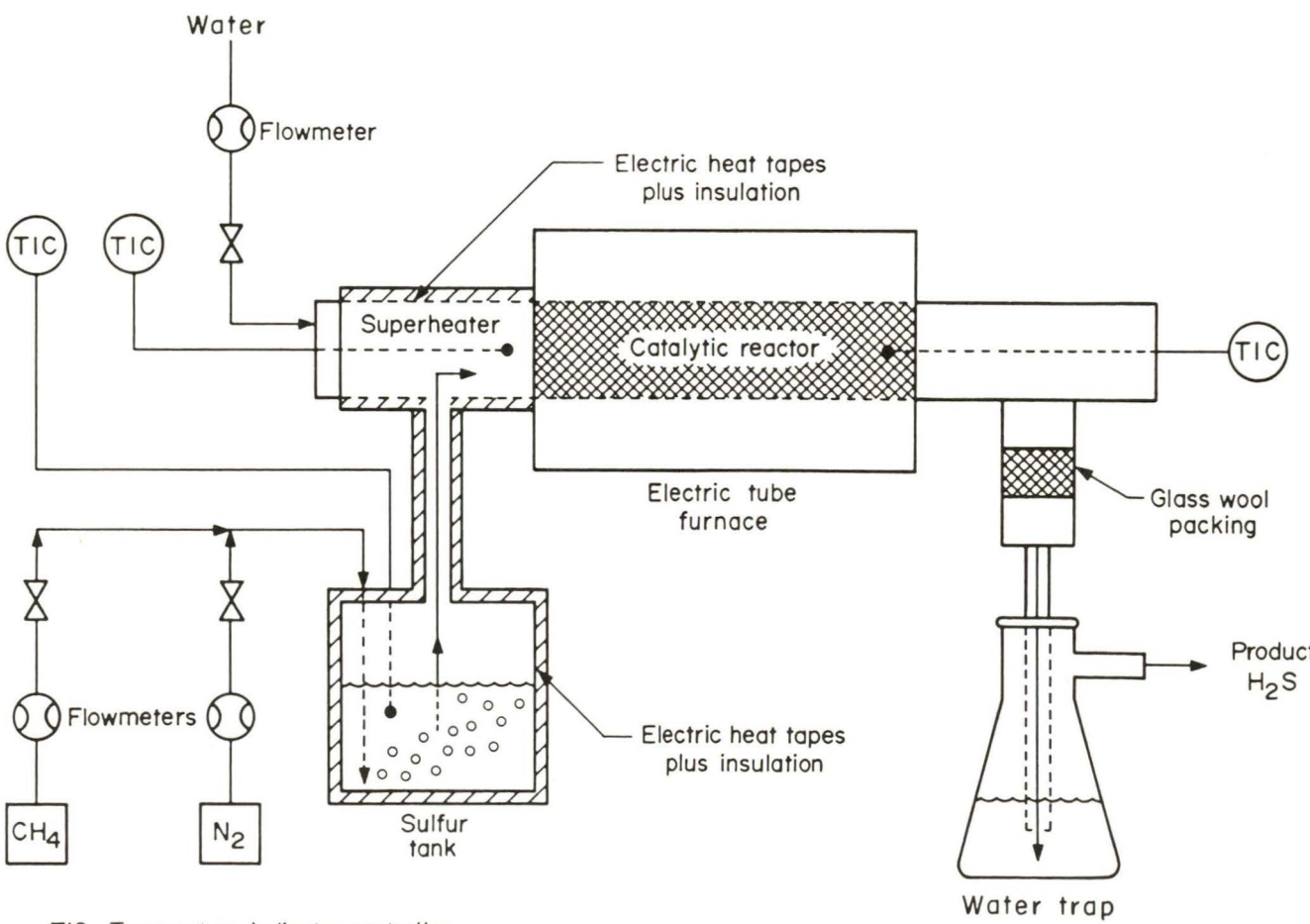
$$CS_2 + 2H_2O \rightarrow CO_2 + 2H_2S. \quad (12)$$

The Bureau's research was directed to the simultaneous reaction of sulfur, CH_4, and steam to produce H_2S.

Bench-Scale Investigations

CH_4, Sulfur, and Steam Tests

Crane (*12*) studied the production of H_2S from CH_4, sulfur, and steam. Figure 12 depicts the bench-scale reactor for preparation of H_2S in one stage. Figure 13 shows the



TIC Temperature indicator controller.

Figure 12.—Bench-scale apparatus for preparation of H_2S.

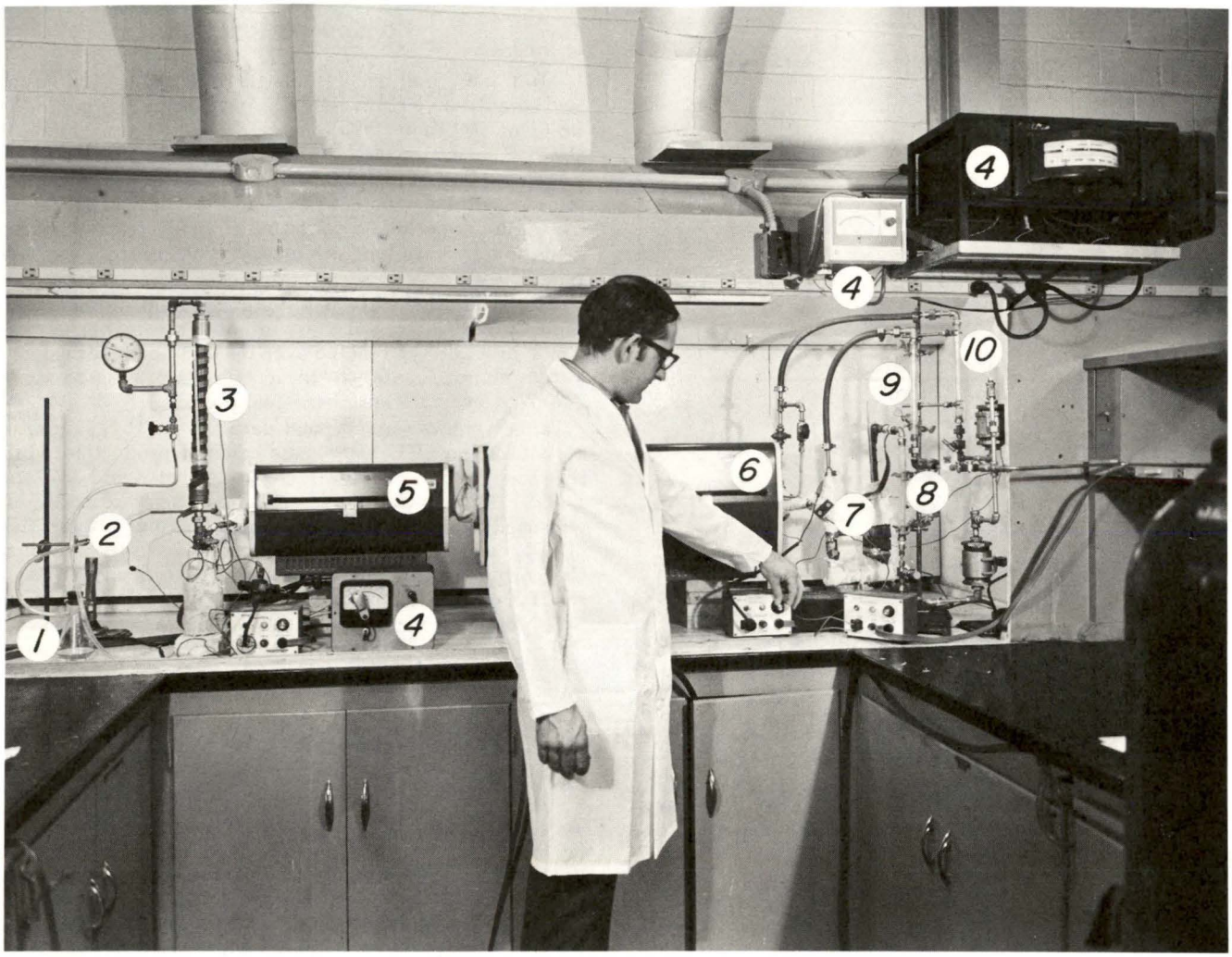


Figure 13.—Laboratory catalytic H_2S generator. *1*, Water trap; *2*, H_2S product; *3*, sulfur condenser; *4*, temperature indicator controller; *5*, catalytic reactor; *6*, superheater; *7*, sulfur tank; *8*, N_2 flowmeter; *9*, CH_4 flowmeter; *10*, water flowmeter.

bench-scale H_2S generator. This H_2S generator used a 1-in-diam stainless steel tube packed with a 9-in-long bed of minus 8- plus 14-mesh activated alumina. Figures 14 and 15 show the effect of temperature and space velocity,[4] respectively, on the CH_4, sulfur, and steam one-stage reaction efficiency. The percentage of CH_4 converted to H_2S represents the reaction efficiency. To provide an excess of water and sulfur to the reaction, investigators added 10 pct more water and from 10 to 20 pct more sulfur than the stoichiometric requirements. The space velocity at 640 mm Hg pressure for the data in figure 14 ranged from 460 h^{-1} at 1,148° F to 510 h^{-1} at 1,328° F because the feed rates were held constant while the temperature was varied. Reaction efficiency leveled at about 93 pct at a temperature of 1,292° F and a space velocity of 500 h^{-1}. At these conditions, a typical product gas analyzed, in dry vol pct, 78.4 H_2S, 19.6 CO_2, 0.66 COS, and 1.34 CH_4. Figure 15 illustrates that at a temperature of 1,220° F, the reaction efficiency decreased with an increase in the space velocity.

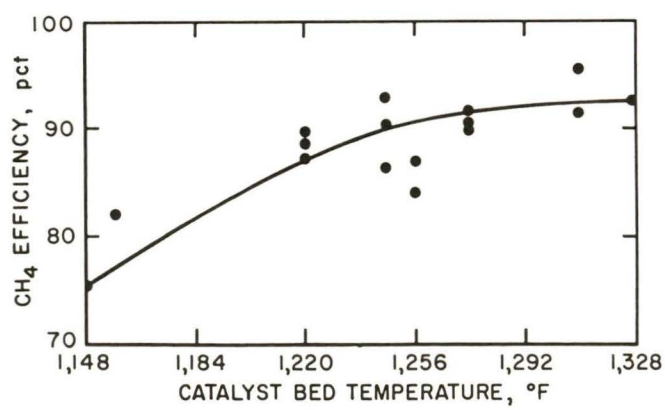


Figure 14.—Effect of temperature on CH_4, sulfur, and steam reaction.

[4]For the purpose of this report, space velocity is defined as the hourly volume of gas at the operating temperature and pressure, divided by the total catalyst bed volume.

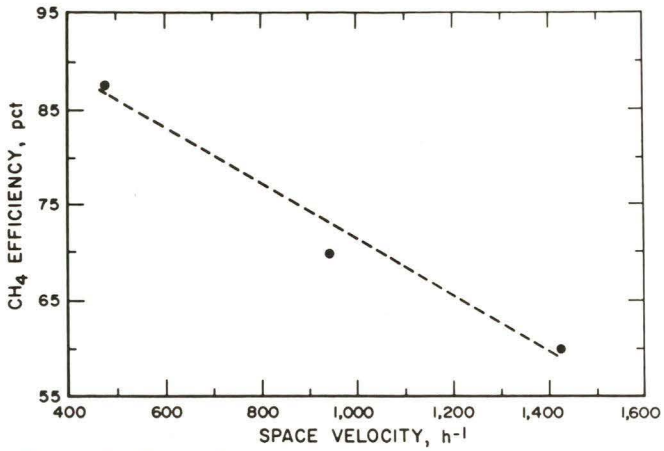


Figure 15.—Effect of space velocity on CH_4, sulfur, and steam reaction at 1,220° F.

Other Reducing-Gas Tests

Reductants other than CH_4, such as H_2, CO, C_2H_6, and CH_3OH, were tested in the 1-in-diam catalytic reactor using minus 8- plus 14-mesh activated alumina catalyst. Equations 9, 13, 14, and 15, shown in chapter 1, give the overall reactions for these reductants. Table 5 shows the reactions, conditions, and results of these tests. The reaction of H_2 and sulfur to produce H_2S (equation 9), is considered a commercial process (*19*). The conditions for the reaction of C_2H_6 or CH_3OH with sulfur and steam (equations 14 and 15) are not too different from those for the CH_4, sulfur, and steam reaction. The reaction of CO with sulfur and steam (equation 13) was studied in more detail, and investigations determined the optimum reaction temperature to be 842° F. At this temperature and a space velocity of 4,800 h^{-1}, 94 pct of the CO reacted to form H_2S.

Catalyst Tests

Various catalysts were tested in the production of H_2S from CH_4, sulfur, and steam in the 1-in-diam reactor. Test conditions included a temperature of about 1,292° F, a space velocity of 400 h^{-1}, and 10 pct more sulfur and 20 pct more steam than the stoichiometric requirement. Granular catalysts sized to minus 8- plus 14-mesh were used in the investigations. Activated alumina and cobalt-molybdenum catalysts were purchased commercially. By soaking activated alumina catalyst in a metal nitrate solution, filtering, drying, heating in an oxidizing atmosphere, and heating in a reducing atmosphere of hydrogen, investigators prepared iron-, chromium-, and nickel-impregnated catalysts. Table 6 shows that the use of activated alumina resulted in the best reaction efficiency and the lowest COS content in the product gas.

Continuous Test Unit

After successful bench-scale testing of the CH_4, sulfur, and steam reaction, investigators scaled the H_2S generator up about 100 times for the citrate CTU. Figure 16 depicts the H_2S generator section of the CTU. This generator used a metered flow of high-temperature silicone oil to displace molten sulfur at about 275° F into a sulfur superheater. The sulfur superheater consisted of an electrically heated, 2-in-diam by 16-in-long, Alonized,[5] type 310 stainless steel pipe. CH_4 and water were metered and then superheated in an electrically heated, 1-in-diam, type 316 stainless steel pipe. Superheated CH_4, sulfur, and steam at between 1,202° and 1,382° F reacted over 1/4-in-diam spherical activated alumina catalyst in a 4-in-diam by 54-in-long, Alonized, type 310 stainless steel pipe.

Table 7 shows some typical data for the H_2S generator section of the CTU at various rates of production while the reactor temperature was controlled between 1,337° and 1,382° F. Also, in these investigations, 10 pct excess sulfur was used to provide sufficient sulfur for complete reaction of CH_4, and 75 pct excess steam was used to hydrolyze COS or prevent COS formation. The results show that as the H_2S production rate was increased, the CH_4 conversion to H_2S decreased and the CH_4 conversion to COS increased.

STEAM STRIPPING

Regeneration of SO_2 absorbents by steam stripping has received the attention of several investigators. In the 1930's, H. F. Johnstone of the University of Illinois conducted the most thorough studies on stripping SO_2 from ammonia, NaOH, or methylamine, and water systems (*26-27*). He suggested the use of buffered weak organic acids for SO_2 absorption and steam stripping (*28*). Until 1970, the most significant industrial use of steam stripping SO_2-loaded absorbents was made by the American Smelting and Refining Co. (ASARCO) (*16, 21*). In the ASARCO process, dimethylaniline is used to absorb SO_2 from smelter gases, followed by steam stripping to recover SO_2.

Since 1971, Boliden Aktiebolag Ronnskarsverke, Skelefteham, Sweden, has been using cold water in a commercial operation to absorb SO_2 from smelter gases. The SO_2 is recovered from the water by steam stripping and liquefaction (*7*). In 1976, Boliden pilot-tested a citrate absorbent to treat waste gases. For a 3,000-std-ft^3/min pilot plant, results (*15*) show that 90 pct of the SO_2 can be removed and recovered from flue gas containing 1.0 pct SO_2, using 4 lb of steam per lb of SO_2.

[5]A proprietary process of Alon Processing Inc., Tarentum, PA. This process of vapor-aluminum diffusion provides an aluminum-enriched surface that is generally very resistant to both sulfidation and oxidation.

Table 5.—Summary of results of H_2S generation tests using various reductants

Reductant	Reaction	Catalyst bed		H_2S anaysis, dry vol pct	Reaction efficiency, pct
		Temperature, °F	Space velocity, h^{-1}		
H_2	(9) $H_2 + S \rightarrow H_2S$	842-1,202	1,200-2,400	99	98-99
CO	(13) $CO + S + H_2O \rightarrow H_2S + CO_2$	752- 932	600-4,800	49	90-95
C_2H_6	(14) $C_2H_6 + 7S + 4H_2O \rightarrow 7H_2S + 2CO_2$	1,112-1,292	240- 480	77	80-90
CH_3OH	(15) $CH_3OH + 3S + H_2O \rightarrow 3H_2S + CO_2$	1,112-1,292	240- 480	71	80-90

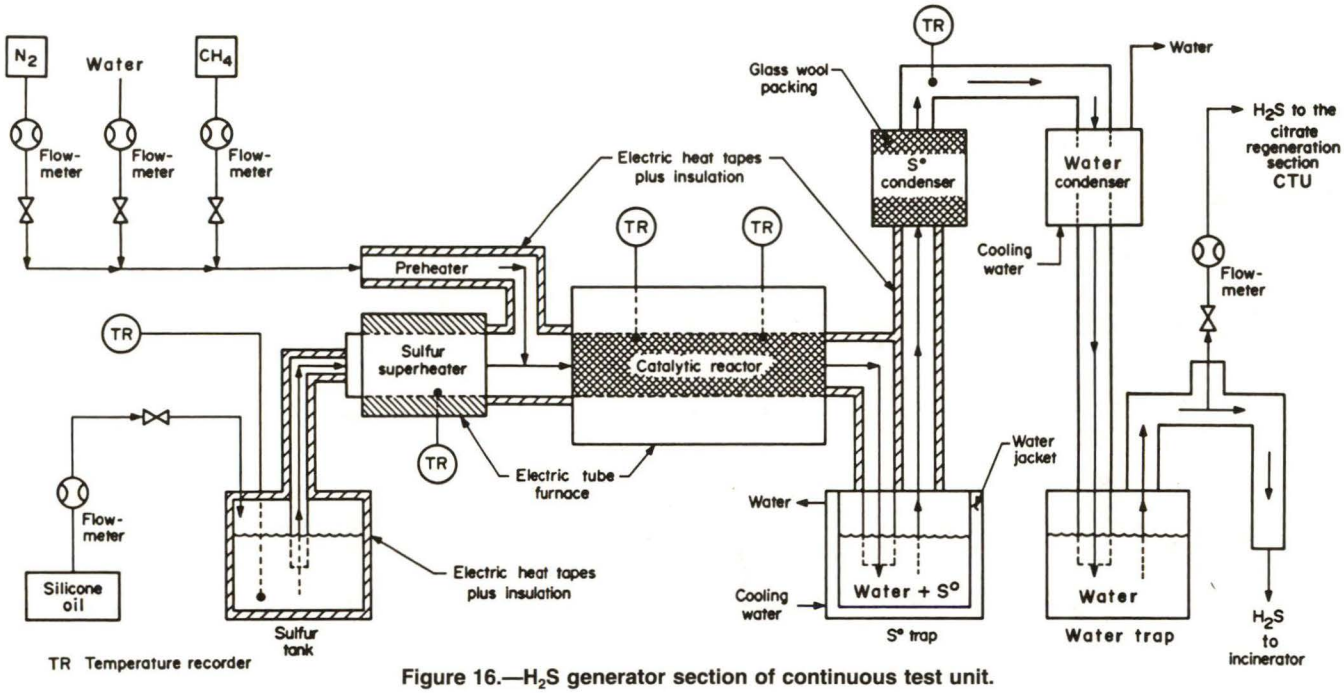


Figure 16.—H_2S generator section of continuous test unit.

Table 6.—Effect of catalyst type on production of H_2S by reaction of CH_4, sulfur, and steam in a 1-in single-stage tube reactor

Catalyst	Conversion efficiency, pct	COS in product, dry vol pct
Alumina:		
Activated	98.0	0.31
Nickel impregnated	96.4	.42
Iron impregnated	89.5	.34
Chromium impregnated	89.2	.33
Cobalt-molybdenum impregnated	85.7	3.10
Crushed firebrick	57.7	3.66
No catalyst	52.3	2.64

Table 7.—Typical results for H_2S generator section of continuous test unit

H_2S production rate, ft^3/min	Space velocity, h^{-1}	Product gas analysis, dry vol pct				CH_4 conversion, pct
		H_2S	CO_2	COS	CH_4	
0.25	226	79.5	19.9	0.5	0.1	97.1
0.50	434	79.3	19.8	.4	.5	95.1
0.74	596	78.8	19.7	1.2	.3	92.9

Bureau investigators started research on steam stripping as an adjunct to the citrate process in October 1971 (*44*). As an alternative to H_2S regeneration, steam stripping offers several options. The high-purity SO_2 stripped from the scrubbing solution can be liquefied, used for manufacture of H_2SO_4, or reduced to elemental sulfur with coke (*9, 33*). Other advantages of steam regeneration over chemical regeneration with H_2S include the reduction of both production costs and the potential hazards of working with H_2S gas.

Bench-Scale Investigations

For atmospheric pressure and reduced-pressure batch stripping tests and continuous, integrated absorber-stripper tests, 2-in-diam glass columns packed with 1/4-in ceramic saddles were used. Figure 17 shows the CTU with 30-in-high absorber (1) and stripper (2). In pressurized batch tests, a 2-in-diam by 15-in-high type 316 stainless steel column packed with 1/4-in ceramic saddles was used. This column was heated with a 1,600-W heat tape (fig. 18).

Batch Tests

Atmospheric and Reduced Pressure

In the batch tests, 0.5*M* citrate buffered solutions loaded with 20 g/L SO_2 were used. The loaded solutions were pumped at a flow rate of 50 mL/min through a heat exchanger that raised the solution temperature to the boiling point (201° F at 640 mm Hg and 165° F at 380 mm Hg), then to the top of an insulated 30-in-high stripper. Steam was injected into the bottom of the stripper tower and passed countercurrently to the solution through the tower. The tower was operated at atmospheric pressure (640 mm Hg) except when the effect of pressure was investigated. Steam usage was measured by condensing the steam in the SO_2-steam mixture leaving the top of the stripper. The degree of SO_2 removal was determined by assaying the stripped solution for SO_2.

Figure 19 graphically illustrates the effect of buffer solution pH and reduced pressure on steam efficiency. These results show that steam consumption was less at lower pH but was not reduced by using the lower pressure.

In the stripping test at reduced pressure, 0.5*M* citric acid buffered with 0.75*M* NaOH was used. The pressure in the stripper was maintained at 380 mm Hg. In the preheater, the SO_2-loaded solution was raised to 165° F, which is the boiling point of the solution at this pressure. This temperature was maintained in the stripper. The results clearly indicated that steam consumption was not reduced when the stripper was operated at reduced pressure. However, the test did show that a low-temperature steam could be used for steam stripping if the pressure in the stripper is reduced.

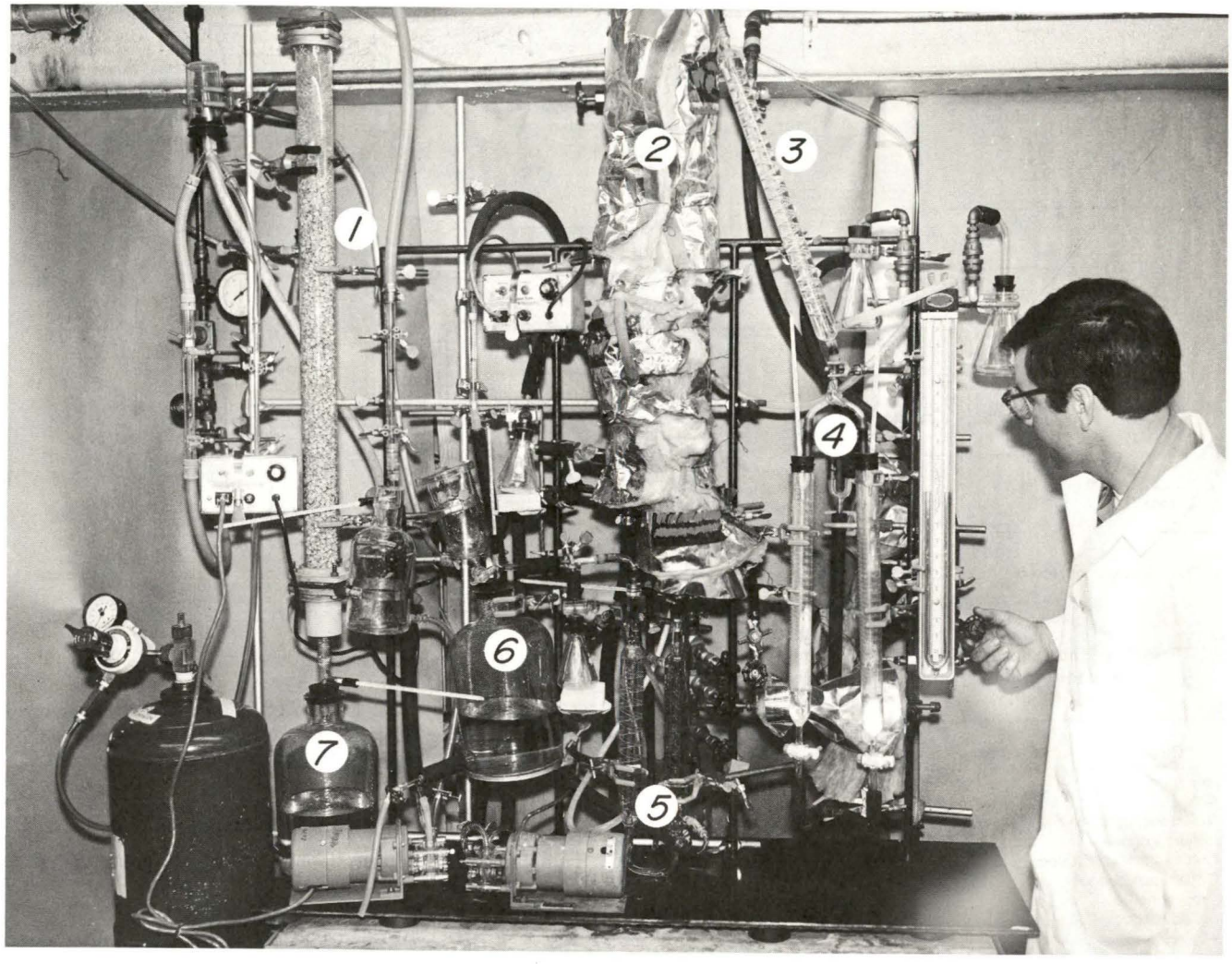


Figure 17.—Laboratory absorber-stripper system. *1,* Absorber; *2,* stripper; *3,* condenser; *4,* condensate measuring system; *5,* heat exchangers; *6,* stripper solution; *7,* loaded solution.

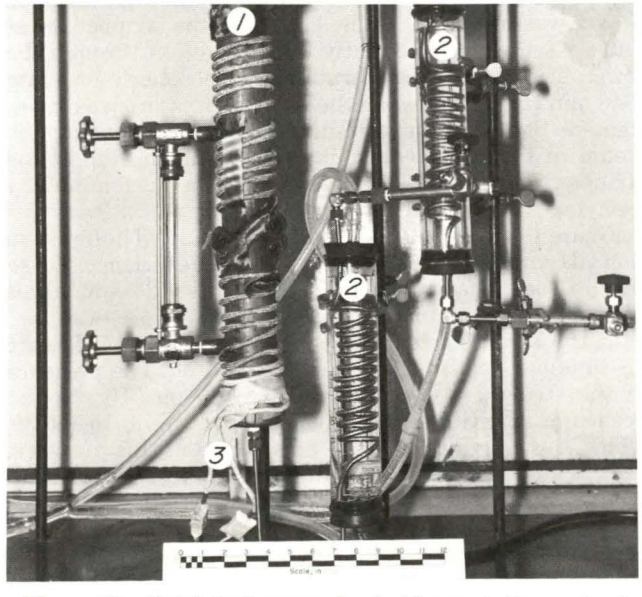


Figure 18.—Batch test pressurized stripper. *1,* Pressurized stripper; *2,* heat exchanger; *3,* heat tape.

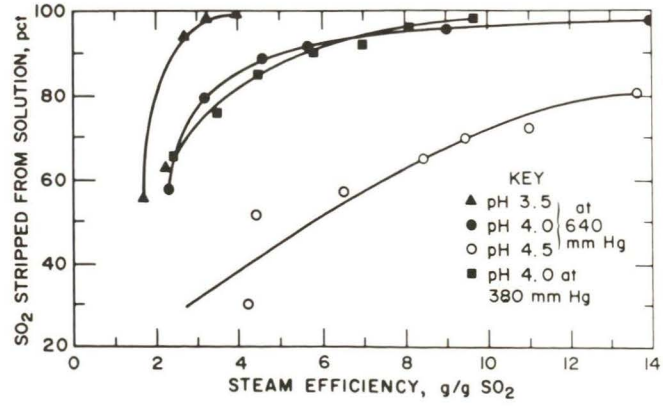


Figure 19.—Effect of pH and pressure on steam efficiency.

Table 8.—Effect of stripper pressure on steam consumption

SO_2 in feed gas, vol pct	Citric acid conc,[1] *M*	Solution flow rate, mL/min	Solution SO_2 loading, g/L		Stripper pressure, $lbf/in^2(ga)$	Stripping steam recovery, g/min	Steam efficiency, g/g SO_2
			Rich	Lean			
0.25	0.3	8.7	8.8	1.5	0	3.6	55.9
		8.7	8.9	1.2	100	1.2	18.1
1.0	.75	8.6	23.4	5.4	0	3	19.4
		8.7	23.4	6	100	1	6.7
2.0	1.25	8.1	37.3	7.3	0	3.5	14.4
		8.0	37.3	7.9	100	1.1	4.7

conc Concentration.

[1]Solution pH was maintained at 4.7.

[2]Steam efficiency = $\frac{\text{[stripping steam recovered (g/min)]}}{\text{[rich sol loading (g/L } SO_2\text{)} - \text{lean sol loading (g/L } SO_2\text{)] [sol flow (L/min)]}}$

Elevated Pressure

Further batch testing was undertaken to determine if steam consumption could be reduced by stripping at a higher pressure. In these tests, SO_2-loaded citrate solution was pumped through the high-pressure stripper (fig. 18) pressurized to 100 $lbf/in^2(ga)$. Solution loadings were chosen to simulate 90-pct SO_2 recovery from a powerplant stack gas (0.25 pct SO_2), a lead smelter sintering-machine tail gas (1.0 pct SO_2), and a copper smelter reverberatory gas (2.0 pct SO_2), in an absorber operating at 75 pct of equilibrium. The lean citrate solution pH was maintained at 4.7 in all tests.

Test results, presented in table 8, show that steam consumption decreased significantly with increased stripper pressure.

Continuous Tests

The objective of continuous tests was to relate steam consumption to SO_2 recovery in the integrated absorber-stripper system. This included evaluating citrate solution concentrations and pH, stripping tower heights, simulated industrial gas concentrations, and sulfate formation in the solution.

A 30-in-high absorber (fig. 17) was arbitrarily chosen for the early tests. However, further investigation showed that a 60-in-high absorber improved absorption by about 5 pct (from 90 to 95 pct). Therefore, all continuous test data presented here were obtained using a 60-in-high absorber tower.

The absorber tower operated isothermally at 113° F and 640 mm Hg. Twenty liters per minute of simulated waste gas was treated in all tests. Solution flow rates through the absorber were chosen to allow operation at about 60 pct of SO_2 equilibrium. The stripping tower was operated isothermally at 201° F and 640 mm Hg. A stripping tower height of 30 in was arbitrarily chosen for all tests except those in which the effect of stripper height was evaluated.

Buffer Solution Evaluation

Citrate solution concentrations between 0.05*M* and 0.5*M* were studied. Each solution was evaluated for a minimum of 6 h. Simulated waste gas containing 0.5 vol pct SO_2 was used in the investigation. The citrate solution pH was 4.5. Although the results presented in table 9 are not strongly conclusive, they indicate that 0.2*M* to 0.3*M* citrate solution had sufficient buffer capacity to obtain about 90 pct SO_2 recovery from the simulated waste gas. Also, the tests showed that the lowest steam consumption for 90-pct SO_2 absorption was obtained with 0.2*M* to 0.3*M* citrate solutions.

In the absorption of SO_2 from a waste gas stream, a high solution pH is desirable because of the acidic nature of the dissolved SO_2. Conversely, a low pH is advantageous for ease of desorption. Therefore, an optimum pH should exist for a particular set of operating conditions. To determine the optimum pH, a series of tests was run in which 0.5 pct SO_2 gas was treated with 0.3*M* citrate solution and the pH of the starting solution was varied. The results of these tests, shown in table 10, tend to confirm that an optimum pH does exist. With citric acid, the best absorption and steam stripping efficiency were obtained at pH 4.75.

Table 9.—Effect of citric acid concentration on steam efficiency and SO_2 absorption

Citric acid concentration, *M*	Steam efficiency, g/g SO_2	SO_2 absorption, pct
0.05	17.2	61
0.10	12.8	82
0.20	11.7	90
0.30	11.8	89
0.40	11.9	88
0.50	12.2	86

Table 10.—Effect of citrate solution pH on steam efficiency and SO_2 absorption

Solution pH	Steam efficiency, g/g SO_2	SO_2 absorption, pct
4.25	12.7	83
4.50	12.2	86
4.75	11.5	91
5.00	12.2	86

Stripping Tower Height

To investigate the effect of stripping tower height on steam efficiency, a series of tests was made using stripper heights of 15, 30, and 60 in (fig. 20). For 90-pct SO_2 removal from 0.5 pct SO_2 gas, 22 g of steam per g of SO_2 was required in the 15-in-high stripper, whereas about 12.5 g of steam per g of SO_2 was required in the 60-in-high stripper. By extrapolation or interpolation, an economic stripping tower height can be determined for scale-up for a CTU.

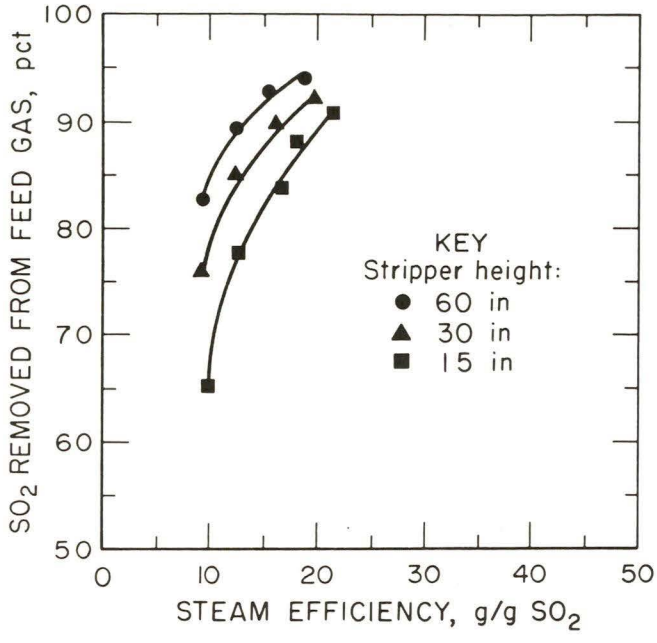


Figure 20.—Effect of stripper height on steam efficiency.

Simulated Industrial Gas

Since SO_2 concentrations in waste gas vary depending on the industry, simulated waste gases ranging from 0.25 to 2.0 vol pct SO_2 were treated in the absorber-stripper system (fig. 17). Such gases would be produced from coal-burning powerplants and nonferrous smelters. As shown in table 11, steam requirements increased as the concentration of SO_2 in the waste gas decreased. This is the natural consequence of an equilibrium (reversible) process. A high SO_2 concentration in the waste gas produces a high SO_2 solution loading. Conversely, low SO_2 concentrations produce low solution loadings. To strip the SO_2 from the solution, lower SO_2 concentrations in the gas or vapor phase are required. Thus, as solution loading decreases, increasing amounts of steam are required to achieve the necessary SO_2 dilution in the vapor.

Table 11.—Steam requirements for 90-pct SO_2 removal from waste gases

SO_2 in waste gas, vol pct	*Steam efficiency, g/g SO_2*
2.0	5
1.0	8
0.50	12
0.25	30

SO_4^{2-} Formation

The formation of SO_4^{2-} is common to all wet SO_2 scrubbing processes. When the waste gas is scrubbed, small amounts of oxygen become dissolved in the scrubbing solution. The dissolved oxygen reacts with the absorbed SO_2 to form SO_4^{2-}. For example, in the Wellman-Lord process, 8 to 10 pct of the SO_2 handled by the system is oxidized (*39*). Approximately 1.6 pct of the SO_2 is oxidized in the citrate process. The oxidation in the integrated absorption, steam stripping operation ranged from 0.4 to 0.7 pct of the SO_2 in the waste gas.

In earlier work on the basic citrate process using H_2S to precipitate sulfur and regenerate the absorbent solution, $S_2O_3^{2-}$ was thought to inhibit the oxidation of SO_2 to SO_4^{2-} by complexing the SO_2. However, $S_2O_3^{2-}$ is not formed in the steam stripping process. Therefore, a series of 6-h tests was made to evaluate the effect of $S_2O_3^{-2}$ in the absorber-stripper system by adding different amounts of $Na_2S_2O_3$. The results are shown in table 12. These results show that in the steam stripping process, $S_2O_3^{2-}$ contributes SO_4^{2-} rather than inhibits SO_4^{2-} formation. The high temperature in the stripper probably decomposes some of the $S_2O_3^{2-}$ to SO_4^{2-}.

Table 12.—Effect of $S_2O_3^{2-}$ on SO_4^{2-} formation in steam stripping

$S_2O_3^{2-}$ concentation, M	*SO_4^{2-} formed per liter of solution,[1] g*
0	0.33
0.05	.27
0.10	.29
0.15	.61
0.20	.76
0.25	.96

[1]During 6-h test.

Continuous Test Unit

Continuous atmospheric pressure tests were conducted using a 75-in-high stripper and a 12-ft-high absorber (fig. 21). The towers were 4 in. in diam and packed with 1/2-in ceramic saddles. On top of the stripper was a 4-in-diam reflux section containing 9 in of saddle packing. The stripping steam was generated by boiling the citrate solution with two 2,000-W immersion heaters in a 10-L capacity stainless steel tank (reboiler) at the bottom of the stripper.

Continuous increased-pressure tests were conducted using a 66-in-high stripper (fig. 22) and the 12-ft-high absorber. The absorber was constructed of Plexiglas acrylic sheet, and the stripper was constructed of type 316 stainless steel. Both towers were 4-in. in diam and packed with 1/2-in ceramic saddles. Stripping steam was generated in a reboiler at the bottom of the stripper by a 4,500-W stainless steel immersion heater. The loaded citrate solution was heated to the stripper operating temperature in a series of type 316 stainless steel heat exchangers.

Atmospheric Pressure Tests

Tests were conducted to determine (1) optimum solution flow rates and (2) optimum citric acid concentration for various strength SO_2 gases. Once the optimum citric acid concentration was determined, new SO_2-citrate distribution curves were obtained to aid in the design and scale-up of the steam stripping process.

The absorber tower was operated isothermally at 113° F and 640 mm Hg while the stripper was operated isothermally at the boiling point of the citrate solution and 640 mm Hg. The lean citrate solution pH was maintained at 4.7 in all tests.

Optimum Solution Flow Rates

To determine the optimum solution flow rates, a series of tests was run in which 0.25, 0.50, and 1.0 vol pct SO_2

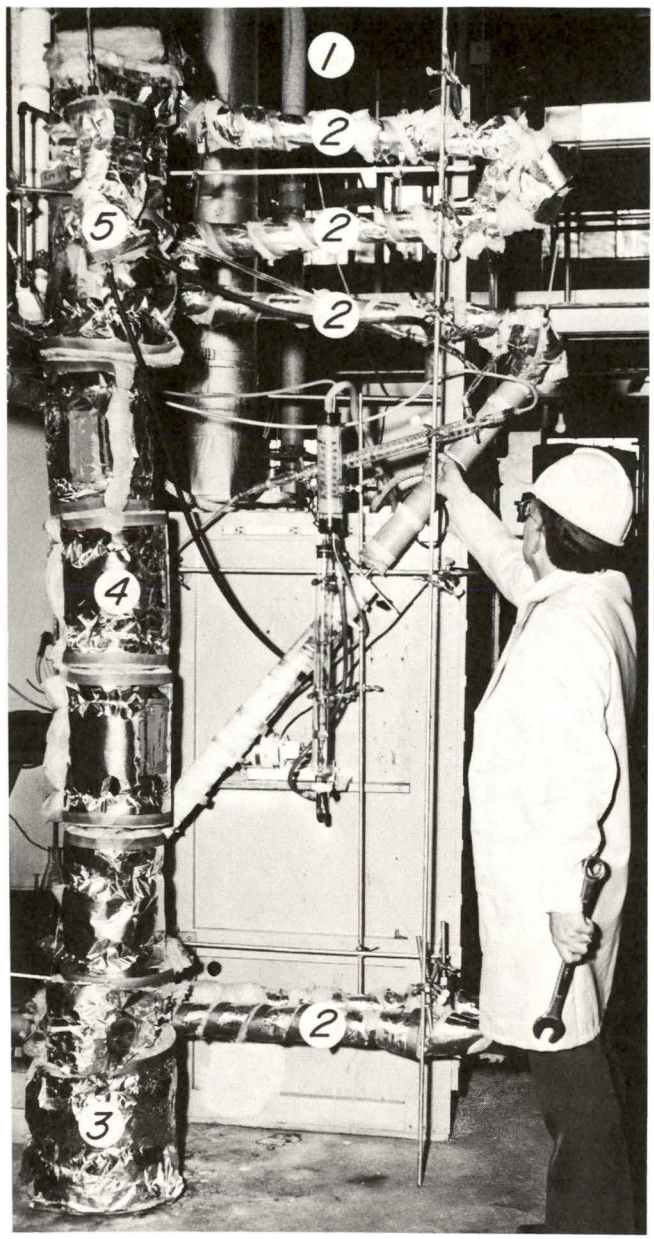


Figure 21.—Continuous test unit atmospheric pressure stripping. *1*, Absorber; *2*, heat exchangers; *3*, reboiler; *4*, stripper; *5*, reflux section.

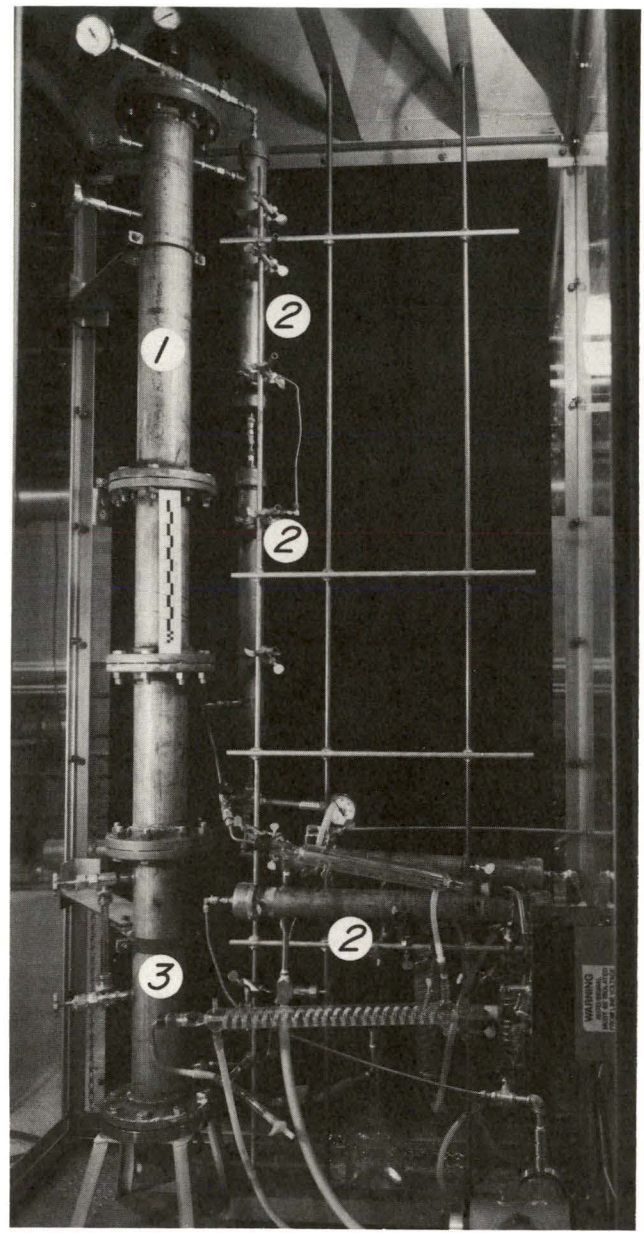


Figure 22.—Continuous test unit pressurized steam stripping. *1*, Stripping tower; *2*, heat exchangers; *3*, reboiler.

gases were treated with 0.3*M* citric acid solution. The objective was to recover 90 pct of the SO_2 from the simulated waste gas. Test results (table 13) show that increased SO_2 concentrations required increased solution flows. These data also again show that steam requirements decreased as SO_2 concentrations increased.

Table 13.—Effect of SO_2 gas concentration on solution flow rate and steam efficiency

SO_2 in feed gas, vol pct	Solution flow rate, L/min	Steam efficiency, g/g SO_2	SO_2 absorption, pct
0.25	0.33	26.4	90.8
0.50	.40	14.1	90.7
1.0	.71	7.7	91.6

Optimum Citric Acid Concentrations

To determine optimum citric acid concentrations, a series of tests was run in which 0.25, 1.0, and 2.0 vol pct SO_2 gases were treated with various citric acid concentrations. Results of the tests (table 14) show that higher citric acid concentrations increased SO_2 loadings and SO_2 recovery without increasing the solution flow rate. To recover 90 pct of the SO_2, citric acid concentrations required were (1) 1.25*M* for 2.0 vol pct SO_2, (2) 0.75*M* for 1.0 vol pct SO_2, and (3) 0.3*M* for 0.25 vol pct SO_2.

Table 14.—Effect of citric acid concentration on SO_2 absorption and steam efficiency

SO_2 in feed gas, vol pct	Citric acid conc, *M*	Solution flow rate, L/min	Solution SO_2 loading, g/L		Steam efficiency, g/g SO_2	SO_2 absorption, pct
			Rich	Lean		
2	1.50	0.57	41.8	9.5	4.6	90.8
	1.25	.57	39.2	6.9	4.7	90
	1	.57	31	2.9	5.7	78
1	.75	.56	21.6	4.9	7.7	92
	.5	.57	18.9	4	8.4	75
0.25	.3	.41	8.7	2.9	26.7	90.8

conc Concentration.

Distribution Curves

Steady-state SO_2-citrate distribution curves were obtained by the dynamic method in which metered SO_2 and N_2 were mixed and bubbled into citrate solution. The solution was contained in an insulated vessel equipped with an agitator. The vessel was heated with a resistance heater, and the temperature of both phases was monitored. To maintain a near-constant solution concentration, the wet offgas was passed through a cold-water condenser and the condensed water returned to the vessel. The SO_2 concentrations in the solution and offgas were checked until they reached steady state.

Curves were determined for 0.3*M*, 0.75*M*, 1.0*M*, and 1.25*M* citric acid solutions at pH 4.7 and the boiling points as well as at 113°, 131°, and 149° F. These curves are presented in figures 23 and 24.

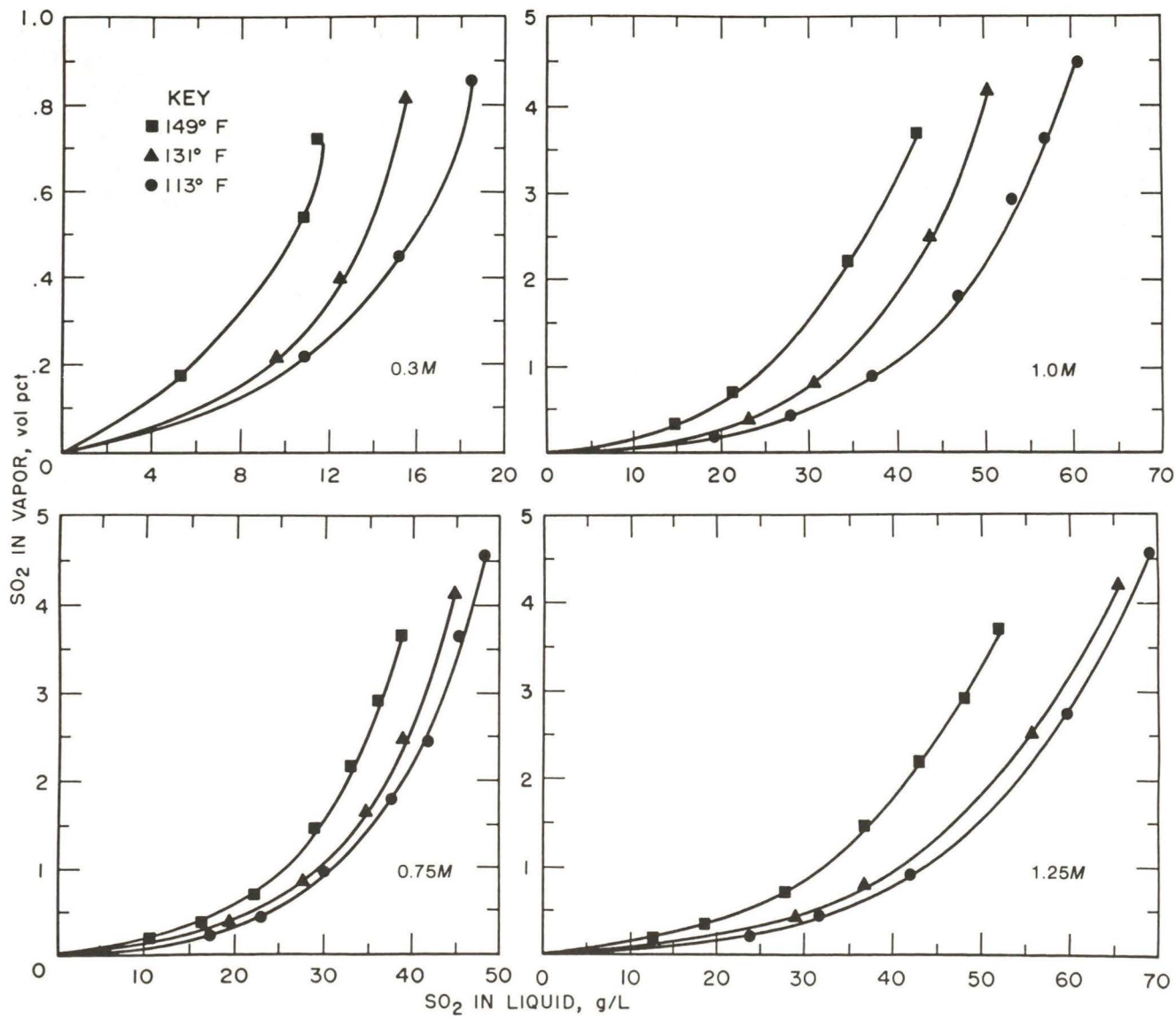


Figure 23.—SO_2 distribution curves, using various citrate solution concentrations at pH 4.7.

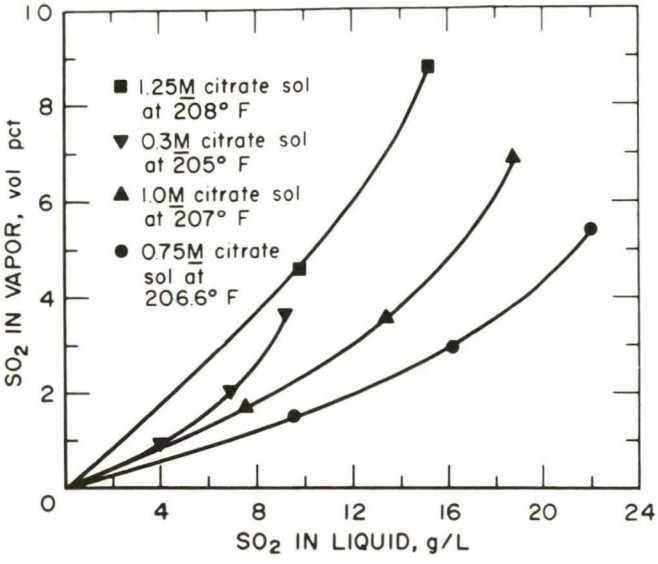


Figure 24.—SO_2 distribution curves at solution boiling points.

Mass Transfer Rates

Mass transfer rates (K_Ga, K_La) for the absorber, stripper, and reflux sections were calculated to provide information for sizing packed towers (*14*). The steam stripping operation was treated as a desorption process, with steam acting as an inert purge gas. Rates calculated for treatment of 0.25, 1.0, and 2.0 vol pct SO_2 gases were rounded to the nearest whole number and are presented in table 15. K_Ga is given as pound-moles of SO_2 absorbed per cubic foot of packing per hour per atmosphere of driving force, and K_La as pound-moles of SO_2 stripped per cubic foot of packing per hour per mole fraction of driving force. The numbers given in table 15 may be used to design absorbers, strippers, and reflux sections.

Table 15.—Mass transfer rates (K_Ga, K_La) for steam-stripping continuous test unit

SO_2 in feed gas, vol pct	Absorber K_Ga[1]	Stripper K_La[2]	Reflux K_La[2]
2.0	12	5	8
1.0	13	9	7
0.25	17	2	11

[1]Pound-moles of SO_2 absorbed per cubic foot of packing per hour per atmosphere of driving force.
[2]Pound-moles of SO_2 stripped per cubic foot of packing per hour per mole fraction of driving force.

Elevated-Pressure Tests

Tests were conducted with the stripper pressurized in the range of 5 to 150 lbf/in^2(ga). Tests were limited to the treatment of 1.0 and 2.0 vol pct SO_2 gases, since lower tenor gases require excessive amounts of steam for treatment (*34-36*). The 2.0 vol pct gas was treated with 1.25*M* citrate solution, whereas the 1.0 vol pct SO_2 gas was treated with 0.75*M* citrate solution. The solutions were buffered to pH 4.7.

To investigate the effect of stripper pressure on steam consumption, a series of tests was made treating 11 std ft^3/min gases (approximate design capacity of the stripper when operated at atmospheric pressure for 90-pct SO_2 recovery) with the stripper operating at 0 to 5, 75, and 150 lbf/in^2(ga). The solution flow rate was maintained at 500 mL/min.

Test results (fig. 25) show that pressurizing the stripper decreased steam consumption. For example, 90-pct SO_2 removal from a 1.0 vol pct SO_2 gas required 4.1 g steam per gram SO_2 at a stripper pressure of 150 lbf/in^2(ga) but 7.1 g steam per gram SO_2 at 5 lbf/in^2(ga).

No test results are shown for treatment of 2 vol pct SO_2 gas above 75 lbf/in^2(ga) because the 1.25*M* citrate solution decomposed rapidly at 100 lbf/in^2(ga) and above. Therefore, a lower concentration of citric acid and a higher solution flow rate would be recommended to treat 2 vol pct SO_2 gas at pressures above 100 lbf/in^2(ga).

SO_4^{2-} FORMATION AND REMOVAL

The citrate process requires an SO_4^{2-} removal step primarily because of the oxidation of SO_2 and decomposition of $S_2O_3^{2-}$. A convenient method for SO_4^{2-} removal is the crystallization of $Na_2SO_4 \cdot 10H_2O$.

SO_4^{2-} Formation

Research was conducted on the oxidation of SO_2 to SO_4^{2-} in the citrate system using a bench-scale absorption column at 113° F with 0.5*M* citrate solution buffered at pH 4.5. Except as noted, sulfur was produced by H_2S precipitation in a stirred reactor at 140° F. The sulfur was recovered by filtering and centrifuging, and the regenerated citrate solution was recycled to the absorption column. Results of tests using various synthetic gases are given in table 16. Six tests were run using 0.5 vol pct SO_2, and a simulated powerplant gas containing 0.25 vol pct SO_2 was used in the seventh test.

The first test showed a small amount of oxidation occurring in the absorption column alone. The second test showed that some oxidation did occur in the H_2S precipitation reactor or sulfur recovery equipment. As shown in the third test, the SO_2 oxidation, although still not excessive, was nearly double that of the second test, in the presence of 3.6 vol pct O_2. This figure did not increase appreciably when 21 pct O_2 was used in the fourth test. When NO was present, SO_2 oxidation increased from 0.98 to 1.34 pct. The addition of NO_2 to the feed gas resulted in a substantial increase in oxidation of SO_2 to SO_4^{2-}. The highest oxidation of 6.7 pct occurred with the simulated powerplant gas containing 0.25 vol pct SO_2, 3.6 vol pct O_2, 950 ppmv NO, and 100 ppmv NO_2. In general, the tests showed that (1) very little oxidation occurs in the absence of nitrogen oxides, (2) a slight increase in oxidation occurs in the presence of NO, and (3) the presence of NO_2 with NO results in appreciable increase in oxidation.

Table 16.—Oxidation of SO_2 to SO_4^{2-} during SO_2 removal from various feed gases using the citrate system

Test	Synthetic gas composition				Oxidation, pct
	SO_2, vol pct	O_2, vol pct	NO, ppmv	NO_2, ppmv	
1	0.5	0	0	0	[1]0.37
2	.5	0	0	0	.47
3	.5	3.6	0	0	.84
4	.5	21	0	0	.98
5	.5	3.6	1,000	0	1.34
6	.5	3.6	1,025	100	3.60
7	.25	3.6	950	100	6.70

[1]Citrate solution circulated through absorption tower; no sulfur precipitation or solution regeneration.

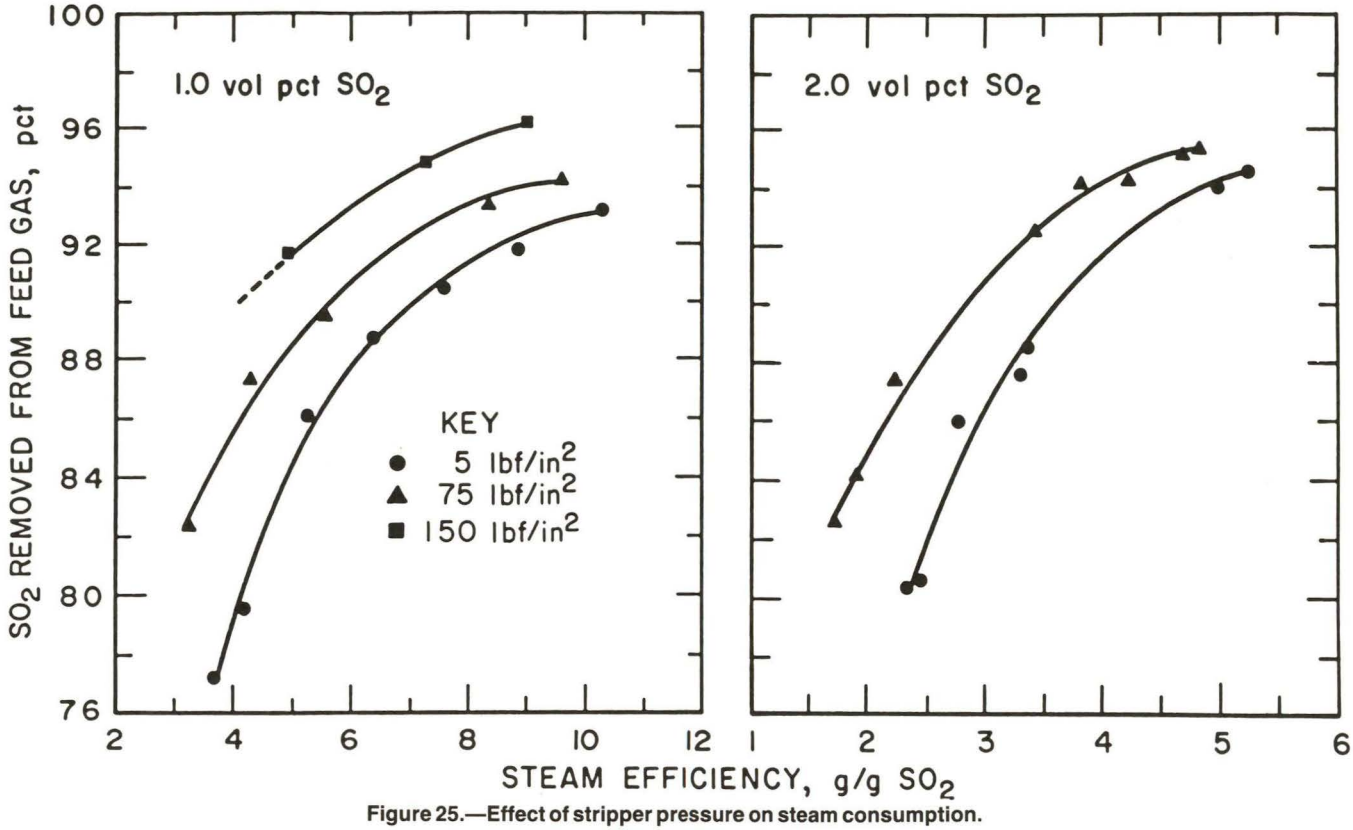


Figure 25.—Effect of stripper pressure on steam consumption.

Decomposition of $S_2O_3^{2-}$ occurred primarily in the sulfur melting step of the citrate process. Tests were conducted for 100 h in an autoclave at 275° F. For these tests, 1*M* citrate solution at pH 4.5 contained 40 g/L $S_2O_3^{2-}$. Test results showed 70 pct of the $S_2O_3^{2-}$ decomposed. However, the test time represented about 300 melting cycles, and therefore approximately 0.1 g/L $S_2O_3^{2-}$ decomposed per cycle, which represents an oxidation of 0.06 g/L SO_2. For 90-pct removal of SO_2 from a powerplant gas containing 0.25 pct SO_2, solution loading could be 5 g/L SO_2. Therefore, the decomposition of $S_2O_3^{2-}$ represents about 1.2 pct oxidation of SO_2 to SO_4^{2-}.

SO_4^{2-} Removal

Crystallization tests were conducted to determine the amount of $Na_2SO_4 \cdot 10H_2O$ that could be removed from citrate solutions. Citrate solutions were cooled from about 113° to 41° or 32° F. Table 17 shows sulfate removals from typical citrate solutions simulating actual process solutions containing 0.2*M* $S_2O_3^{2-}$ and 0.50*M* or 1.0*M* SO_4^{2-}. Since $Na_2SO_4 \cdot 10H_2O$ would not precipitate at 41° or 32° F from 0.25*M* SO_4^{2-} solutions, sulfate could not be removed using this procedure. Sulfate removal efficiency ranged from 56 to 74 pct. The $Na_2SO_4 \cdot 10H_2O$ produced was easily washed free of citrate and $S_2O_3^{2-}$ with 34° F water, using only 25 pct of the water present in the solution before crystallization.

Table 17.—Crystallization of $Na_2SO_4 \cdot 10H_2O$ from citrate solutions

Citrate concentration, *M*	SO_4^{2-} concentration, *M*	Pct SO_4^{2-} removed at—	
		32° F	41° F
0.25	0.5	69	61
	1	74	72
0.5	.5	NA	56
	1	71	65
1.0	.5	72	62
	1	72	68

NA Not available.

CITRATE DECOMPOSITION

Batch and continuous test results showed that citrate concentration in the scrubbing solution decreased with operating time. This citrate loss may be explained by reactions reported by Rochelle and Gibson (*50*). They proposed that at 266° to 338° F citrate decomposes to aconitic acid, which reacts with bisulfite ion to form sulfotricarballylic acid. Also, they suggest that sulfotricarballylic acid has a buffer capacity similar to that of citrate. Bureau investigators determined that the citric acid decomposition probably proceeds as follows:

Citric acid → aconitic acid → itaconic acid
→ citraconic acid → mesaconic acid.

Batch test results on the stability of citric acid and $S_2O_3^{2-}$ during the sulfur melting operation are presented in table 18. The solution was heated for 100 h in an autoclave at 275° or 302° F with or without sulfur and $S_2O_3^{2-}$. Citric acid underwent a slow decomposition; the rate was dependent upon temperature and concentration. However, the amount of decomposition was not alarming because these tests represented approximately 300 melting cycles. For example, the decomposition at 302° F amounted to only about 1 lb citric acid per st of sulfur melted. More importantly, the autoclaved citrate solution showed no loss in capacity to absorb SO_2.

Continuous tests of citrate decomposition were conducted during the steam stripping investigations in which 11 std ft^3/min of 1.0 vol pct SO_2 gas was treated. The initial citrate concentration was 0.75*M* (144 g/L). The test results (table 19) show that the citrate solution decomposed with increased time and temperature to as low as 0.28*M* citrate concentration (53 g/L) under the most severe conditions. However, citrate decomposition did not affect SO_2 loadings.

Table 18.—Citric acid decomposition during sulfur melting in autoclave

Citric acid concentration, *M*	Temp, °F	Added sulfur and 40 g/L $S_2O_3^{2-}$	$S_2O_3^{2-}$ loss, pct	Organic loss, pct	
				By titration	By chromatograph
1.0	275	No	NA	29 ± 1	28 ± 4
	275	Yes	70	27 ± 1	23 ± 4
	275	Yes	70	28 ± 1	24 ± 4
	302	No	NA	53 ± .5	47 ± 3
0.5	275	No	NA	16 ± 9	13 ± 6

NA Not available.

Table 19.—Effect of stripper temperature on citrate decomposition and absorption capacity during steam stripping

Stripper temp, °F	Operating time, h	Citrate conc,[1] g/L	SO_2 in solution, g/L	
			Loaded	Stripped
307	12	130	25.7	6.3
221 to 230	22	120	28.0	8.0
327 to 345	9	98	25.8	5.6
360	16	53	25.7	6.6

conc Concentration.

[1]Initial concentration, 144 g/L.

Citrate concentrations and solution loading presented in table 19 are final samples of each set of test conditions.

Tables 18 and 19 show that the quantity of citrate decomposed tended to increase with increased time and temperature.

SUMMARY

Laboratory investigations showed the Bureau's regenerable citrate FGD process to be capable of substantially complete removal of SO_2 from simulated industrial waste gases. In the case of H_2S regeneration, most of the SO_2 was converted to elemental sulfur. Only about 2 pct was converted to SO_4^{2-}, regardless of the SO_2 and oxygen content of the feed gas. Investigations showed that the SO_4^{2-} could be removed from the citrate solution by cooling a solution that contained at least 0.5*M* SO_4^{2-} to at least 41° F and precipitating $Na_2SO_4 \cdot 10H_2O$. The steam stripping regeneration investigations showed several technical advantages such as simplicity of operation, optional products, and reduced hazard. However, steam stripping regeneration may only be applicable to flue gases containing over 1 vol pct SO_2 because of the cost of steam. Elevated-pressure steam stripping improved the stripping efficiency. In the steam stripping regeneration process, the rate of oxidation of SO_2 to SO_4^{2-} ranged from 0.4 to 0.7 pct of the SO_2 in the waste gas.

Because of the successful laboratory studies and the ability to produce a marketable sulfur from a variety of feed gases, research on the basic citrate process was continued.

CHAPTER 3.—PILOT PLANT INVESTIGATIONS

By W. I. Nissen, L. Crocker, and D. A. Martin

BACKGROUND

The encouraging results obtained in continuous laboratory tests on simulated smelter gases justified further testing on actual smelter gases. The Bureau, in cooperation first with the Magma Copper Co. and later with the Bunker Hill Co., designed, constructed, operated, and tested citrate process pilot plants at a copper smelter and a lead smelter. In November 1970, a pilot plant to process copper reverberatory furnace gas commenced operations and testing at the San Manuel smelter in Arizona (*51-52*). Private industry showed much interest in the Bureau's work at the copper smelter and encouraged continued development. This interest led to two independent citrate process pilot plant projects. One project investigated FGD at a Pfizer, Inc., coal-fired steam-generating station near Terre Haute, IN (*10, 31, 58*). This project was completed by a private industrial group consisting of Arthur G. McKee and Co., Peabody Engineered Systems, and Pfizer, Inc. The Pfizer pilot plant processed 2,000 std ft^3/min of flue gas having an average SO_2 concentration of 1,000 ppmv and removed in excess of 95 pct of the SO_2. In another project, a Bureau cooperative agreement with the Bunker Hill Co. provided for pilot plant testing of FGD at the Bunker Hill Co.'s lead smelter in Kellogg, ID (*12, 44-47*). This chapter describes the two Bureau pilot plants and test results.

SAN MANUEL PILOT PLANT

Discussions with officials of Newmont Mining Corp. and its subsidiary Magma Copper Co. resulted in arrangements to cooperatively test the citrate process. Assembly of the plant began during the summer of 1970. The pilot plant was sized to handle up to 300 std ft^3/min of flue gas containing from 1 to 2 vol pct SO_2, which would result in a gross production of 1,000 to 2,000 lb/d. To expedite assembly of the plant, equipment on hand or immediately available from suppliers was installed. Figure 26 shows the San Manuel flowsheet, and figure 27 is a photograph of the plant. For this plant, sulfur conversion to H_2S was omitted as being premature. A 13-st load of liquid H_2S stored in a tank truck supplied the necessary H_2S for the process.

Gas Cleaning and Cooling

Initially, the plant used a package unit containing two 10-hp, high-speed fans installed in series after a venturi scrubber to draw flue gas from the waste heat boiler of the copper reverberatory furnace. This flue gas passed through a dry cyclone and the venturi scrubber where the gas was cleaned and cooled from approximately 700° F to between 104° and 122° F. Fresh water replaced a 2- to 3-gal/min scrubber bleed of the 6- to 10-gal/min recycling venturi scrubber solution for control of the cooled gas temperature, particulate loading, and pH. The pressure drop through the venturi scrubber was approximately 50 in H_2O. Under these conditions, most of the H_2SO_4 mist and essentially all of the dust were removed from the gas. Unfortunately, condensation in the fans caused severe corrosion of the cast-iron impellers and required that the venturi scrubbing unit be replaced. The venturi scrubber was replaced with another package unit incorporating a low-pressure-drop venturi (4 in H_2O), impingement scrubbing, and electrostatic precipitation. Fan corrosion was eliminated by installing a 30-hp fan on the hot side of the scrubbing unit. However, this scrubbing unit had lower removal efficiencies than did the high-pressure-drop venturi scrubber.

SO_2 Absorption

In the San Manuel plant, the cleaned and cooled gas passed upward through a 14-in-diam (1-ft^2) tower containing 1-in plastic saddles. Initially, the tower was constructed of clear plastic with space for a 12-ft packing height. Later, the packing height was increased to 28 ft by adding two 8-ft-long polyvinyl chloride (PVC) sections. A demister pad at the top of the tower removed solution droplets from the exhaust gas. Regenerated and clarified solution sprayed on top of the packing percolated down through the packing, absorbed SO_2 from the flue gas, and accumulated in a sump. SO_2-loaded solution in the sump flowed by gravity to a 200-gal reactor feed tank. Pressure drops were 3 and 7.5 in H_2O, respectively, with 12 ft and 28 ft of packing, at a gas flow of 200 std ft^3/min and a solution flow of 5 gal/min.

Solution Regeneration and Sulfur Precipitation

Solution regeneration and sulfur precipitation reactions with pure H_2S occurred in a closed, agitated, and baffled 70-gal stainless-steel tank. A 6-in-diam radial turbine impeller, rotating at from 800 to 1,200 r/min, mixed the loaded solution and H_2S gas. Loaded solution was pumped from the reactor feed tank to the reactor through a flowmeter. Liquid H_2S stored in the tank truck at 250 lbf/in^2(ga) was vaporized in a heat exchanger and reduced in pressure to about 30 lbf/in^2(ga). This H_2S gas then passed through an automatic control valve that maintained a pressure of H_2S above the slurry in the reactor at from 4 to 30 in H_2O. H_2S flowed into the reactor through an open pipe underneath the impeller. The gas flow was measured with a flowmeter. Retention time of the slurry in the reactor ranged from 5 to 15 min, depending upon the solution flow rate.

Sulfur Separation and Solution Recovery

The slurry of sulfur and regenerated solution flowed from the reactor tank through a liquid gas trap to a 200-gal gently agitated holding tank where complete flocculation of the sulfur occurred. From the holding tank, the slurry flowed by gravity to a 54-in-diam by 40-in-deep thickener

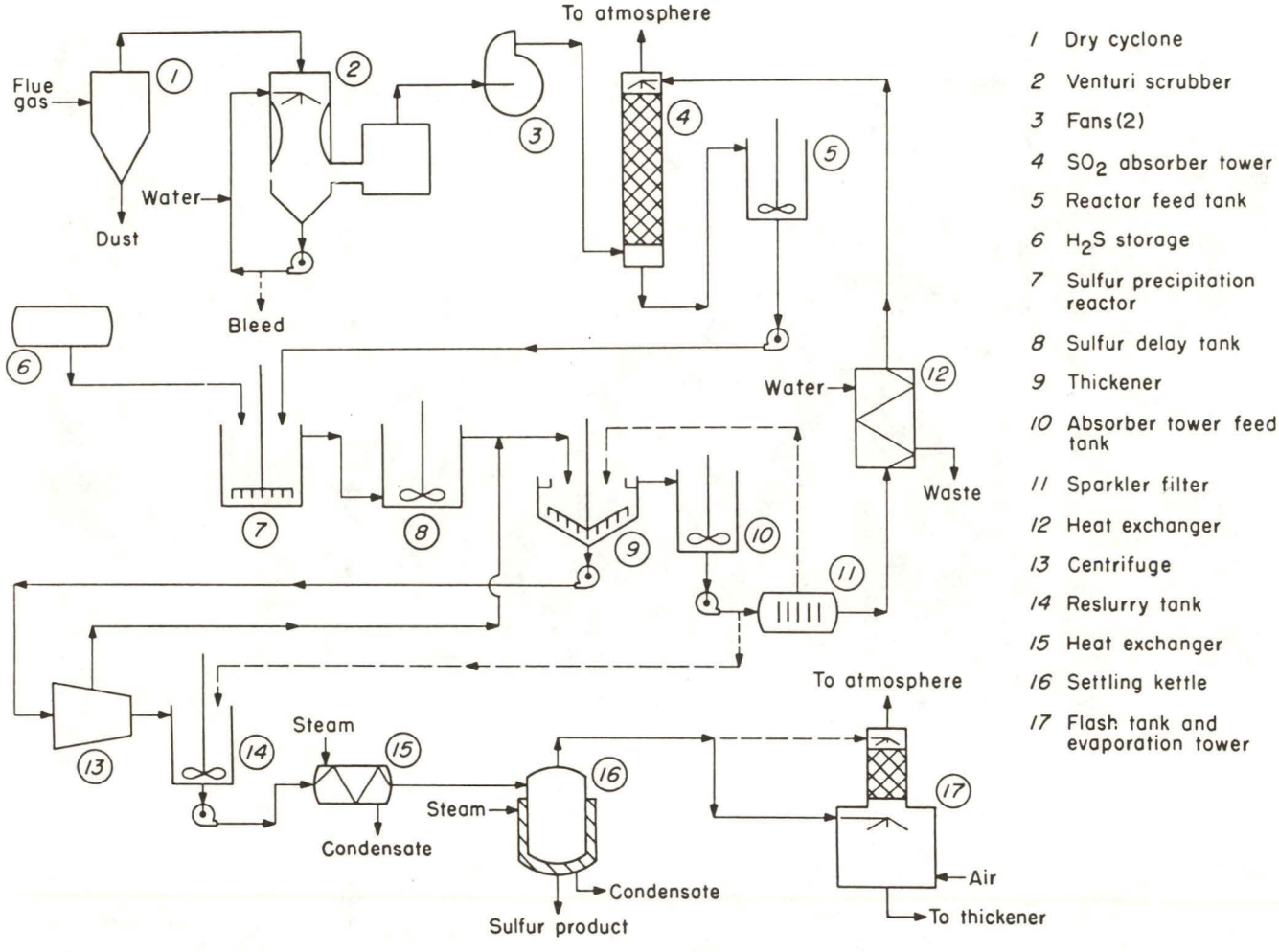


Figure 26.—San Manuel pilot plant flowsheet.

where most of the sulfur settled. The underflow from the thickener was pumped to a 6-in-diam solid bowl centrifuge that increased the solids content from 5 pct to between 40 and 60 pct. The centrifuge cake discharged to a holding tank while the filtrate returned to the thickener. Solution overflowing the thickener contained some flocs of sulfur. This solution flowed first to the absorption tower feed tank and then was pumped through a filter before flowing to the spray nozzle at the top of the absorption tower. An in-line, water-cooled heat exchanger cooled the recycled solution when required.

The centrifuge sulfur cake was repulped with regenerated solution to a consistency of about 20 pct solids, which could be moved with a Moyno positive-displacement auger-type pump through a steam-heated shell-and-tube heat exchanger where the sulfur slurry temperature was raised to about 275° F. The molten mixture of sulfur and solution flowed to a steam-jacketed, glass-lined settling kettle of about 20-gal capacity where molten sulfur settled and was intermittently withdrawn through an automatic level control valve. Molten sulfur from the settling kettle was cooled in steel pans holding about 200 lb. Solution free of sulfur was continuously discharged from the top of the kettle through a pressure-regulating valve set at about 35 lbf/in^2(ga). The hot solution flowing from the kettle was cooled and partially evaporated in an air-swept tank. The cool solution flowed by gravity to the absorption tower feed tank.

Instrumentation and Control

Except for the addition of H_2S and removal of sulfur from the settling kettle, pilot plant operations were controlled manually. Continuous analyzers sampled, analyzed, and recorded the SO_2 and O_2 concentrations of the feed gas. An analyzer, developed in the laboratory (*5*), sampled and analyzed the SO_2 in the exhaust gas. An orifice meter was used to measure the flue gas flow. The pH of the regenerated solution and the loaded solution were continuously measured and recorded. Temperatures of solutions and gases were continuously recorded. Regenerated solution, sulfur slurry, and gas flows were manually controlled. A small on-site laboratory was equipped for rapid analysis of SO_2 and citrate in the solutions.

Test Results

During the operation, frequent mechanical failures made it impossible to achieve sustained, around-the-clock operation and required one shutdown of 2 months while awaiting delivery of replacement gas cooling and cleaning equipment. Despite these difficulties, pilot plant testing

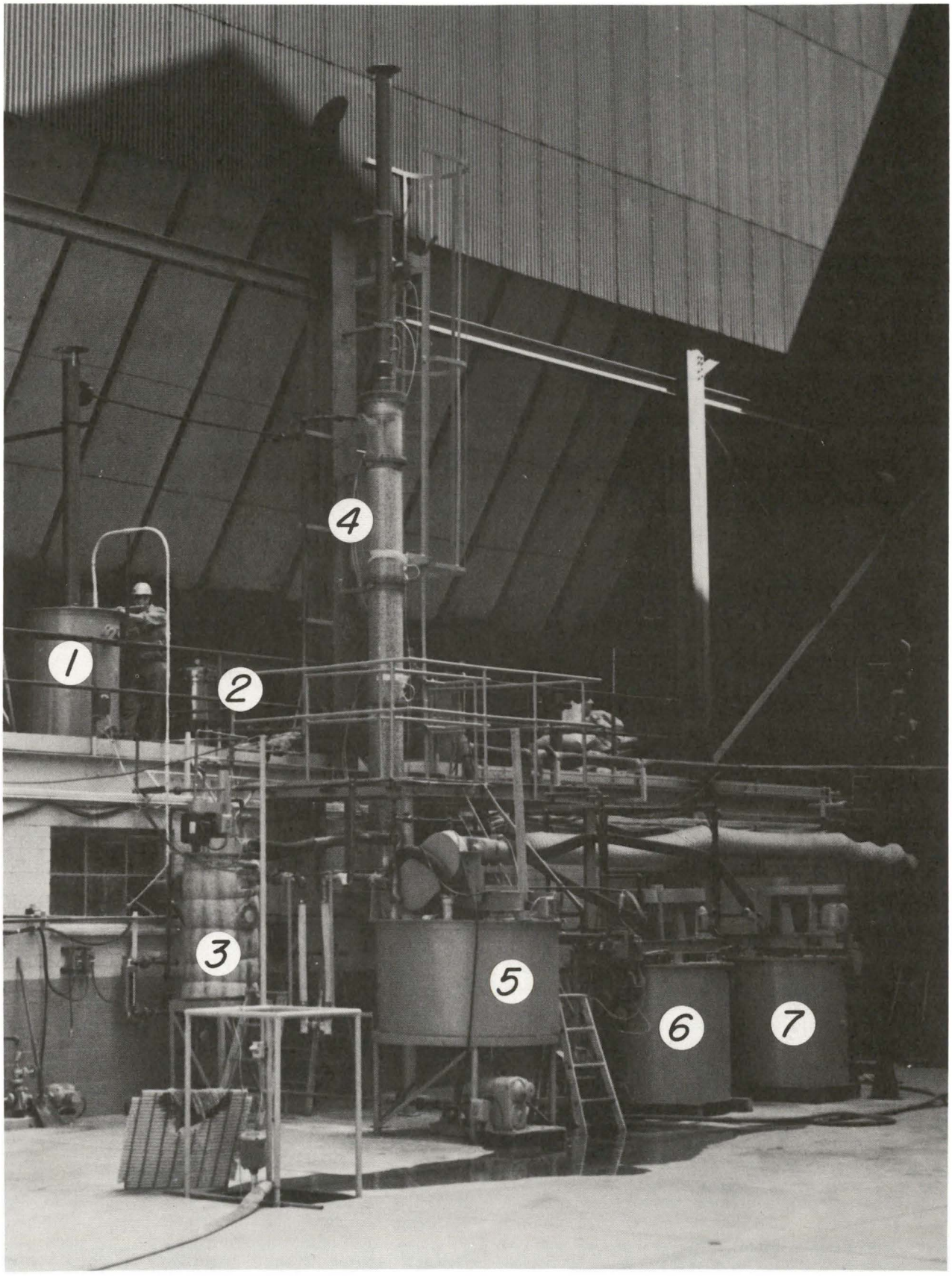


Figure 27.—Pilot plant at San Manuel. *1*, Flash tank and evaporation tower; *2*, sparkler filter; *3*, sulfur precipitation reactor; *4*, SO_2 absorber tower; *5*, thickener; *6*, absorber tower feed tank; *7*, reactor feed tank.

demonstrated (1) the citrate process will readily remove and recover 90 to 99 pct of the sulfur contained as SO_2 in copper reverberatory furnace flue gas, (2) the regeneration of solution and precipitation of sulfur with H_2S is easily controlled and highly efficient, and (3) the precipitated sulfur can be continuously recovered as a high-quality product by a combination of thickening, centrifuging, and melting.

Table 20 summarizes results obtained during separate tests, each involving from 10 to 40 h of reasonably steady-state continuous operation at gas flow rates of 90 to 300 std ft^3/min and SO_2 concentrations of 1.07 to 1.66 vol pct. Feed gas temperatures ranged from 108° to 126° F and the pH of the regenerated solution from 3.1 to 3.8.

These test results show comparable SO_2 removal efficiencies under a variety of operating conditions. However, increased pH and tower packing height improved SO_2 loading. Although the data presented were selected, the SO_2 removal efficiency for the entire test program averaged over 90 pct and rarely fell below 80 pct. Generally, when the recovery was less than 90 pct, the poor removal of SO_2 could be correlated with low pH of the regenerated solution, high gas and solution temperatures, or inadequate flow of solution for the amount of SO_2 in the flue gas. Occasionally, low SO_2 recovery stemmed from incomplete regeneration of the solution because of a deficiency of H_2S.

BUNKER HILL PILOT PLANT

At the Bunker Hill Co.'s smelter, lead concentrates were sintered in a Lurgi updraft sintering machine. Strong and weak SO_2 gases were emitted from the sintering operation. The strong gas from the feed end of the sintering machine, containing from 4 to 5 vol pct SO_2, was sent to a contact H_2SO_4 plant for SO_2 recovery. The weak tail gas containing from 0.5 to 1 vol pct SO_2 was filtered in a baghouse and vented through a stack to the atmosphere. In an effort to improve air quality, the Bunker Hill Co. expressed interest in testing the citrate process on the sintering machine tail gas. At the same time, the Bureau needed an industrial cooperator to further develop the citrate process. On October 2, 1972, the Bunker Hill Co. and the Bureau executed a cooperative agreement to pilot-test the citrate process at the Bunker Hill lead smelter.

Design and Construction

Bureau engineers and contractors designed the Bunker Hill pilot plant based on the 300-std ft^3/min San Manuel pilot plant and on laboratory investigations. Contracts to design, fabricate, and install the plant were awarded to Morrison-Knudsen Co., Inc., Boise, ID. Home Oil Co., Ltd., of Canada, a major subcontractor, designed the H_2S generator section. Engineers designed this plant to treat 1,000 to 1,500 std ft^3/min of 0.5 vol pct SO_2 from either one of two possible sources—either acid plant feed gas diluted with air approximately eightfold to simulate the weak tail gas or actual weak gas from the lead smelter sintering machine, which was reported to be about 0.9 vol pct SO_2.

Generally, the plant was constructed of materials known to resist the corrosive effects of SO_2-loaded gas and liquid streams. Fiberglass-reinforced polyester (FRP), PVC, or bitumen-lined carbon steel were used to fabricate process piping and vessels where temperature permitted. Type 316 stainless steel was used where high temperature or structural strength were factors. Carbon steel was used where the gas temperatures were above the H_2SO_4 dewpoint. The H_2S generator process piping and vessels were all fabricated from suitable stainless steels because of high temperature and corrosive effects of feedstock and products.

The Bureau contracted for the construction of the Bunker Hill pilot plant in three phases:

Phase 1. SO_2 absorption, solution regeneration, and sulfur recovery section.

Phase 2. H_2S generator section.

Phase 3. Flue gas cooling and cleaning section.

The contractor constructed phase 1 of the project between March and December 1973, and acceptance testing began in January 1974. The plant operated on H_2S from a 13-st-capacity tank trailer during construction and operational checkout of the H_2S generator section. Construction of phase 2 was started in December 1973, and after some design modifications, the H_2S generator was ready for acceptance testing in April 1975. Phase 3 of the plant was constructed during 1974. Starting in January 1975, this section supplied a cool and clean weak gas from the lead sintering machine to the absorber. By the end of April 1975, the completed plant was in operation and the tank trailer of H_2S was no longer needed.

Pilot-Plant Description and Operation

The block diagram in figure 28 shows the process for the complete pilot plant. From the plant's initial operation in January 1974 until completion of testing in May 1976, the pilot plant logged over 5,400 h and produced about 55 net short tons of sulfur. During that time, the H_2S generator produced H_2S gas for the citrate process for 3,090 h. The gas cooling and cleaning section was operated as needed to test the respective components and to provide cool, clean, humidified gas to the SO_2 absorption section.

Gas Cooling and Cleaning

The SO_2 absorption, solution regeneration, and sulfur recovery section of the pilot plant (fig. 29) operated for about 1 yr starting in January 1974. A precleaned H_2SO_4 plant feed gas was diluted with air to about an 8:1 ratio to obtain the required 0.5 vol pct SO_2 feed gas for which the plant was designed. After installation and acceptance of the gas cooling and cleaning section, shown in figures

Table 20.—SO_2 removal results for San Manuel pilot plant

Packing height, ft	Gas flow rate, ft^3/min	SO_2 in feed gas, vol pct	Citrate solution			SO_2 in offgas, ppmv	SO_2 absorption, pct
			pH	Flow rate, gal/min	SO_2 loading, g/L		
12	90	1.46	3.1	5	5.3	725	95.2
	100	1.48	3.3	5	4.5	890	92.6
28	150	1.66	3.6	5	10.0	85	99.5
	210	1.09	3.8	3	16.2	135	98.7
	300	1.07	3.6	5	14.1	700	93.5

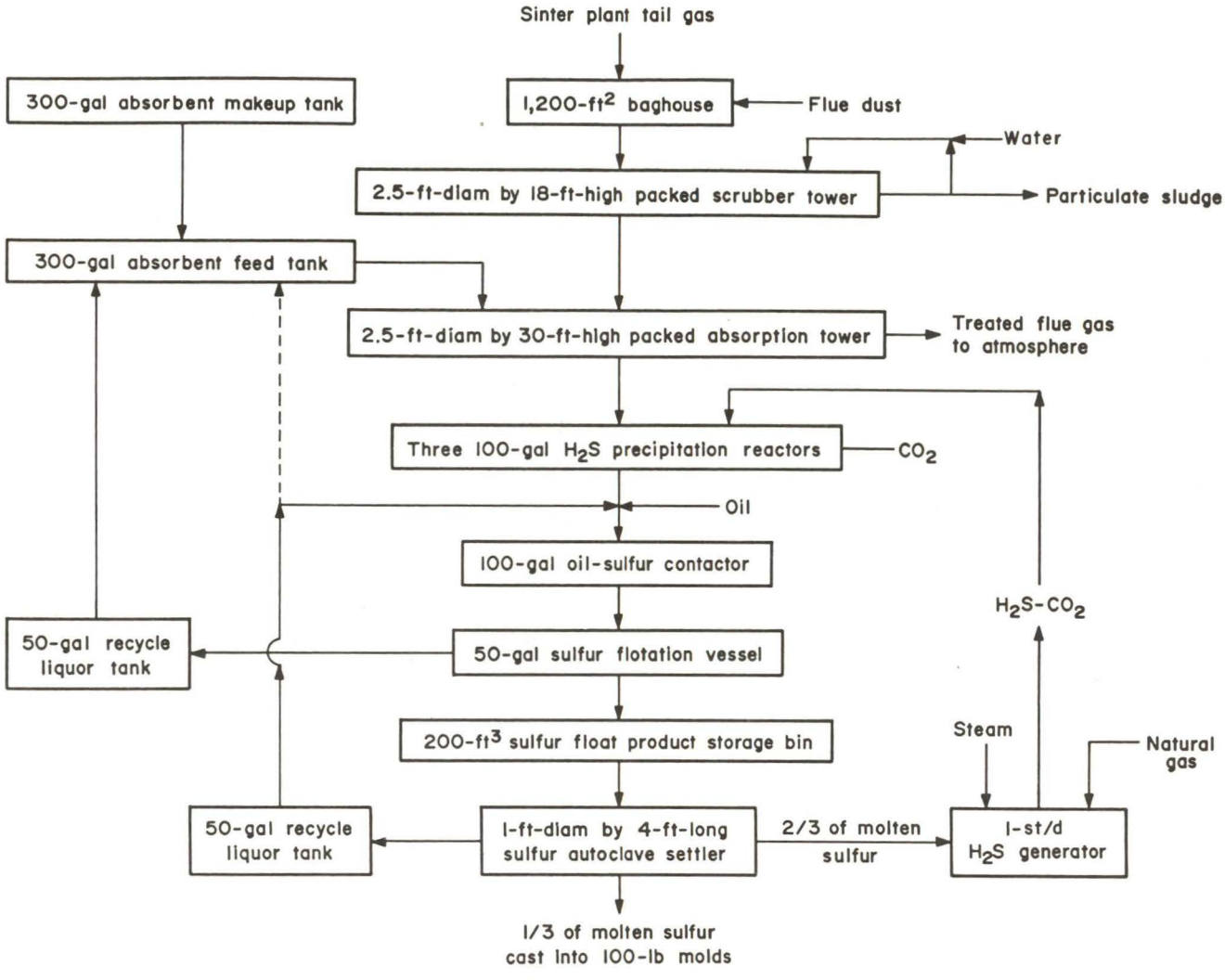


Figure 28.—Bunker Hill pilot plant flowsheet.

30 and 31, the source of the pilot plant feed gas was switched to the weak gas from the Bunker Hill Co.'s lead smelter sintering machine. An induced draft fan moved the weak gas through the gas cooling and cleaning section and into the SO_2 absorber. A valve located at the main weak gas duct controlled the weak gas flow. Weak gas was drawn from the main duct through a 150-ft, 10-in-diam insulated carbon steel pipeline to the first unit in the pilot plant, a 3.5-ft-diam by 24-ft-high dust knockout tank. This tank was originally intended to cool and condition the weak gas with a water spray for subsequent H_2SO_4 mist removal. However, the weak gas temperature averaged only 266° F. As a result, heat losses from the weak gas pipeline and dust knockout tank required heating of the weak gas to prevent acid mist condensation and corrosion of carbon steel equipment. A gas-fired preheater was installed in a branch pipeline to heat the weak gas before the gas entered the dust knockout tank. The weak gas also proved to be higher in SO_2 than was reported and more variable in concentration; thus, to achieve an average 0.5 vol pct SO_2 feed gas for the pilot plant required dilution of the weak gas with air and combustion gas.

Following the dust knockout tank, a carbon steel baghouse containing 1,200 ft^2 of Orlon acrylic fiber bags removed 99.6 pct of the particulates from an inlet gas containing 65 mg/ft^3. The gas-fired preheater automatically controlled the baghouse inlet temperature at about 239° F. A pulsed air jet periodically cleaned the bags. Subsequently, dust was removed from the baghouse. Next, a 2.5-ft-diam by 18-ft-high prescrubber tower constructed of FRP and packed with a 6-ft-high bed of 1-in polypropylene saddles scrubbed 95 pct of the remaining dust in the gas. The resulting exit gas from the prescrubber contained about 0.013 mg/ft^3 particulates. Also, the prescrubber removed about 91 pct of the SO_3 from the prescrubber inlet gas, which contained 0.23 mg/ft^3 SO_3. Recycled prescrubber solution flowed at 25 gal/min. A small purge flow of about 0.2 gal/min was maintained to keep the prescrubber solution pH about 1.5 and avoid solids buildup. A level controlled solenoid valve operated to replace the purge flow with plant water. The purge flow joined other lime-neutralized smelter acid plant wastes for disposal.

Finally, to control the temperature of the SO_2 absorption tower for testing and process evaluation, it was necessary to humidify and heat the gas after leaving the prescrubber. This was done by adding steam directly and then passing the gas through a shell-and-tube heat exchanger. This ability to humidify and heat the gas permitted evaporation and temperature control in the SO_2 absorption tower.

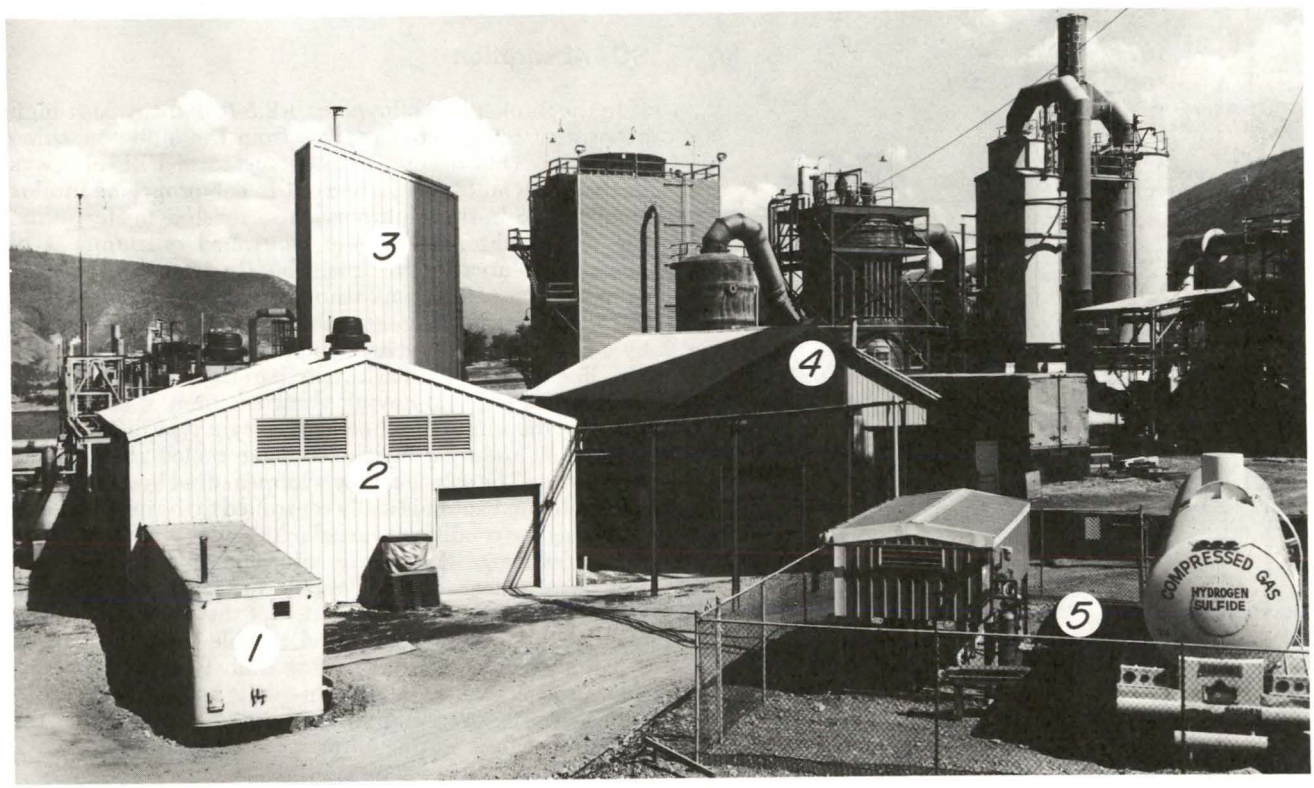


Figure 29.—Overview of Bunker Hill pilot plant from west. *1*, Trailer housing laboratory and control room; *2*, citrate plant building; *3*, cupola containing absorber tower; *4*, shop and storage building; *5*, H_2S vaporizer shed and supply tank.

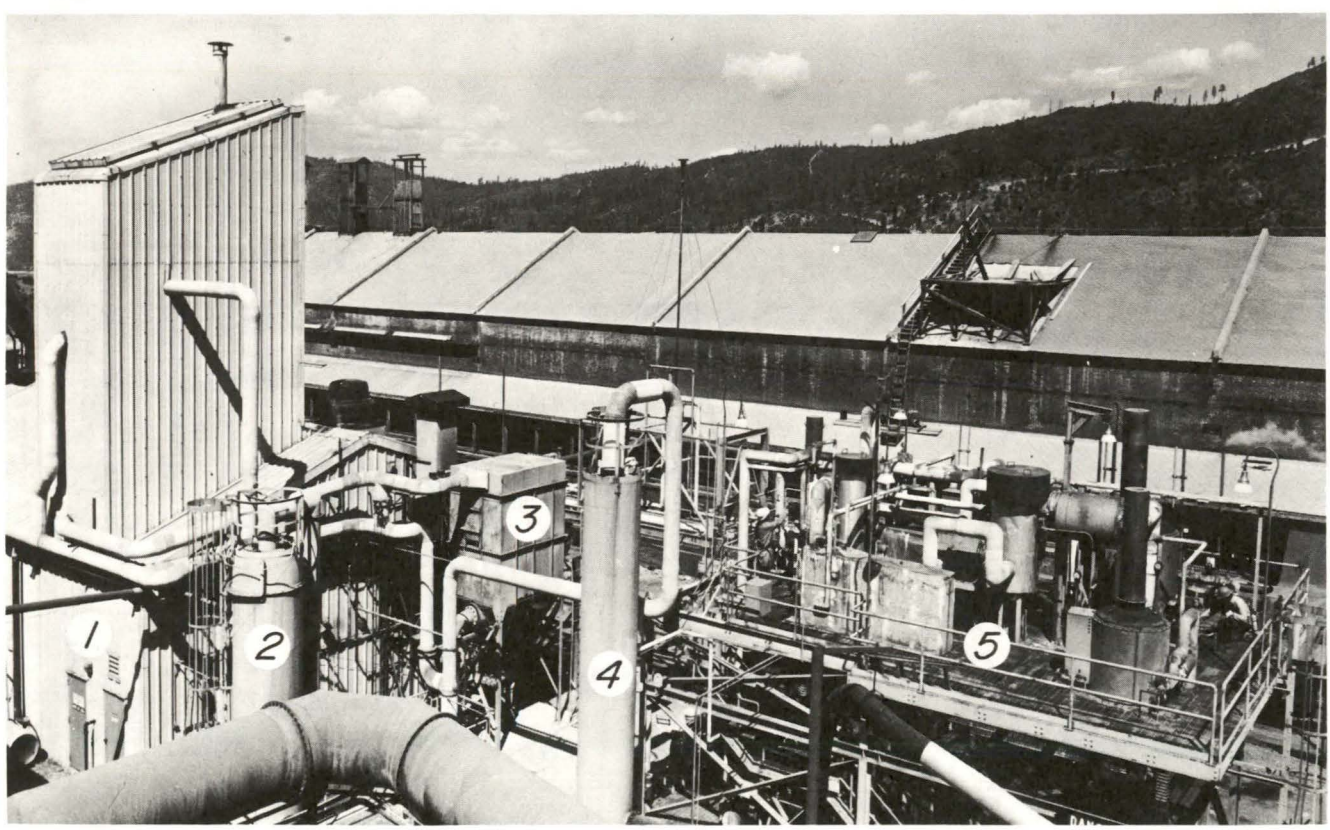


Figure 30.—Overview of Bunker Hill pilot plant from southeast. *1*, Citrate plant building; *2*, electrostatic precipitator; *3*, baghouse; *4*, dust knockout tank; *5*, H_2S generator.

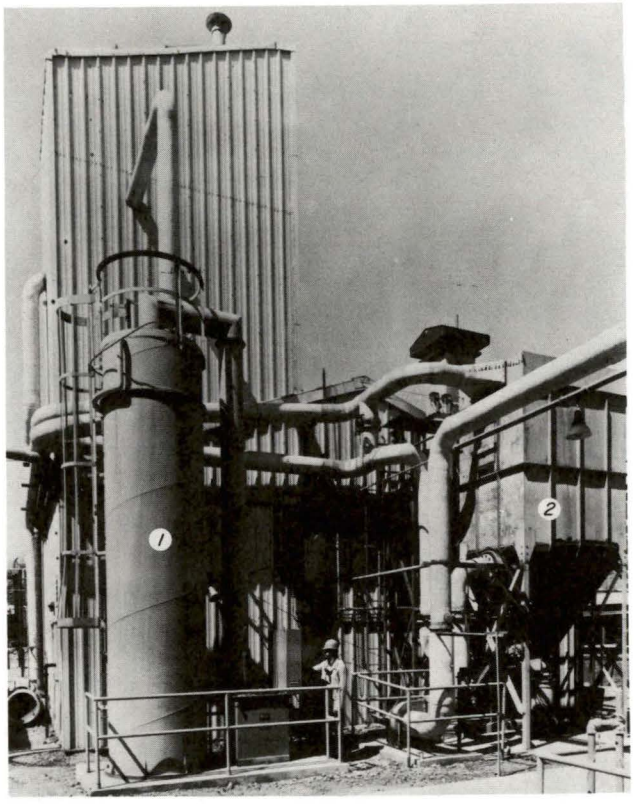


Figure 31.—Gas cooling and cleaning section (Bunker Hill pilot plant). *1*, Electrostatic precipitator; *2*, baghouse.

SO_2 Absorption

In the Bunker Hill pilot plant, a 2.5-ft-diam by 30-ft-high absorption tower removed SO_2 from the sinter machine weak gas. This tower was constructed of FRP and was packed with an 18-ft-high bed of 1-in polypropylene Intalox saddles. A 6-in-thick stainless steel mesh demister in the top of the absorption tower controlled entrainment of absorber solution in the gas. The absorber solution was pumped from a feed tank through clarification filters (fig. 32) and a heat exchanger to a distributor above the packing by a sealless magnetic drive pump, at rates ranging from 5 to 15 gal/min. Dual-backwash, porous type 316 stainless steel filters (fig. 32) having a surface area of about 6 ft^2 clarified the solution. When necessary, a type 316 stainless steel shell-and-tube heat exchanger cooled the solution with water. The solution flow was measured by a float-type flowmeter and automatically controlled to the desired flow.

Among the conditions varied in the pilot plant tests were concentration of the citrate solution, solution flow rate, feed gas SO_2 concentration and flow rate, and feed gas and solution temperatures. Operation of the absorption tower was generally satisfactory and trouble-free. The normal amount of sulfur carryover (less than 1 pct of the sulfur float product) was handled by periodic backwashing of the filters. The backwash sulfur slurry was returned to the conditioner tank in the sulfur recovery section.

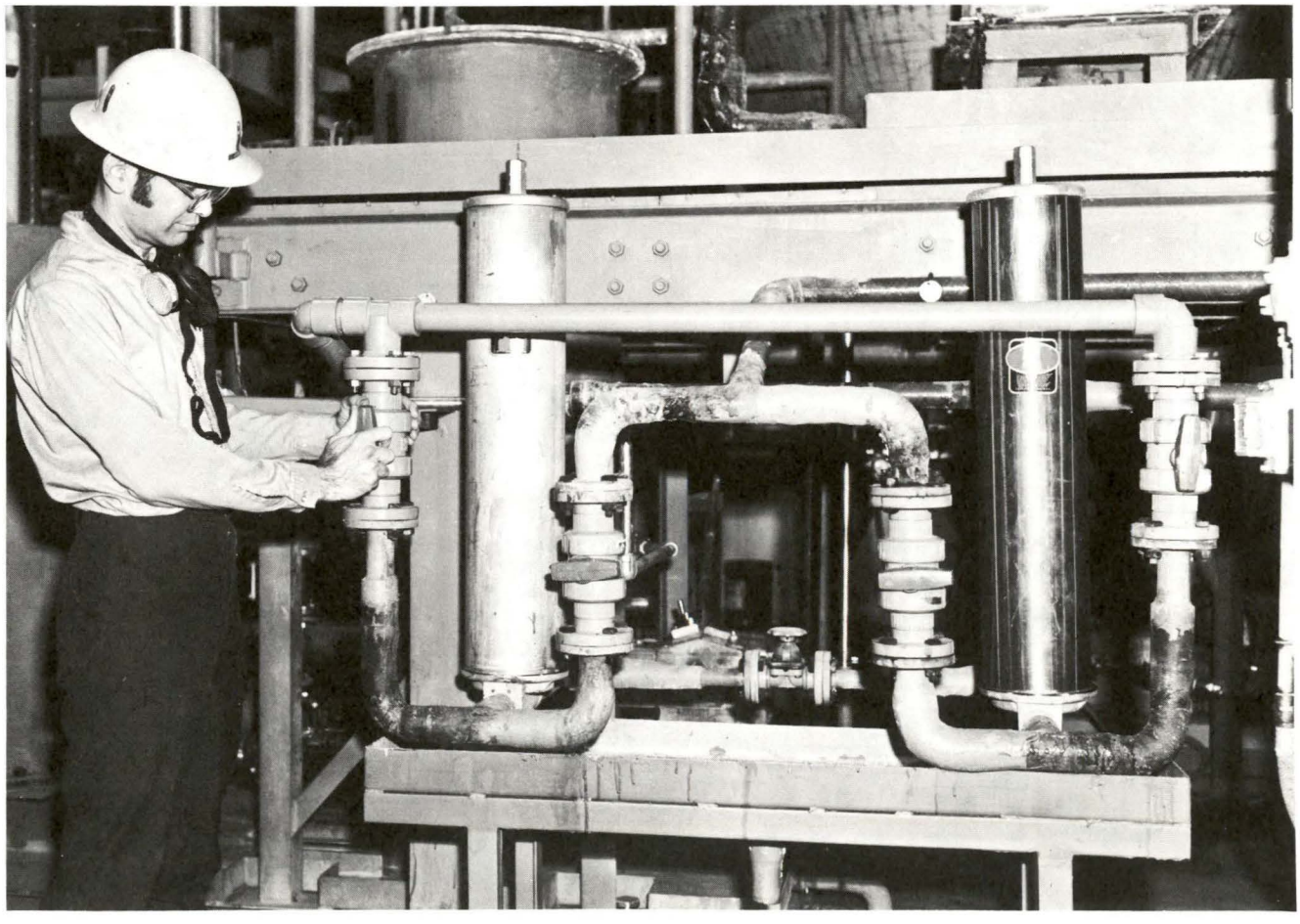


Figure 32.—Citrate solution clarification filters (Bunker Hill pilot plant).

SO_2 Absorption Results

Initially, the phase 1 section of the plant was operated to determine optimum conditions for SO_2 absorption. Table 21 shows the effect of citrate solution concentration, absorption temperature, and solution and gas flow rates on the SO_2 removal efficiency during the phase 1 operation in which diluted acid plant feed gas was treated and the H_2S for regeneration was supplied from the tank trailer. The SO_2 removal efficiencies were based on feed and offgas analyses. These tests were made using pure H_2S to regenerate the solution in a single 100-gal reactor operating at an agitator speed of 220 r/min and a temperature of about 149° F. Citrate solution concentrations of 0.25*M* and 0.5*M* were tested. Investigators varied the absorption temperature from 95° to 147° F, the solution flow rates from 5 to 10 gal/min, and the gas flow rates from 1,000 to 1,500 std ft^3/min. The range of values for concentration of SO_2 were from 0.30 to 0.54 vol pct, the regenerated solution pH ranged from 4.2 to 4.7, and the solution loadings were from 6.3 to 21.3 g/L SO_2. These loadings represent from 50 to 95 pct of the equilibrium loading values, which are shown in figures 5 and 6 (chapter 2). Only in tests where the absorption temperature was 147° F or the solution flow was 5 gal/min did the absorption efficiency decrease to any extent. The design SO_2 loading for the pilot plant was 10.8 g/L SO_2 when treating 1,000 std ft^3/min of 0.5 vol pct SO_2 gas with 10 gal/min of 0.5*M* citrate solution at a temperature of 113° F. This design loading represents about 60 pct of the equilibrium loading. The test that came closest to the design in loading and conditions resulted in a 99.4-pct SO_2 removal efficiency.

Although the pilot plant was designed to test SO_2 feed gases in the 0.5 vol pct SO_2 range, a few tests were run with SO_2 feed gas concentrations of 0.10 vol pct or less. With reference to SO_2 content, such a gas might be typical of the flue gas from a coal-burning powerplant firing medium-sulfur-content coal (1 to 2 pct S). Table 22 shows the effect of low-SO_2 feed gas compared with results using a higher SO_2 feed gas. All tests in table 22 used 78 dry vol pct H_2S gas from the H_2S generator to regenerate the solution in two 100-gal reactors operating at an agitator speed of 220 r/min and a temperature of about 149° F. The citrate solution concentration was between 0.4*M* and 0.5*M*. The most significant results of these tests were an SO_2 loading of 4.1 g/L SO_2, which represents 83 pct of the equilibrium loading value, and an SO_2 removal efficiency of 95 pct. The results in table 22 suggest that the process may be applicable to flue gases from coal-fired powerplants.

Table 23 shows the effect of H_2S excess on the SO_2 removal efficiency and pH of the regenerated solution. The H_2S excess plus the stoichiometric H_2S was fed to the solution regeneration section. Although this excess was lost to the incinerator, it raised the partial pressure of H_2S in the reactors.

Tests reported in table 23 were made using 78 dry vol pct H_2S gas from the H_2S generator to regenerate the solution in either two or three 100-gal reactors operating at an agitator speed of 220 r/min and a temperature of about 149° F. A solution flow of 10 gal/min was used, and the solution concentration ranged from 0.45*M* to 0.6*M* citrate. The absorption temperature was between 93° and 97° F. The flow rate of the feed gas was about 1,100 std ft^3/min.

Table 21.—Effect of citrate solution concentration, absorption temperature, and solution and gas flow rates on SO_2 removal efficiency at Bunker Hill pilot plant

Feed gas		Citrate solution		Absorption temperature, ° F	SO_2 in offgas, ppmv	SO_2 removal efficiency, pct
SO_2, vol pct	Flow rate, std ft^3/min	Flow rate, gal/min	SO_2 loading, g/L			
EFFECT OF GAS FLOW RATE AT 0.25*M*						
0.32	1,000	10	6.3	97	51	98.4
.30	1,500	10	9	99	57	98.1
EFFECT OF GAS FLOW RATE AND TEMPERATURE AT 0.5*M*						
0.46	1,200	10	11.5	104	41	99.1
.42	1,000	10	8.9	102	33	99.2
.47	1,000	10	9.8	113	28	99.4
.47	1,000	10	10.1	131	52	98.9
.37	1,000	10	7.5	147	163	95.6
EFFECT OF SOLUTION FLOW RATE AT 0.5*M*						
0.44	1,000	8	12	97	110	97.5
.47	1,000	7	14.5	99	103	97.8
.54	1,000	5	21.3	95	405	92.5

Table 22.—Comparison of SO_2 removal efficiency from feed gases containing about 0.1 versus about 0.5 vol pct SO_2

Feed gas		Citrate solution			Absorption temperature, ° F	SO_2 in offgas, ppmv	SO_2 removal efficiency, pct
SO_2, vol pct	Flow rate, std ft^3/min	Flow rate, gal/min	SO loading,$_2$ g/L	Regenerated pH			
0.09	1,000	7.5	2.4	4.8	99	1	99.9
.12	1,300	7.5	4.1	4.9	135	60	95
.46	1,000	10	9.6	4.3	97	110	98.6

Table 23.—Effect of excess H_2S on SO_2 removal efficiency and pH of regenerated solution

Feed gas		Citrate solution		Regeneration reactor H_2S excess,[1] pct	SO_2 removal efficiency, pct
Type	SO_2, vol pct	Loading, g/L SO_2	Regenerated pH		
Sintering machine weak gas	0.38	9.0	4.3	15.1	98.4
Simulated weak gas[2]	.31	7.3	4.1	6.1	97.4
	.44	10.3	4.1	2.5	94

[1] H_2S excess plus stoichiometric H_2S was fed to solution regeneration section.
[2] Commercial SO_2 gas diluted to simulate sintering machine weak gas.

SO_2 Absorption Rates

Scientists and engineers often use the overall mass transfer coefficient, K_Ga, to express gas absorption rates (*14*). The K_Ga value for the absorption of SO_2 in citrate solution may be used to design gas absorption equipment of different sizes to do the same job. The coefficients are given as pound-moles of SO_2 absorbed per hour, per volume of absorber packing, per atmosphere of driving force, and are corrected for atmospheric pressure. Table 24 shows a few mass transfer coefficients for tests at the Bunker Hill pilot plant.

The first requirement for calculating K_Ga is an equilibrium SO_2-loading curve for the temperature, pressure, and solution concentration being used. Figures 5 and 6 (chapter 2) show these curves. Interpolation and pressure correction are necessary if the conditions of the test vary from conditions for which the curves are made.

For the K_Ga values given in table 24, the citrate solution concentrations were 0.5*M* citric acid, 1.0*M* NaOH, and about 0.25*M* $S_2O_3^{2-}$. As stated previously, the absorption tower packing height was 18 ft. The absorption tower cross-sectional area was 4.91 ft^2. The atmospheric pressure at the Bunker Hill pilot plant was 0.92 atm. For all the examples given in table 24, the gas flowed at about 1,000 std ft^3/min.

The formula for calculation of K_Ga is

$$K_Ga = \frac{N}{HA \ln \text{mean } \Delta p},$$

where N = SO_2 absorbed, lb mol/h,
H = tower packing height, ft,
A = tower packing cross-sectional area, ft^2,

and

$$\ln \text{mean } \Delta p = \frac{(\Delta p_1 - \Delta p_2)P}{\ln (\Delta p_1/\Delta p_2)} = \text{driving force, atm,}$$

where $\Delta p_1 = Y_1 - Ye_1$ = SO_2 pressure at bottom of tower, atm,
$\Delta p_2 = Y_2 - Ye_2$ = SO_2 pressure at top of tower, atm,
and P = pressure correction factor, atmospheric pressure at test conditions divided by atmospheric pressure at sea level.

The values Δp_1 and Δp_2 are driving force factors, that is, the difference between actual SO_2 concentration, Y_1, in the gas and the concentration at equilibrium, Ye_1 (for the tower bottom) and $Y_2 - Ye_2$ (for the tower top). Units used are atmospheres partial pressure of SO_2. Usually, Ye_2 is assumed to be zero since the solution going back to the tower top is completely regenerated.

In table 24, the average K_Ga was 10.1 for the citrate system at Bunker Hill.

Solution Regeneration

The H_2S precipitation solution regeneration section is shown in figure 33. It consisted of three 100-gal, baffled, type 316 stainless steel reactors. Each was stirred with a 17.5-in-diam, six-blade radial turbine-type impeller. These variable-speed agitators were capable of 230 r/min and a tip speed of 1,050 ft/min.

The first reactor was fed by gravity through a variable-level control and siphon breaker from the absorption tower bottom. Sulfur slurry flowed by gravity through the three-reactor cascade. The H_2S could be fed into any of the three reactors countercurrent to the flow of slurry and was introduced under the reactor impeller through an open 3-in pipe. A steam jacket on the first reactor provided for temperature control. The other reactors were insulated to conserve heat.

When one reactor and pure H_2S from the tank trailer were used, H_2S was supplied on a demand basis. That is, the H_2S supply system was automatically controlled to maintain 0.5 lbf/in^2(ga) of H_2S pressure over the solution. This mode of operation did not waste H_2S. However, at startup, it was necessary to vent the reactor to displace the air from the system to an H_2S incinerator.

When H_2S generator product (78 pct H_2S) was used, the H_2S requirement was determined by following the degree of solution regeneration and analyzing the reactor offgas for H_2S. During operation, it was necessary to vent the reactor to displace the CO_2 and unreacted H_2S from the system to the H_2S incinerator.

Table 25 presents some typical regeneration data with citrate scrubbing solutions. Agitation was the same in all tests, 1,050 ft/min impeller tip speed. The SO_2 loadings are concentrations in the reactor feed, not steady-state SO_2 concentrations in the reactors. The final reactor effluent solutions averaged less than 0.5 g/L SO_2. The pH of the

Table 24.—Overall mass transfer coefficient (K_Ga) for SO_2 absorption at Bunker Hill pilot plant

Solution flow rate, gal/min	Absorption temperature, °F	Gas analysis, vol pct SO_2		Solution analysis, g/L SO_2		Driving force (1n mean Δp), 10^{-4} atm	Molecular weight absorbed (N), lb mol/h SO_2	Mass transfer coefficient (K_Ga)[1]
		Feed	Stack	Lean	Rich			
10	95	0.22	0.0030	0.2	4.9	4.3	0.37	9.7
10	95	.53	.0066	.0	11.1	8.6	.87	11.4
13	113	.41	.0060	.0	6.6	8.3	.67	9.1

[1] Pound-moles of SO_2 absorbed per hour per cubic foot of absorber packing per atmosphere of driving force.

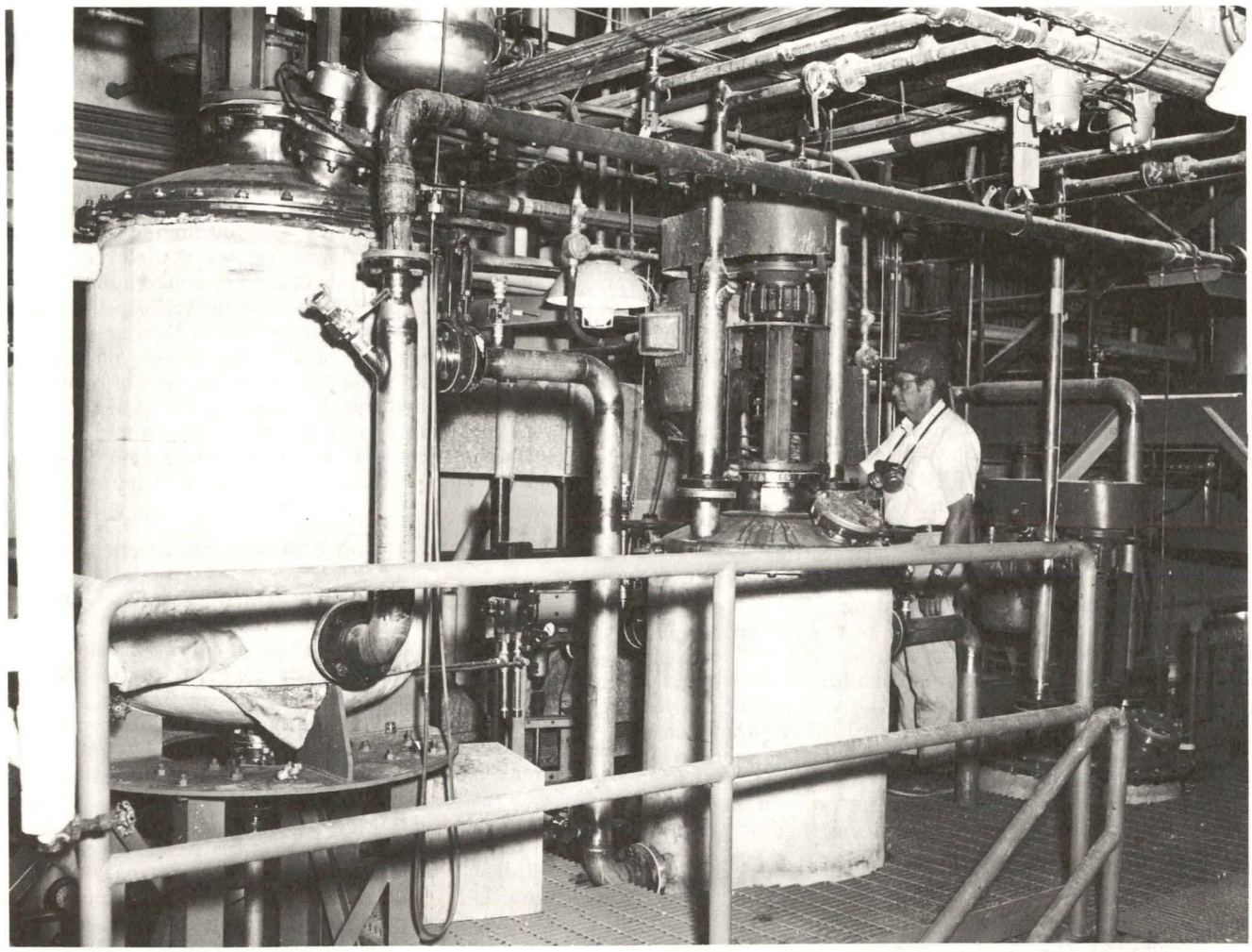


Figure 33.—Solution regeneration reactors (Bunker Hill pilot plant).

Table 25.—Regeneration data for SO_2-loaded citrate solutions at Bunker Hill pilot plant

SO_2 loading, g/L	Reactors in use	Feed rate, gal/min	Av retention time, min	H_2S in feed gas, dry vol pct	H_2S excess, pct	SO_2 reduction rate	
						lb/h	lb/(h·gal)
10.2	1	8.3	12	100	0	41	0.41
15.6	1	7.1	14	100	0	55	.55
21.3	1	5.0	20	100	0	53	.53
11.0	2	10.0	20	78	9	55	.27

loaded solutions in these tests averaged 4.4. These solutions also contained 0.25*M* $Na_2S_2O_3$.

The data indicate that 100 gal of reactor volume is sufficient to treat 50 lb/h SO_2 with pure H_2S. With 78 pct H_2S, a 200-gal reactor volume was required.

From the operational standpoint, one problem involved the presence of dissolved H_2S and some colloidal sulfur in the regenerated solution. The H_2S would evolve from solution in the sulfur flotation cell and contaminate the air. The colloidal sulfur could not be removed by flotation. Injecting about 5 pct of the SO_2-loaded solution from the absorption tower into the conditioner tank solved this problem. This technique eliminated the excess H_2S and dissolved the colloidal sulfur.

Sulfur Separation and Solution Recovery

After leaving the reactors, the regenerated solution containing about 1.5 pct S overflowed to a 50-gal, stirred, type 316 stainless steel conditioner feed tank. From this tank the sulfur slurry, at a temperature of about 127° F, was pumped to a 100-gal FRP conditioner tank. The conditioner tank was stirred by a variable-speed agitator equipped with two 16-in-diam axial impellers. The lower impeller mixed the hydrocarbon flotation reagent kerosene and the upper impeller, located just below the surface, broke up the accumulations of floating sulfur. The mixture of floating sulfur and regenerated solution overflowed through a 3-in-ID sloping line to the sulfur flotation vessel. An agitator tip speed of 700 ft/min was sufficient for good sulfur flotation.

By design, 6 to 12 g/min kerosene were added to the conditioner by a chemical feed pump. This quantity of kerosene amounted to about 1 to 2 pct of the gross sulfur production. The average sulfur content of the float product was 48 pct solids under these conditions. Later, the

kerosene addition point was changed from the bottom of the conditioner tank to a point just above the overflow line. At the same time the kerosene feed pump was replaced with a smaller pump. These changes improved kerosene dispersion. Only about 0.2 pct of the gross sulfur production was needed. The percent solids of the float product was the same when the new addition point and less kerosene were used.

The sulfur flotation vessel was a 50-gal-capaciity, rectangular, type 316 stainless steel tank, with a bottom outlet and an inclined chute with a drag-type belt conveyor, shown in figure 34. The sulfur, in the form of 40 to 50 pct solids powder, floated to the top of the regenerated solution and was continuously skimmed off by the blades of the conveyor. At the end of the conveyor, sulfur discharged into a 200-ft^3-capacity, type 316 stainless steel storage bin. The clear solution flowed from the bottom of the sulfur flotation vessel through a level controller into a 65-gal-capacity cone-bottom FRP settler tank. Here, a small amount of sulfur that failed to float (usually less than 1 pct) was settled and recycled to the conditioner tank by a slurry pump. A vertical baffle in the settler tank separated a small amount of floating sulfur that escaped from the sulfur flotation vessel. This floating sulfur was periodically removed manually and added to the sulfur storage bin. The carryover of floating and sinking sulfur indicated deficiencies in the design of the sulfur flotation circuit. The clarified solution, after leaving the settler tank, overflowed by gravity into a 300-gal-capacity FRP absorber feed tank. Thus, the cycle was completed for the mainstream of absorbent solution.

Flotation of sulfur with air alone (no addition of kerosene to the conditioner) was tried because it resulted in improved purity of the product sulfur. Sulfur produced with air flotation contained 0.04 pct C, whereas that produced with kerosene flotation contained 0.15 pct C. Flotation with air also reduced reagent costs and eliminated the need for a kerosene recovery system. The flotation of sulfur with air involved the addition of 5 to 10 L/min air through a porous stainless-steel diffuser tube located in the bottom of the sulfur flotation vessel. The sulfur pickup conveyor worked just as well as with oil-floated sulfur, and the clarity of the underflow solution was also very good. However, the percent solids of the separated sulfur was only 8 to 20 pct, compared with the 40 to 50 pct solids sulfur produced by kerosene flotation. Assuming an average 14 pct solids with air flotation, the weight of solution that would have to be heated in the process of melting sulfur is increased by about six times. The cost of the additional heat, plus the decomposition of citrate and formation of sulfate that occurs in the autoclave, must be weighed against the advantages of the air flotation method.

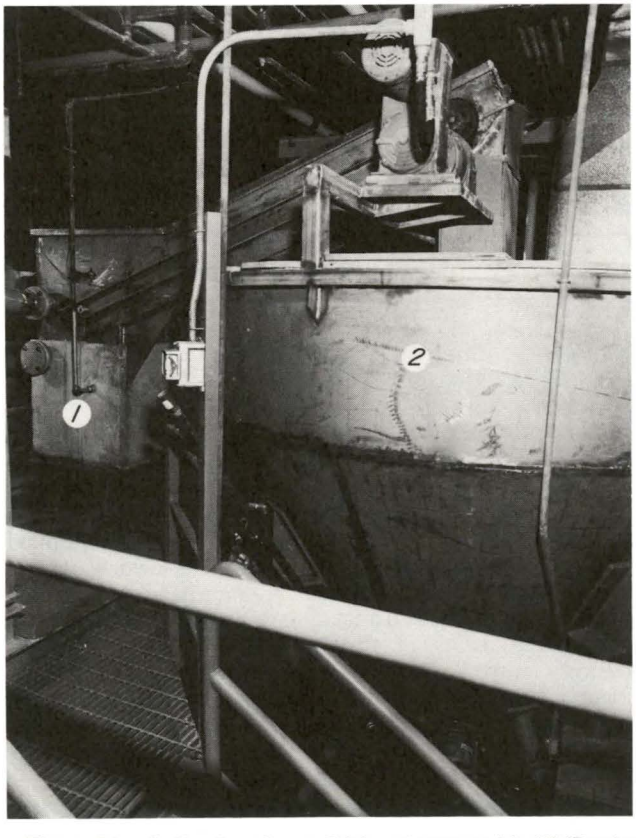


Figure 34.—Sulfur flotation cell (*1*) and storage bin (*2*) (Bunker Hill pilot plant).

Sulfur Melting and Solution Recovery

The sulfur melting was done during day shift only. The sulfur float product accumulated in the 200-ft^3 storage bin for the other 16 h. This mode of operation allowed the use of a commercial-size progressing, cavity-type slurry pump for moving the sulfur into the melter. This pump was installed directly on the bottom of the storage bin, and sulfur was fed through an 8-in gate valve into the bridge-breaker of the pump. A bin vibrator and a timed blast of air that discharged into the sulfur every 30 s near the bottom of the bin prevented bridging of sulfur and aided sulfur feed to the pump. Downstream of the pump, the sulfur was melted with steam at a rate of 300 to 400 lb/h in a 14-ft^2-area concentric-tube heat exchanger. After exiting from the heat exchanger, the melted sulfur was separated from the remaining absorbent solution in a 57-gal-capacity, type 316 stainless steel autoclave settler, shown in figure 35. The sulfur settler operated at a pressure of about 35 lbf/in^2(ga) and a temperature of 284° F. The pressure in the heat exchanger and autoclave settler was controlled by automatic release of solution from the top of the autoclave settler. After release, the solution traveled through a water-cooled concentric-tube heat exchanger and a knockout pot into a 50-gal-capacity cone-bottom FRP kerosene separator tank. The cooled solution was withdrawn from the bottom of this tank through a level controller and flowed by gravity to the absorber feed tank. Kerosene that floated to the surface was allowed to accumulate and then was periodically floated out through an overflow line to a tank for reuse. In practice, there was little recovery of kerosene when its usage was held below 1 pct of the gross sulfur produced because of vaporization losses. The kerosene that dissolved in the sulfur amounted to about 20 pct of the total kerosene based on carbon analysis of the sulfur product. No attempt was made to recover kerosene lost out of the tank vents because of the small amount involved—about 15 lb/d.

An automatic level-control valve on the bottom of the autoclave settler permitted sulfur withdrawal from the settler. Two-thirds of the sulfur produced was transferred by pressure of the settler through steam-jacketed lines to the H_2S generator sulfur storage tank where it was maintained as a molten liquid for use as required. The remaining sulfur was cast into 100-lb blocks and stored, as shown in figures 35 and 36.

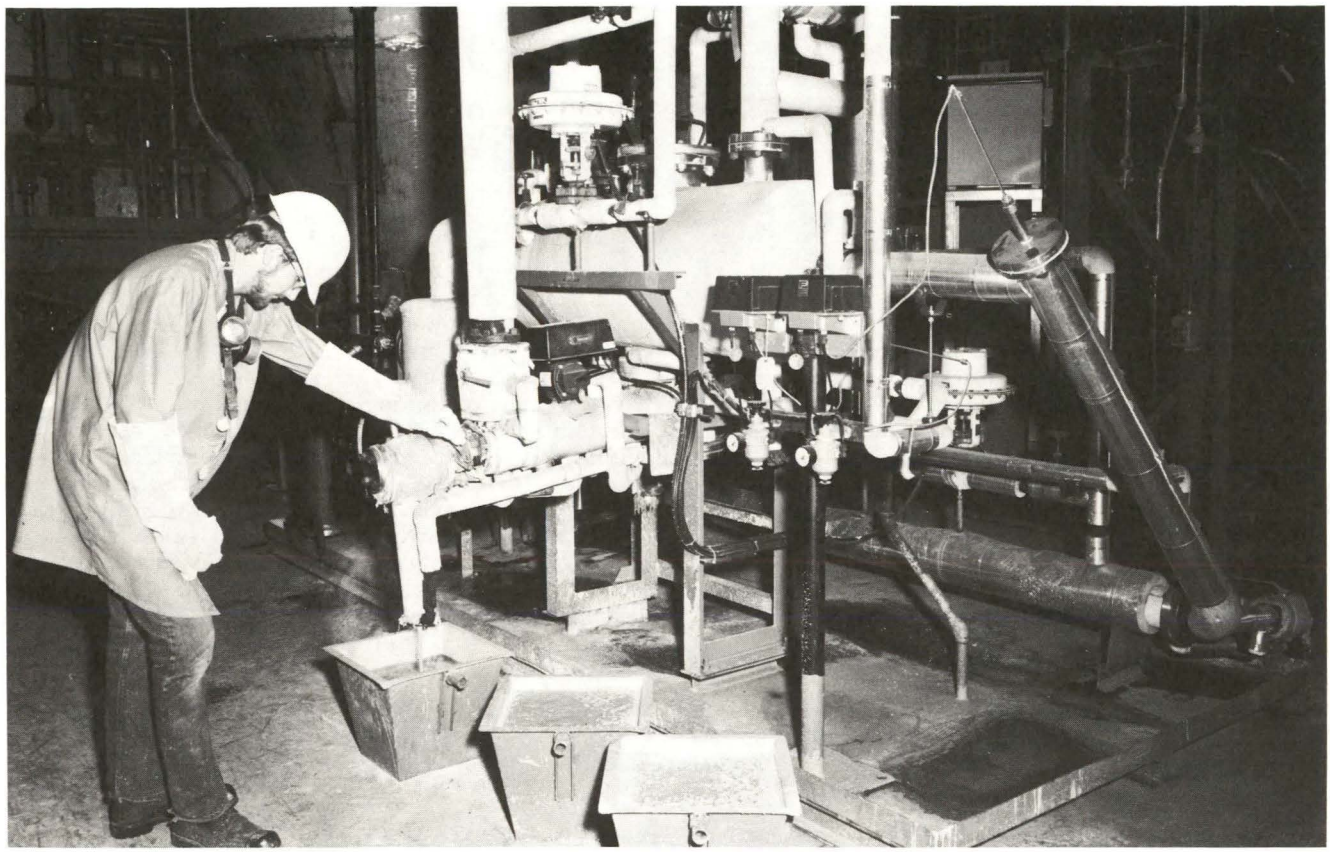


Figure 35.—Sulfur melter and sulfur molds (Bunker Hill pilot plant).



Figure 36.—Solid sulfur product (Bunker Hill pilot plant).

A high-purity, bright-yellow sulfur was produced and used successfully for H_2S generation. However, the carbon and other impurities combined with sulfur and formed a black, flakelike material that caused sticking of the sulfur pump check valves. Table 26 gives typical analyses of the quality of sulfur floated with kerosene and air. Except for the carbon content, the sulfur produced by either kerosene or air flotation was nearly identical. In spite of the higher carbon content, the kerosene-floated sulfur would be acceptable for H_2SO_4 manufacture.

Solution Makeup

The absorbent solution was prepared in a 300-gal stirred FRP absorbent makeup tank. The ingredients and order of mixing for a 250-gal batch of 0.5*M* citrate solution were as follows: water, 150 gal; citric acid, 200 lb; soda ash (Na_2CO_3), 100 lb; $Na_2S_2O_3$, 128 lb; and water to final volume. Because CO_2 would be released in the chemical reaction, Na_2CO_3 was added slowly to prevent a boilover. The $Na_2S_2O_3$ was added last to prevent decomposition. About 1,000 gal were needed to fill the pilot plant system. The drain lines of the two tanks, makeup and feed, were also interconnected to provide extra system surge capacity.

Chemical Usage—Inventories

The important chemical makeup requirements for the SO_2 absorption, solution regeneration, and sulfur recovery section of the pilot plant included citric acid, Na_2CO_3, and kerosene. The pilot plant was designed so that solution losses from spills, leaks, etc., could be collected in a common sump. The plant concrete floor was sloped to trenches that

Table 26.—Bunker Hill pilot plant sulfur product analysis, percent

Type of flotation	Ash	Water	Carbon	Sulfur
Kerosene	0.05	0.25	0.17	99.6
	.07	.25	.15	99.5
Air	.03	.28	.04	99.5
	.08	.15	.04	99.7
	.006	.03	.024	99.9

drained into the sump. The sump pump discharged into a 300-gal stirred FRP spill tank. All of the spilled solution was measured and sampled for analysis before it was dumped into the chemical sewer. Solution inventories and samples were taken at the end of operating periods (usually about every 2 weeks), and citric acid losses were calculated. Averaging the citrate loss tests during runs, when upsets or solution losses were minimized, showed that about 20 lb of citric acid was lost per net short ton of sulfur produced. About 90 lb Na_2CO_3 per net short ton of sulfur was required to neutralize H_2SO_4 and to make up fresh citrate solution. At the conclusion of the pilot plant operation, the kerosene requirements were reduced to about 4 lb per net short ton of sulfur produced.

H_2S Generation

The H_2S generator (fig. 37) indicated as a single block in figure 28, is depicted in some detail in the flow diagram (fig. 38). Solid lines in this diagram indicate flows for a two-stage reaction, considered to be a proven process. The dashed lines indicate provision to bypass reactor 2 for experimentation with a single-stage reaction. The design capacity of the plant was 0.4 to 1.25 st/d H_2S. Molten sulfur produced in the pilot plant was transferred to a sulfur feed tank from which it was pumped through a filter to remove carbon and ash impurities and to a gas-fired superheater. The sulfur was vaporized and superheated to about 1,350° F. Natural gas containing about 92 vol pct CH_4 at 1,200° F from a second superheater was combined with the hot sulfur vapor ahead of reactor 1. The sulfur-CH_4 reaction produced H_2S and CS_2 over a catalyst in this reactor.

The H_2S-CS_2 product gas was first air-cooled to about 800° F and then further cooled in a steam-cooled heat exchanger to about 300° F. Excess sulfur was condensed in the reactor product cooler and was removed from the gas mixture in the first sulfur knockout tank.

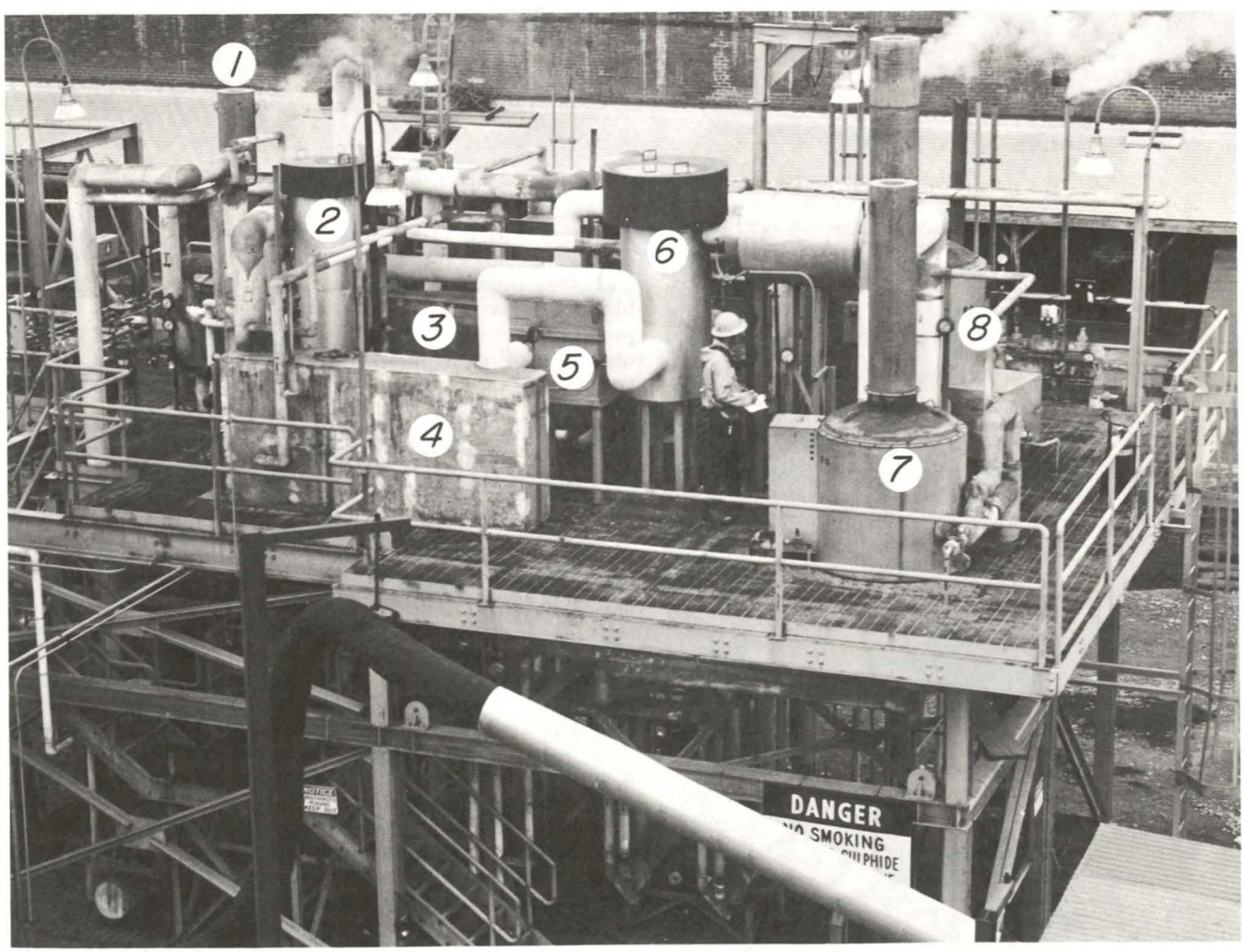


Figure 37.—H_2S generator (Bunker Hill pilot plant). *1*, Steam superheater; *2*, reactor 2; *3*, steam cooler 1; *4*, steam cooler 2; *5*, air cooler 2; *6*, reactor 1; *7*, natural gas superheater; *8*, sulfur superheater.

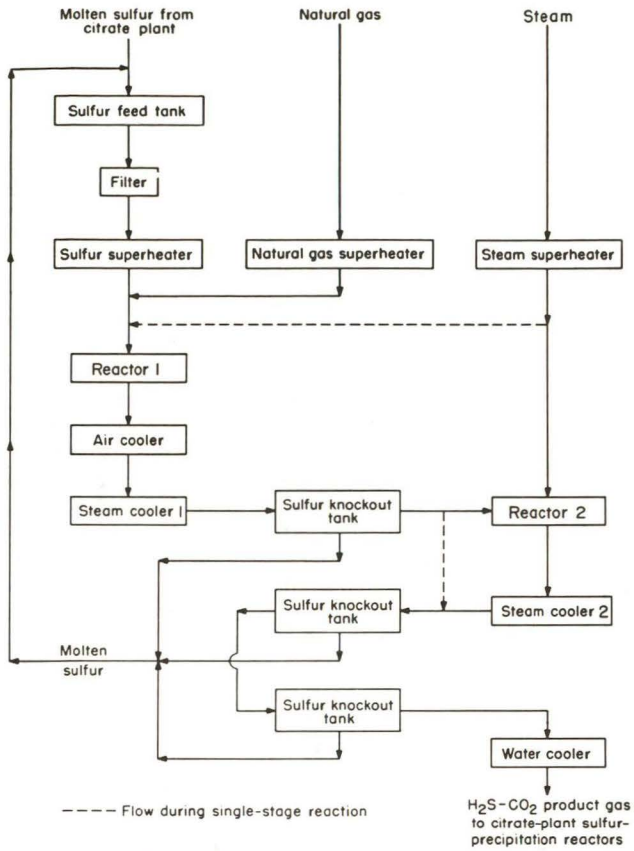


Figure 38.—Flowsheet for H_2S generator at Bunker Hill pilot plant.

A third superheater produced steam at 800° F. The steam combined with the cooled H_2S-CS_2 gas prior to entering reactor 2. In this reactor, the CS_2 was hydrolyzed to H_2S and CO_2 in a catalyst bed at 700° F.

A side reaction, during the CS_2 hydrolysis, resulted in the formation of COS. In the laboratory, this reaction was depressed by feeding excess steam and favored by high reaction temperatures.

A steam-cooled heat exchanger cooled the reactor 2 product gas to 300° F to condense free sulfur. The condensed sulfur was removed in two additional knockout tanks. Sulfur that collected in all three knockout tanks was periodically drained to the sulfur feed tank. Product gas from the second reactor, containing H_2S, CO_2, and some water vapor, was cooled to about 149° F in a water-cooled heat exchanger and then fed to the solution regeneration section of the citrate pilot plant.

After pretesting, the operation of the H_2S generator was integrated with the operation of the SO_2 absorption, solution regeneration, and sulfur recovery sections. Two operating problems developed during continuous operation. The first, and probably the most chronic, was plugging of the cold H_2S product lines and valves with sulfur. This was partially solved by modifying the final sulfur knockout tank to cool the product gas with a water jacket. This mode of operation required periodic steam heating to clear the sulfur out of the knockout tank. The second problem, plugging of the sulfur superheater coil with metal sulfides, was due to high-temperature corrosion.

Reactor 2 was bypassed as indicated in figure 38 after achieving reliable operation with two stages. This allowed reaction 10 (chapter 1) to take place in reactor 1:

$$CH_4 + 4S + 2H_2O \rightarrow CO_2 + 4H_2S. \qquad (10)$$

The operation proceeded without any additional problems; the only noticeable difference was that the product H_2S contained more COS and CH_4.

Next, both the steam and natural gas superheaters were eliminated. All reactant feed materials were superheated in the sulfur superheater. Again the plant worked satisfactorily; the only noticeable difference was that the temperature of the superheater could be reduced about 100° F without affecting the H_2S product quality. This difference was probably due to an increase in the overall reaction time. The advantages of a single-stage operation would be the elimination of capital equipment and possibly reduced corrosion in high-temperature equipment.

Between April 1975 and May 1976, the H_2S generator operated for about 3,090 h and produced the H_2S required for SO_2 reduction in the citrate process. During the latter 2,369 h of this time, the one-stage operation was used.

Table 27 summarizes results of the H_2S generator operation under reasonably steady-state continuous operation. During this time, sulfur was fed to the H_2S generator while the natural gas and steam flows were varied to change the H_2S production rate. Throughout most of the H_2S generator operation, the sulfur flow was about 160 lb/h. This flow provided between 150 and 300 pct excess sulfur, which was recovered and recycled. The large amount of excess sulfur was used to prevent overheating of the sulfur vaporizer coil and to transfer heat to the first reactor. During the two-stage operation, 25 pct excess steam was used to prevent COS formation. During the one-stage operation, where the CS_2 hydrolysis occurred at a higher temperature, 50 pct excess steam was necessary to achieve low COS in the product gas. The first reactor inlet and outlet skin temperatures both averaged about 1,050° F. While operating with two stages, the second reactor inlet and outlet temperatures averaged 430° F and 655° F, respectively. In addition to the principal gas analyses listed in table 27, the H_2S product gas contained about 1 dry vol pct N_2 and traces of CS_2, CO, and O_2.

Table 27.—Bunker Hill pilot plant H_2S generation results using natural gas reductant

Number of—		Natural gas flow, lb/h	H_2S production, st/d	H_2S product analysis, dry vol pct			
Reactor stages	Superheaters			H_2S	CO_2	COS	CH_4
2	3	12.2	1.15	79	19	0.7	0.4
2	3	8.1	.75	79	19	.5	.2
2	3	6	.55	79	19	.3	.2
1	3	10	.95	78	18	1.5	2
1	2	9	.85	77	17	2.4	2.1
1	1	7	.65	78	18	1.6	1

The test results showed that the two-stage operation of the pilot plant made the most efficient use of natural gas and produced the least amount of undesirable COS. The decrease in CH_4 utilization during the one-stage operation, as indicated by the higher CH_4 in the product gas, may have been caused by the increased space velocity through the first reactor. The COS in the H_2S product gas was vented from the sulfur precipitation reactors and incinerated to SO_2 and CO_2. By all methods of operation, the H_2S generator produced a gas that analyzed between 77 and 79 dry vol pct H_2S and was suitable for the SO_2 reduction.

The quantities required for the H_2S generator for each

short ton of H_2S produced were (1) sulfur, 1,900 lb, (2) CH_4, 5,600 std ft^3, and (3) steam, 1,000 lb.

SO_2 reduction was tried with a gas of lower H_2S content. This gas could be produced with a CO-H_2 mixture from a coal gasifier. This would eliminate the need for natural gas reductant in the citrate process. Reactor 1 was operated at 900° F, which reduced the reaction rate and produced a lower strength H_2S gas. This gas contained, on a dry-volume-percent basis, 56 H_2S, 15 CO_2, 24 CH_4, 1 COS, 0.5 CS_2, 2 N_2, and trace CO and O_2. This gas, used for a short period of time in the pilot plant, was suitable for SO_2 reduction.

Morrison-Knudsen Co., Inc., under a cooperative agreement with the Bureau, tested other gaseous reductant feeds to replace natural gas for H_2S generation. Table 28 summarizes results of the H_2S generator operation using C_3H_8, CH_3OH, and CO as reductant feeds. Using a one-stage operation, the sulfur superheater vaporized and heated the sulfur, reductant, and steam. The test conditions were similar to those used in producing H_2S from sulfur, natural gas, and steam.

Table 28.—H_2S generation results using C_3H_8, CH_3OH, and CO reductants

Reductant	Reactor skin temp, °F		H_2S production, lb/h	H_2S product analysis,[1] dry vol pct				
	Inlet	Outlet		H_2S	CO_2	COS	CS_2	N_2
C_3H_8	1,080	1,030	54.2	76.1	20.2	1.7	1.4	0.6
CH_3OH ...	1,100	1,100	54.2	74.2	21.6	2.6	0	1.6
CO	1,000	1,050	27.7	50.1	46.8	2.2	0	.9

[1] H_2S product also contained a trace of CO.

The test results showed that all reductants resulted in the production of an H_2S gas that could be used in the citrate process. The lower temperatures needed for H_2S production from sulfur, CO, and steam may reduce the energy requirement and corrosion in the sulfur superheater coil and high-temperature process piping.

Safety

Safety was an overriding consideration in design, construction, and operation of the pilot plant. Trace quantities of H_2S may not be harmful and are detectable by the characteristic foul odor. However, the ability to detect the odor is destroyed by high concentrations. Concentrations of only 0.1 pct H_2S are lethal. For this reason, the pilot plant emergency ventilation system was designed and installed for a complete air change in the building every 2 min. The emergency ventilation fan took suction from a ducted hood in the immediate vicinity of the reactors where H_2S leaks were most likely to occur.

The pilot plant was equipped with an H_2S detector alarm system that consisted of remote H_2S detection sensors, one in the solution regeneration reactor area, two in the H_2S storage tank area, three in the H_2S generator area, and one in the control room adjacent to the central H_2S alarm system control panel. An audible bell system was set to alarm at an H_2S concentration of 10 ppm, followed by a wailing horn that sounded if a concentration of 25 ppm was reached. The emergency ventilation fans were set to start and an automatic valve on the H_2S supply line was set to close if the 25-ppm level was reached in the process area. During actual pilot plant operation, the H_2S concentration rarely reached a level that set off the alarms. However, 0- to 4-ppm concentrations were frequently encountered. These concentrations, although rarely high enough to show on the H_2S sensors, were objectionable. A program was set up for inspection of H_2S-indicating cards. These cards, sensitive to a fraction of 1 ppm H_2S, made it possible to detect very small leaks and repair them before the alarm system ever became activated. A commercial syringe-type detector, which involves drawing an air sample through a sensitized material in a glass tube and observing the length of stain produced, was also used for pinpointing H_2S and SO_2 leaks. This monitoring was not as sensitive as the indicator cards and was more time consuming. A simple substitute for the cards consisted of small strips of filter paper saturated with lead acetate solution that were also sensitive to a fraction of 1 ppm H_2S.

Several types of breathing-air masks were available for working where a serious leak could occur. For small jobs such as disconnecting lines containing residual H_2S, a 30-min backpack unit having a full face mask was used. A 7-min, self-contained, over-the-shoulder-type escape breathing mask was carried at all times for routine inspection of the H_2S storage and vaporization area or the H_2S generator. This mask was not worn unless there was a known or suspected leak of H_2S. This type of mask could also be used longer by attaching it to the hose on a larger compressed breathing-air container. A refill station was provided so air containers could be recharged with breathing air.

The control room and laboratory section of the pilot plant (fig. 39), which was a modified 40-ft trailer, had a separate ventilating system that consisted of a fan, a heater, and a carbon-filled air purification filter on the fan suction. The carbon filter removed SO_2 and smelter dusts from the air.

Provisions were made for disposing of H_2S during upset periods in plant operations. Also, a small continuous stream of CO_2 containing 5 to 15 vol pct H_2S was discharged from the reactor vent, when 78 vol pct H_2S was used for regenerating the absorbent solution. This gas vented through a fan, which acted as a flame arrester, to a natural-gas-fired incinerator. The H_2S was burned to SO_2 before being discharged to the stack. The incinerator was supplied with two burners as a safety factor. Only one was required during routine operation; however, both were used to bring the incinerator up to operating temperature. The entire H_2S generator product could be burned in the incinerator. This permitted operation of the H_2S generator when the SO_2 absorption section was down.

Personnel Requirements

Eleven persons were required for the pilot-plant operation, maintenance, and testing. One employee operated the SO_2 absorption, solution regeneration, and sulfur recovery section; and another operated the H_2S generator. A shift foreman, responsible for both sections, helped operators when needed. An operator was needed to run the sulfur melting section during the day shift. A plant supervisor was also present on day shift. Instrument repair and general troubleshooting were done by the contractor's representative, but most routine maintenance was done by plant operators. At times, it was necessary to schedule a person for the swing shift to finish sulfur melting and help with plant maintenance.

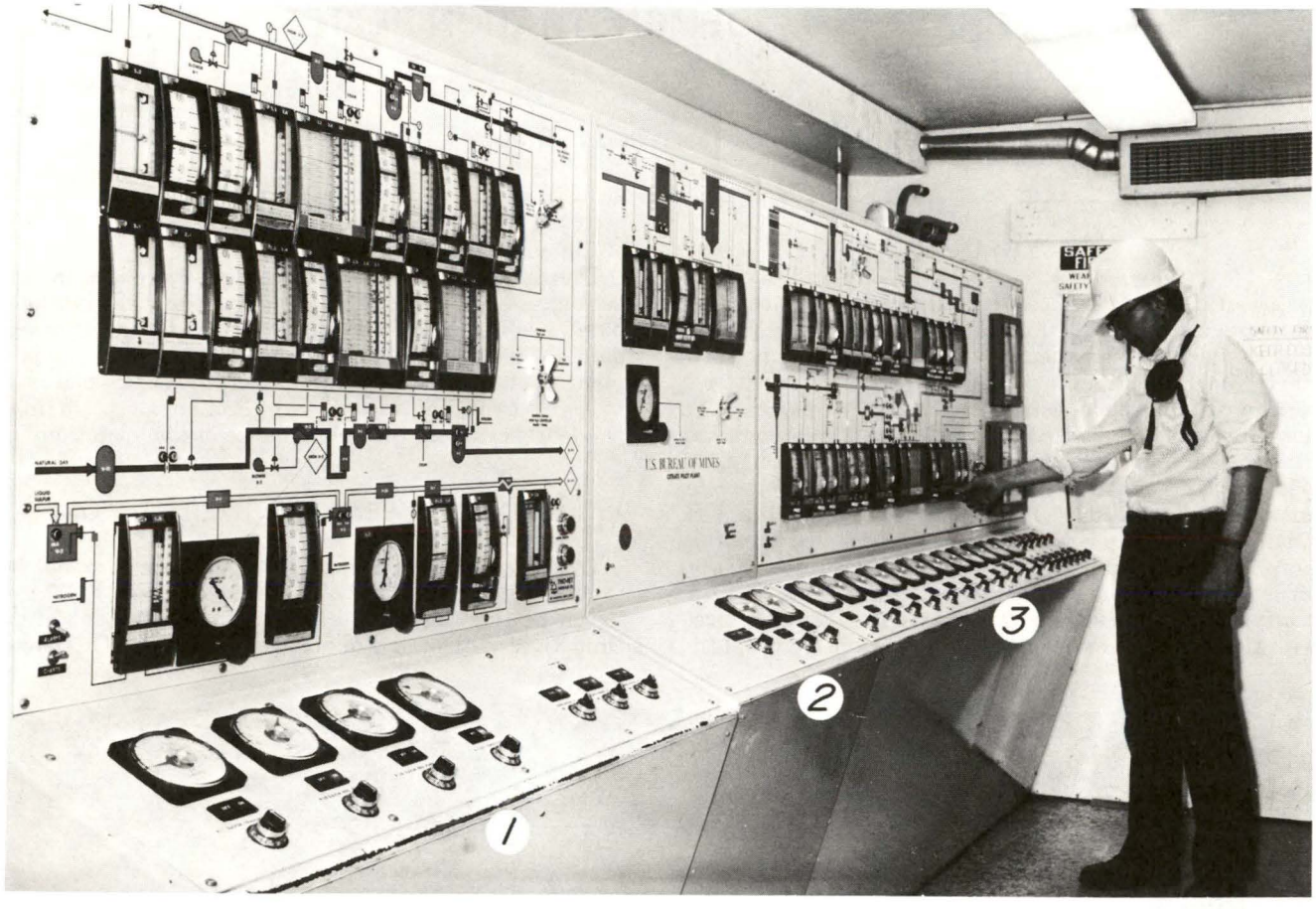


Figure 39.—Control panel (Bunker Hill pilot plant). *1*, H_2S generator section; *2*, gas cooling and cleaning section; *3*, SO_2 absorption, solution regeneration, and sulfur recovery section.

Corrosion Testing

Except for corrosion already mentioned and some problems with FRP joint leaks, all materials of construction used for the gas cooling and cleaning and for the SO_2 absorption, solution regeneration, and sulfur recovery section were satisfactory. To evaluate other stainless steels and alloys, corrosion test specimens were placed in various locations in the Bunker Hill pilot plant prior to the start of operation in January 1974 and were examined after the plant was shut down in May 1976. For equipment handling citrate solution, it appears that type 304 stainless steel would be the most economical choice of metals, except for the gas-cleaning equipment. Although none of the metals was severely attacked, type 304 and type 316 stainless steels showed pitting in the humidifier-scrubber. The best resistance to corrosion in the humidifier-scrubber was shown by the Hastelloy G, Hastelloy C-276, Inconel 617, Inconel 625, Inconel 617 sensitized, and type 317 stainless steels. Again, FRP and PVC plastics were satisfactory where temperature and mechanical strength requirements permitted. It should be mentioned that fluorides, chlorides, or other ions not found in the pilot plant solutions might result in different requirements for other installations.

SUMMARY

Prolonged pilot-plant testing has shown that the Bureau's citrate process is capable of almost complete removal of SO_2 from nonferrous smelter waste gases:

1. Ninety-nine percent of the SO_2 could be removed from either copper smelter reverberatory furnace waste gases containing from 1.07 to 1.66 vol pct SO_2 or lead smelter sintering machine waste gases containing from 0.1 to 0.6 vol pct SO_2.
2. Regeneration of the loaded citrate solution with H_2S and precipitation of sulfur in conventional stirred vessels was readily controlled.
3. Precipitated sulfur could be continuously recovered as a 99.5-pct-pure product by flotation and melting.
4. Seventy-eight dry volume percent H_2S could be readily produced from pilot plant sulfur, natural gas, and steam.
5. A 56 dry vol pct H_2S gas, which might be produced using a synthesis gas (CO-H_2) derived from coal, could be used for solution regeneration.
6. H_2S gas may be produced using the reductants CH_3OH, C_3H_8, or CO.
7. Materials of construction for SO_2 absorption, solution regeneration, and sulfur recovery equipment were satisfactory.

The ability of the citrate process to capture 95 pct of the SO_2, with conversion to sulfur of potential economic value, justified continued study and development on a demonstration plant scale.

CHAPTER 4.—DEMONSTRATION PLANT

By W. I. Nissen and L. Crocker

BACKGROUND

Encouraged by the success of the Bunker Hill pilot plant, the Bureau sought a site for a demonstration of the process on a commercial or industrial scale in 1975. In June 1976, the St. Joe Minerals Corp. was awarded a contract for a commercial-scale demonstration of the citrate process. The host site for the plant was St. Joe's George F. Weaton Power Station near Monaca, PA (*38, 48*). The demonstration plant was built and operated under a cooperative arrangement on a cost-sharing basis between the Bureau, the U.S. Environmental Protection Agency, and St. Joe Minerals Corp. Morrison-Knudsen Co. was awarded the design, construction, and maintenance contract by St. Joe. In turn, Morrison-Knudsen subcontracted for engineering services with the Ralph M. Parson Co. and the Home Oil Co., Ltd., of Canada.

The design of the absorption, sulfur production, and sulfur recovery sections of the plant was based on pilot plant results and Parson's experience with sulfur recovery plants. The design of the H_2S generator was based on pilot plant results and Home Oil's experience with CS_2 plants.

The Bureau contracted with Radian Corp. to independently evaluate the performance of the operation.

GEORGE F. WEATON POWER STATION

The citrate process demonstration plant was retrofitted to one of two coal-fired boilers at the George F. Weaton Power Station (fig. 40), located on the south bank of the Ohio River at Monaca, PA, north of Pittsburgh. This power-

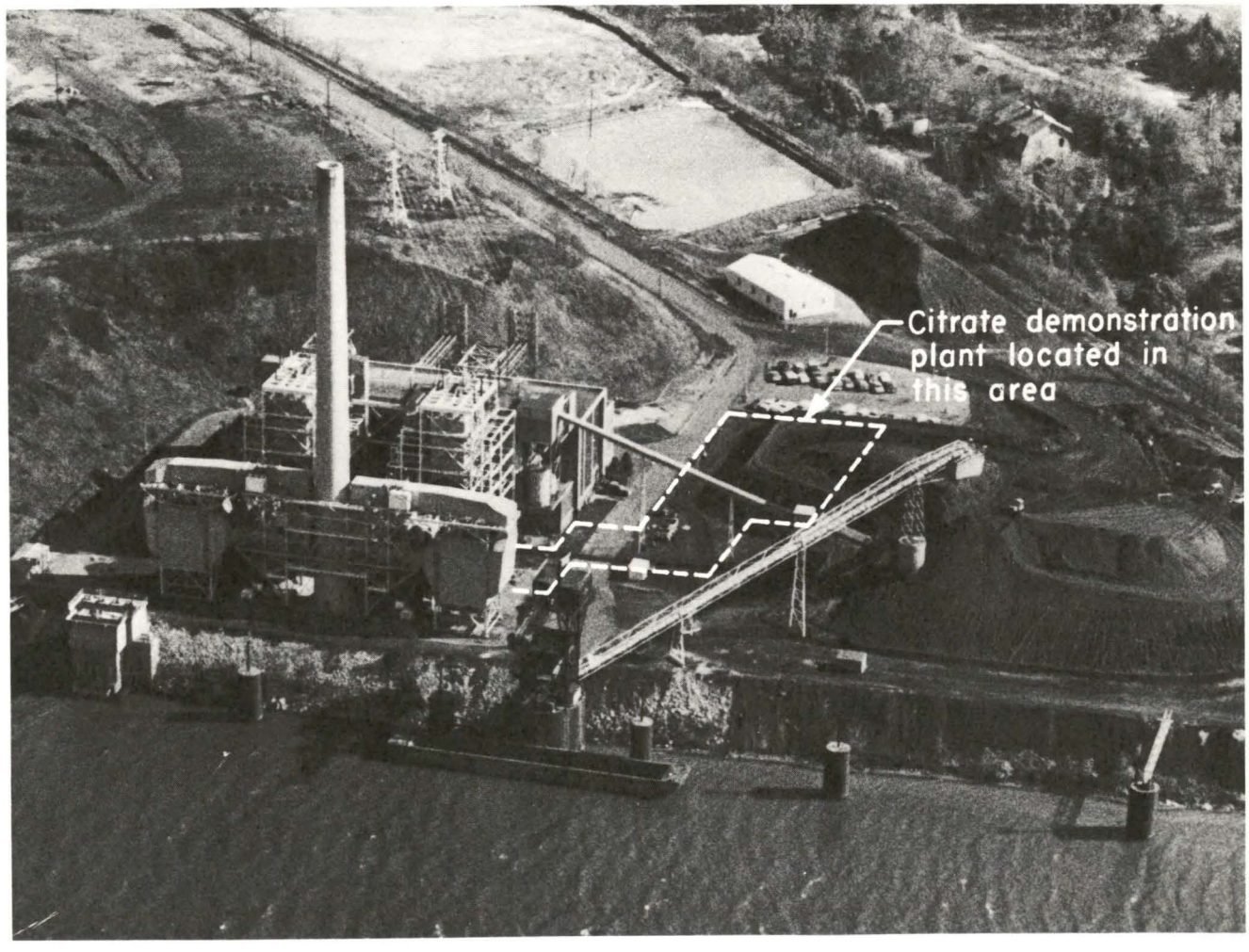


Figure 40.—George F. Weaton Power Station.

plant is a base-loaded, coal-fired electricity generating plant with two identical boiler units, each capable of supplying 60 MW of electrical energy to St. Joe's nearby zinc smelter. Originally, the powerplant could interchange 25 MW of electrical power with the Duquesne Light Co. However, in late 1981, St. Joe installed equipment that made possible the interchange of as much electrical power as the Weaton Power Station would generate.

Particulate control is achieved through a combination mechanical and two-stage electrostatic precipitator, which removes over 99.6 pct of the fly ash. Bottom ash from the boilers and fly ash from the precipitators are slurried and conveyed to a settling pond for decantation, drying, and subsequent disposal.

CITRATE PROCESS DEMONSTRATION PLANT

Construction of the citrate process demonstration plant was completed in November 1979. As shown in the generalized process flowsheet (fig. 41), the citrate process drew SO_2-bearing flue gas from the duct between the electrostatic precipitator and the stack. The nominal design capacity of the plant was 156,000 std ft^3/min of 0.2 vol pct SO_2 gas, which at 90-pct SO_2 removal and a 2-pct oxidation rate would yield approximately 15 lt/d S. The plant was divided into six specific unit operations: (1) gas cleaning and cooling, (2) SO_2 absorption, (3) solution regeneration and sulfur precipitation, (4) sulfur recovery, (5) sulfate removal, and (6) H_2S generation.

Following construction, the demonstration plant commenced preparatory operations (*11*). Unfortunately, in December 1979, St. Joe shut down the Monaca Zinc Smelter, which reduced the electrical load from 120 MW to between 15 and 30 MW. However, for almost 3 yr, efforts continued to prepare the demonstration plant for the planned acceptance test and demonstration test. In September 1982, St. Joe halted preliminary operations and subsequently requested termination of the citrate demonstration contract. During the preliminary operation, the demonstration plant logged over 2,900 h and produced an estimated 250 lt S. St. Joe and the Bureau agreed to terminate the contract in September 1983, without an acceptance test or a demonstration test.

The following describes the plant in greater detail and presents some results of the preliminary operation. The completed plant is shown in figure 42.

Gas Cleaning and Cooling

A forced-draft fan transported the flue gas through a 9-ft-diam duct to the plant. This fan was a double-inlet mechanical-draft type that delivered during preliminary operation up to 208,000 ft^3/min (actual) at 320° F. The fan was constructed of carbon steel and was driven by a 1,000-hp electric motor.

Downstream of the fan, an eductor-type venturi scrubber removed residual fly ash, SO_3, and chlorides (Cl^-) from the flue gas. This venturi also cooled the gas from 320° to 120° F by both humidification and sensible cooling. Sensible cooling requires high solution recirculation rates, and the eductor utilized a 6,000-gal/min flow. Venturi scrubber solution and flue gas separated in the bottom of the vessel that contained the SO_2 absorber. Except for a bleed stream of about 30 gal/min, most of the solution recycled to the venturi scrubber. Two pumps in series transported the recycle solution. These pumps were the centrifugal, horizontal slurry type and delivered 6,000 gal/min in normal operation. The pump casings and impellers were rubber-lined cast iron with Hastelloy C trim. Each pump was driven by a 250-hp electric motor. Makeup water replaced the humdification and bleed stream losses.

The venturi scrubber, which had a 10-ft diam and was 45 ft high, had an acid-proof brick and rubber-membrane lining over a carbon steel shell. The venturi nozzle was fabricated from SiC.

Ash and acids were removed by the bleed stream, which prevented buildup. This bleed stream flowed through a 2-ft-diam by 18-ft-high FRP stripper packed with about 31 ft^3 of 1-in polypropylene saddles. At the same time that the bleed stream flowed through the stripper, a 100-std-ft^3/min stream of air flowed countercurrently, stripped any absorbed SO_2, and returned the SO_2 to the absorption tower.

The SO_2-stripped bleed stream flowed to an acid-brick-lined, agitated, concrete tank where lime was added to neutralize acids. A pump transferred the neutralized bleed stream to the existing ash-settling pond.

SO_2 Absorption

The cooled, cleaned flue gas passed through a polypropylene chevron entrainment separator and a chimney tray having four 6-1/2-ft-diam chimneys into the SO_2 absorber. Initially, flue gas flowed upward through a 26-ft-diam by 20-ft-high packed bed of 2-in polypropylene saddles countercurrent to citrate solution. Because of sulfur plugging in the packed bed, first, from 16 to 18 ft of packing height was removed and, second, spray nozzles were installed, replacing a weir-type citrate solution distributor. Finally, during the last year of operation, all of the packing was removed. The citrate solution selected for preliminary testing was a 0.25*M* citric acid solution buffered with sodium base to a pH between 4.2 and 4.8, which contained about 0.25*M* $Na_2S_2O_3$. In the SO_2 absorber, from 22 to 92 pct of the SO_2 was removed from the flue gas (*11*). Table 29 summarizes the most encouraging SO_2 absorption results. The SO_2 removal efficiency using the initial packed tower was never reliably documented. Therefore, results are reported only for the weir distributor-packed absorber, spray distributor-packed absorber, and spray absorber.

Because none of the preliminary test conditions approached the design capacity of the plant, discussions about the success of the SO_2 removal are difficult. Most of the time, the plant treated only 75 pct or less of the design gas flow, which contained 67 pct or less of the design SO_2 content. The SO_2 removal by the spray tower absorber was remarkable, considering the citrate solution flow was limited to that designed for a packed tower absorber.

The SO_2 absorber and stack were fabricated of carbon steel. The absorber was lined with vinylester reinforced with glass flakes. The lining used in the reheat zone between the absorber and the stack consisted of a corrosion-resistant asphaltic membrane covered with a lightweight heat- and corrosion-resistant insulating brick. The stack was protected with an FRP sleeve.

A pump transported the SO_2-rich citrate solution from the SO_2 absorber to the solution regeneration and sulfur precipitation section. This pump was a centrifugal, horizontal, single-stage type, which delivered up to 1,250 gal/min. The pump was constructed of Chlorimet 3 with Hastelloy C trim and was driven by a 40-hp electric motor. After regeneration, another pump recycled the SO_2-lean citrate solution from a citrate storage tank back to the SO_2 absorber. This lean-solution pump was similar to the rich-

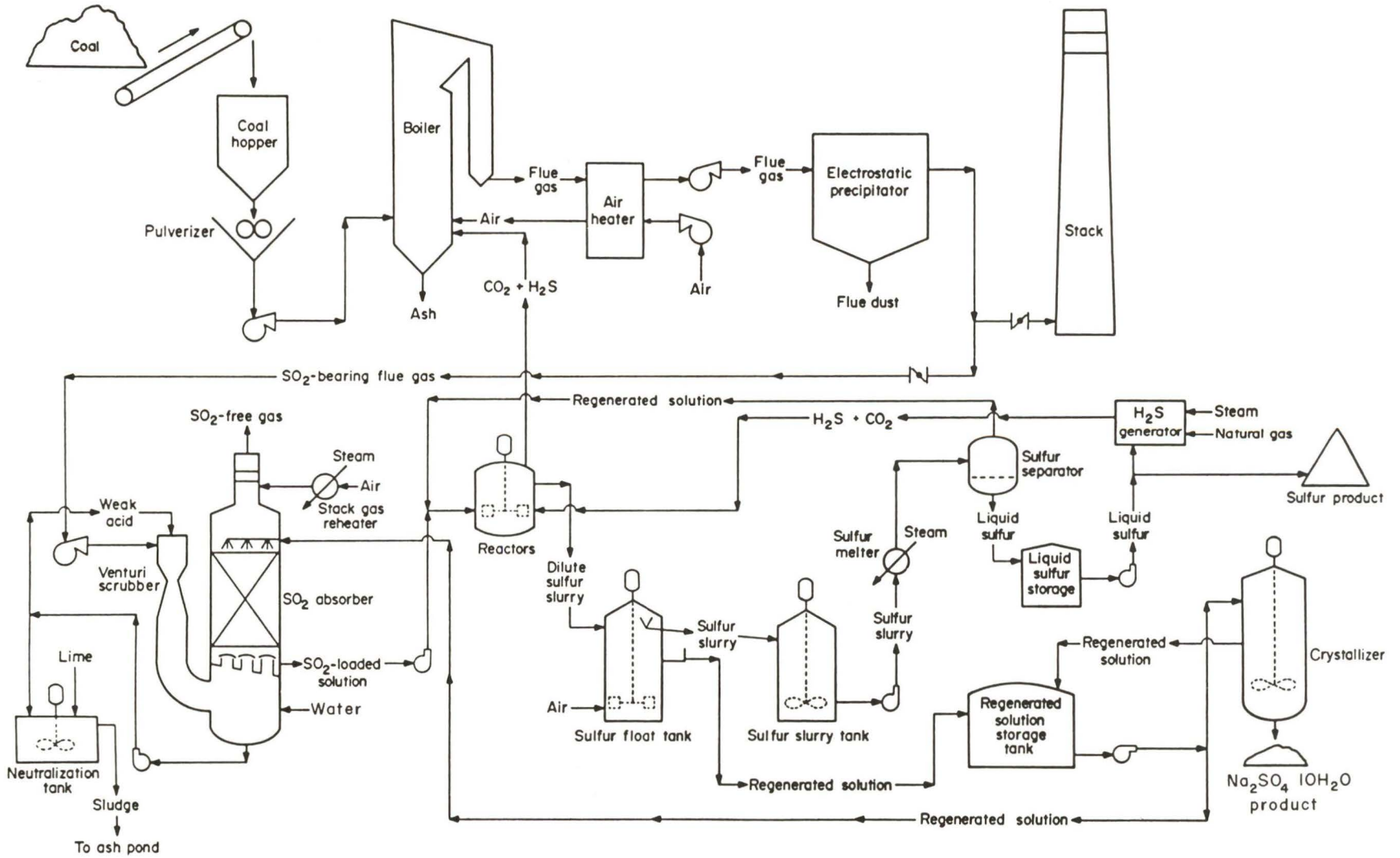


Figure 41.—Powerplant stack gas SO_2 scrubbing—citrate process flowsheet.

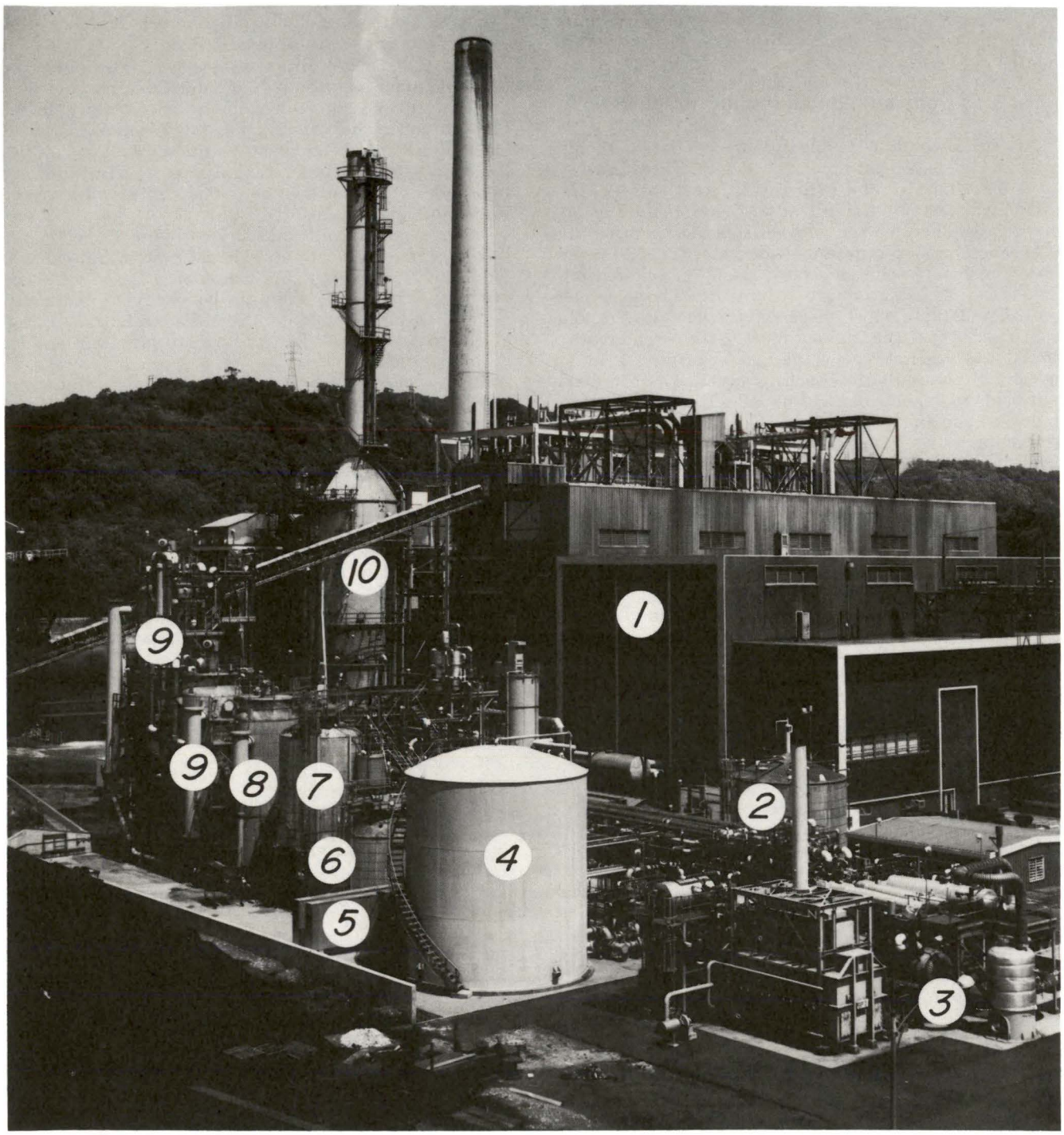


Figure 42.—Citrate process demonstration plant. *1*, George F. Weaton Power Station; *2*, sulfur product storage; *3*, H_2S generator; *4*, citrate solution storage; *5*, sulfur melter; *6*, sulfur slurry tank; *7*, flotation tank; *8*, conditioning tank; *9*, regeneration reactor; *10*, SO_2 absorption tower.

Table 29.—Summary of results of preliminary operation of the citrate process demonstration plant

Flue gas		Type absorber	Lean citrate solution		Absorption temp, ° F	SO_2 in offgas, ppmv	SO_2 removal efficiency, pct
SO_2, ppmv	Flow rate, std ft^3/min		Flow rate, gal/min	pH			
980	90,000	Weir distributor-packed absorber	1,060	4.8	122	118	88
1,250	120,000	Spray distributor-packed absorber	1,030	4.5	129	338	73
1,340	96,000	Spray	1,255	4.8	138	402	70
1,090	113,000	. . do	1,040	4.8	135	392	64

solution pump except that it was driven by a 120-hp motor. During lean-solution recycle, a heat exchanger cooled the solution with river water.

Solution Regeneration and Sulfur Precipitation

Rich citrate solution leaving the absorber flowed through two tandem 13,000-gal-capacity reactors. These reactors were 12-ft-diam by 18-ft-high carbon steel vessels lined with vinylester reinforced with glass flakes. In the reactors, SO_2-rich solution reacted with an H_2S-CO_2 gas from the H_2S generator to precipitate elemental sulfur and regenerate the citrate solution. The H_2S-CO_2 gas flowed into the second of the two reactors through a sparger underneath an agitator, which dispersed the gas into the solution. The H_2S gas that did not react in the second reactor flowed into the first reactor through a sparger. Again, an agitator dispersed the gas. Each agitator had a 67-in-diam, four-blade radial impeller. The impeller turned at 68 r/min and was approximately 4 ft from the bottom of the reactor. The agitators were turned by 100-hp electric motors. All wetted parts of the agitators were Inconel 625.

Reactor offgas, which was mainly CO_2 with small quantities of H_2S, CS_2, and COS, flowed to the boiler firebox for incineration to SO_2. Slurry flowed by gravity through the reactor system, which was stepped, to a digester. The digester was physically similar to the reactors except the agitator had an axial impeller driven by a 3-hp motor. In the digester, any dissolved or entrained H_2S in the slurry reacted with a small stream of SO_2-rich solution from the absorber. From the digester, the slurry flowed by gravity to the sulfur flotation tank.

Sulfur Recovery

Sulfur was separated from the bulk of the solution by air flotation in an agitated 18,500-gal-capacity tank. The flotation tank was 15 ft in diam by 20 ft high and was made of carbon steel lined with vinylester reinforced with glass flakes. In the tank, sulfur froth, aided by air, floated on the surface of the solution. A lobe-type blower supplied air to the tank, and a 25-hp turbo agitator, which had Hastelloy C-276 wetted parts, dispersed the air throughout the solution. The concentrated sulfur froth flowed over a weir to an agitated 18,000-gal-capacity sulfur slurry tank.

Poor flotation was a problem throughout all of the plant operations. Initially, flotation was thought to have been affected by low regenerated solution temperatures. Higher temperatures were thought to aid in the flocculation of collodial sulfur and in the flotation of flocculated sulfur particles. Later, when higher regenerated solution temperatures were attained, it appeared that some sulfur was short-circuiting between the sulfur slurry inlet and the solution outlet and that the turbo agitator caused some reentrainment of the sulfur. The sulfur flotation tank was modified by installing baffles on the sulfur slurry inlet and the solution outlet. These modifications improved flotation but did not solve the problem of carryover of sulfur into the regenerated solution. Plans had been made to replace the turbo agitator with an air-diffuser-type distributor when the plant was shut down.

The sulfur slurry tank was 15 ft in diam by 15 ft high and was made of carbon steel lined with vinylester reinforced with glass flakes. The sulfur slurry tank agitator degassed the sulfur froth and suspended sulfur crystals in the solution. The agitator, which turned at 45 r/min, had two 42-in-diam, four-blade radial impellers. All wetted parts of the agitator were Inconel 625.

Regenerated lean citrate solution flowed from the bottom of the flotation tank through an adjustable overflow weir box that allowed adjustment in the solution level in the flotation tank. The weir box was fabricated of FRP with Hastelloy C trim. Lean citrate solution from the weir box flowed by gravity to a 125,000-gal-capacity citrate storage tank made of carbon steel and lined with vinylester reinforced with glass flakes.

Vapor spaces of all tanks downstream of the reactor system were piped into an exhaust system. An exhaust fan drew vapors containing traces of H_2S and COS and discharged these vapors into the boiler firebox for incineration to SO_2. SO_2 generated from the combustion of H_2S and COS was recycled to the citrate process plant for desulfurization.

Sulfur was separated from the remaining solution by heating the sulfur slurry from 131° F to about 260° F and melting the sulfur with steam in a concentric-tube heat exchanger. A progressing cavity-type pump transported sulfur froth from the sulfur slurry tank to the heat exchanger. This pump, with Hastelloy C and rubber wetted parts, was driven by a 20-hp electric motor. The heat exchanger was designed to exchange 4.11 million Btu/h, operated at about 35 lbf/in^3(ga), and was a jacketed-pipe type with the tube and shell fabricated of Hastelloy C-276 and carbon steel, respectively. Liquid sulfur was separated from the citrate solution by gravity in a 850-gal sulfur separator. The sulfur separator was a pressurized, steam-jacketed decanter vessel fabricated of Hastelloy C-276-clad carbon steel. Liquid sulfur, with a purity of greater than 99.5 pct, flowed from the bottom of the sulfur separator to a heated 56,000-gal carbon steel storage tank. The citrate solution flowed from the top of the sulfur separator to the first reactor in the solution regeneration and sulfur precipitation operation.

Solid impurities were removed from the liquid sulfur by a filter. A pump transferred one-third of the liquid sulfur to loadout for marketing or offsite storage. Another pump transferred the other two-thirds of the liquid sulfur to the H_2S generator, where it was used to manufacture H_2S gas. The sulfur loadout pump, which pumped 50 gal/min at 260° F and 20-lbf/in^2 differential pressure, was driven by a 3-hp electric motor and had a cast-steel case and cast-iron impeller. The sulfur transfer pump, which pumped 15 gal/min at 260° F and 72-lbf/in^2 differential pressure, was driven by a 3-hp electric motor and had a cast-iron case and impeller.

SO_4^{2-} Removal

In the citrate process, up to 1.5 pct of the sulfur in the flue gas forms H_2SO_4 rather than sulfur. The H_2SO_4 can come from the following:

1. SO_3 contained in the flue gas may be absorbed in citrate solution.
2. Absorbed SO_2 in the form of HSO_3 ion may be oxidized during absorption.
3. $S_2O_3^{2-}$, which is a sulfur compound formed during solution regeneration, decomposes during sulfur melting.

The H_2SO_4 was neutralized with NaOH, which formed Na_2SO_4 in solution. $Na_2SO_4 \cdot 10H_2O$ can be crystallized from a chilled citrate solution, thus providing a method to reduce the buildup of Na_2SO_4 in the solution.

A vacuum crystallizer cooled a 5- to 10-gal/min bleed stream of citrate solution and crystallized $Na_2SO_4 \cdot 10H_2O$.

The crystallizer had an approximate 4 st/d capacity of $Na_2SO_4 \cdot 10H_2O$. Wetted parts of the crystallizer were FRP, Hastelloy, or rubber-lined carbon steel.

H_2S Generation

Recovered elemental sulfur, natural gas, and steam reacted to form H_2S. An on-site H_2S generator produced up to 35 st/d H_2S in a fixed-bed catalytic reactor. The design of the H_2S generator was based on a proprietary process developed by Home Oil Co., Ltd., as modified and pilot-plant-tested by the Bureau.

The H_2S generator was designed so that the reaction was at least 95 pct efficient. Impurities besides CO_2 and H_2O include CS_2 and COS. Materials of construction for the H_2S generator process include suitable proprietary stainless steels, Alonized stainless steel, and stainless steel lined with high-temperature refractories. Additionally, the H_2S generator was designed to operate using a CO reductant should natural gas supplies become unavailable.

The H_2S generator consisted of the following main units:

1. A natural gas compressor.
2. An oil-fired sulfur superheater.
3. A catalyst-filled main reactor.
4. A heat exchanger after the main reactor.
5. A catalyst-filled trim reactor.
6. A waste-heat boiler after the trim reactor.
7. A sulfur feed tank.
8. Two product heat exchangers.

Figure 43 shows a schematic diagram of the demonstration plant H_2S generator. The dashed lines show the modifications that were made after corrosion damaged the heat exchanger between the main reactor and the trim reactor. Intergranular corrosion damaged this heat exchanger as well as the main reactor's stainless steel shell. The main reactor was replaced with one having a carbon steel shell. A length of pipe replaced the heat exchanger. Two product heat exchangers were operated alternately. One heat exchanger cooled the product gas while the other was being heated with steam to melt sulfur, which drained to the sulfur feed tank. Product gas flowed through the sulfur feed tank to allow collection of excess sulfur. The main reactor operated at 1,150° to 1,200° F with an excess of sulfur and steam of 10 and 25 pct, respectively. In actual operation, H_2S production rarely exceeded one-third of the design rate because of low SO_2 absorption, low powerplant loads, and a lower sulfur content of the coal. An excess of sulfur and steam was necessary to maintain the temperature of the main reactor. The operation was relatively trouble-free, except for plugging of the H_2S generator product lines entering the regeneration reactors.

Throughout the last year of operation, sulfur carryover from the H_2S generator caused plugging of the H_2S gasline to the regeneration reactors. This prevented operation of the plant for more than 10 days. The plugging problem appeared after the removal of the original product coolers, which failed because of intergranular corrosion. The replacement coolers were of a different design and less efficient. The H_2S product consistently assayed between 70 and 78 vol pct H_2S on a dry basis. Lower strength H_2S gas contained from 10 to 12 vol pct CH_4, which indicated inefficient H_2S generator operation. Good-quality H_2S gas contained, in dry vol pct, 78 H_2S, 19 CO_2, 2 CH_4, 1 COS, and traces of CS_2 and N_2. Usually, over 98 pct of the H_2S was used to regenerate the citrate solution.

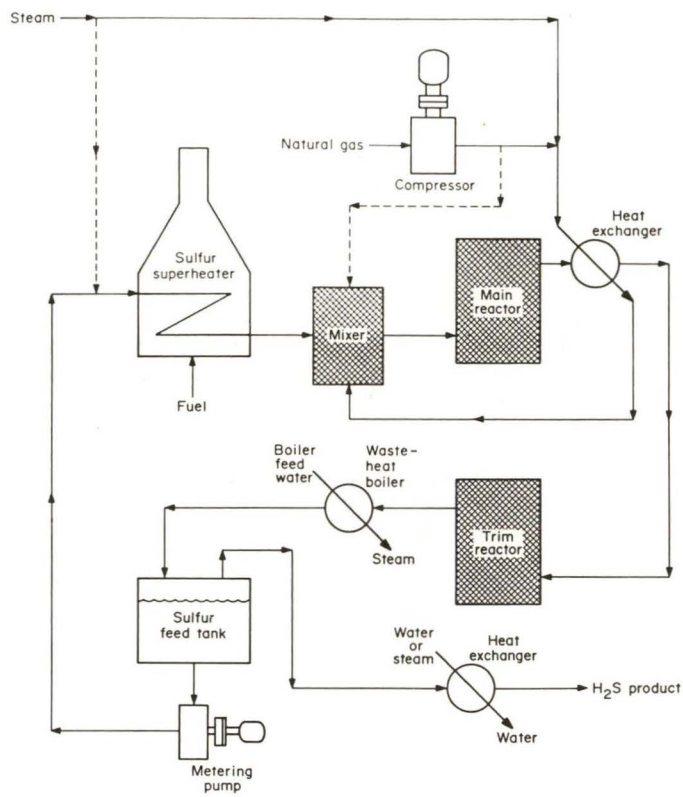


Figure 43.—Schematic diagram of demonstration plant H_2S generator.

Safety

Operator Training

Operator training, which included 2 weeks of classroom instruction on the various phases of plant operation, emphasized safety. Lectures and a movie on the hazards of H_2S gas were included in the training. Demonstrations were conducted on the proper use and care of the self-contained breathing apparatus. Time was allotted for practice in wearing and adjusting the equipment and in refilling empty breathing-air bottles. During plant operations, regulations called for all operators to carry the breathing apparatus when working in an area of possible hazard. The hazard area included the H_2S generator and the regeneration superstructure.

H_2S Monitors

Twelve H_2S monitors, sensitive to only a few parts per million of H_2S gas, were provided throughout the plant. These instruments had indicators and alarms in the control room as well as audible alarms that sounded over the loudspeaker system.

H_2S– indicating cards were kept in selected locations around the plant. These paper cards turn dark in the presence of very small amounts of H_2S and can be used to provide a permanent record of very small H_2S leakage over a long period of time. Cards must be inspected and read manually, the results recorded, and used cards replaced by fresh ones. These cards provided a means of detecting small leaks so that the problem could be corrected.

Engineered Safety Features

Three H_2S vent systems were provided in the plant design. In normal operation, unreacted H_2S gas in the regeneration reactors flowed through a vent system to either of the two powerplant boiler fireboxes for combustion. A second vent system was installed in the various solution storage tank vents. This system, equipped with a blower, collected any fugitive H_2S in the absorbent solution and prevented H_2S emission to the atmosphere. Gases from the second vent system were also burned in the powerplant boilers. The third system, piped to a flare located on the top of the absorber stack, was an emergency vent that received gases from the H_2S gas system. When required, this system burned any H_2S gas in a natural gas flame, which burned constantly at the flare tip.

Personnel Requirements

Two persons per shift were required for the demonstration plant operation. On day shift, a foreman, one utility person, and three maintenance persons were usually also required.

SUMMARY

The full-scale demonstration plant at St.Joe's George F. Weaton Power Station operated intermittently for about 3 yr. A lack of funds prevented completion of a formal demonstration of the process. However, the preliminary test results showed that the Bureau's citrate process is capable of—

1. Removing over 90 pct of the SO_2 contained in a coal-fired powerplant flue gas.
2. Producing an elemental sulfur product with a purity of 99.5 pct that is suitable for the manufacture of H_2S or H_2SO_4.

CHAPTER 5.—CORROSION TESTS AND ANALYSES IN SUPPORT OF THE CITRATE PROCESS

By L. L. Oden and G. Asai[1]

With a section on In-Plant Corrosion Testing and Analysis
By P. F. Ellis II

CORROSION IN H_2S GENERATOR OF BUNKER HILL PILOT PLANT

Background

Between February 1974 and November 1975, the citrate process pilot plant at the Bunker Hill smelter operated for about 5,400 h (*13*). During the initial 2,300 h of plant operation, H_2S was obtained from a commercial vendor and delivered on-site in low-pressure tanks. For the remaining 3,100 h, H_2S was produced on-site by reacting sulfur, natural gas, and steam in an apparatus fabricated largely from 300-series stainless steels. In late 1976, the pilot plant was dismantled, and the H_2S generator was examined for corrosion.

The H_2S generator, shown schematically in figure 38 in chapter 3, was operated in four different modes during its lifetime. Initially, during shakedown trials, mode 1 operation was used, wherein steam, natural gas, and sulfur were superheated in separate coils. Sulfur vapor at 1,300° to 1,380° F and natural gas at about 1,200° F were reacted in catalytic reactor 1. The products were cooled below the dewpoint of sulfur in an air-cooled heat exchanger (air cooler) and a steam-jacketed heat exchanger (steam cooler 1). Unreacted sulfur was removed by a small, gravity-settling, steam-jacketed sulfur knockout trap.

Superheated steam at 750° to 930° F was added after the sulfur trap, and reactants flowed to catalytic reactor 2. The product gases were passed through a steam-jacketed heat exchanger (steam cooler 2), two sulfur knockout traps, and a water-jacketed heat exchanger (water cooler) to provide H_2S containing about 16 pct CO_2 and 16 pct water vapor.

Corrosion specimens were obtained from the generator when it was dismantled. *Specimen 1* was obtained from near the broken end of the original sulfur superheater coil, which failed after only 660 h of operation. Numerous stops and starts were necessary during initial phases of the operation. Accompanying changes from sulfidizing to oxidizing conditions probably contributed significantly to the short life of the original sulfur superheater coil.

Within 4 weeks (730 h integrated operation) after installing the second sulfur superheater coil, the procedure was changed to bypass reactor 2 and steam cooler 2 and inject the superheated steam along with superheated natural gas and sulfur into reactor 1 (mode 2). Then the steam superheater was discontinued (mode 3). Steam, together with natural gas, was injected into the natural gas superheater coil for mode 3 operation, which bypassed reactor 2 and steam cooler 2. The second sulfur superheater coil failed after about 1,340 h of operation. That coil was lost during a cleanup by smelter personnel.

The original sulfur superheater outlet spool, represented by *specimen 2*, was changed when the third and final sulfur superheater coil was installed. The second outlet spool, represented by *specimens 3* and *4*, had been subjected to the severest environmental conditions the third coil had; the third coil therefore was not sampled. Mode 4 operation, in which all reactants were fed to the sulfur superheater coil (reactor 2 and steam cooler 2 were discontinued), was practiced during the 1,100 h that the second sulfur superheater outlet spool was in service. The remaining samples were in place during the entire life of the H_2S generator, about 3,100 h.

Table 30 lists each specimen by number, a short description, the alloy designation based upon chemical analysis, and the best estimate of exposure time and temperature. All pipes were in the wrought and annealed condition. All cast flanges and tees had been annealed, as judged from the respective microstructures.

Corrosion specimens cut from the pipes, tees, and flanges were sized to include weld metal and heat-affected zones in all cases where pipe-flange or pipe-tee junctions were studied. Weld metals were not specifically analyzed for alloy content.

Observations

The piece of 2-in, schedule 160 pipe of *specimen 1* was analyzed near the broken end, which is assumed to be near the outlet end. Corrosion of the inner surface of the pipe was nearly uniform, with only shallow grain-boundary attack and broad, shallow pitting. The pipe exterior was not attacked. The wall thickness had decreased from the original 0.344 in to about 0.125 in, which, based on an assumed exposure time of 660 h, is a rate of 2.9 in/yr. Grain-boundary sulfide penetration of the inner surface of the pipe was 4 to 5 mils, indicating that the corrosion products were rapidly removed. Carbide formation was evident across the pipe section, indicating that extensive sensitization occurred at the operating temperature. Sulfidation, particularly of the grain boundaries, apparently was enhanced by carbide formation, which removed chromium from the matrix. Rapid thinning of the wall by grain removal and continuous intergranular formation of the brittle carbide phase across the pipe section are most likely responsible for the loss in ductility and subsequent failure by thermal fatigue of the original sulfur superheater coil.

[1]Metallurgist, Albany Research Center, Bureau of Mines, Albany, OR.

Table 30.—Description of corrosion specimens obtained from Bunker Hill pilot plant H_2S generator

Specimen	Location	Description	Exposure[1]		
			Time, h	Operational mode[2]	Temp, °F
1	Original sulfur superheater coil	2-in, schedule 160, type 310 SS pipe. . .	660	1	~1,350
2	Original sulfur superheater outlet spool	2-in, schedule 160, type 310 SS pipe and flange.	2,000	All	~1,350
3	2d sulfur superheater outlet spool	2-in, schedule 160, type 310 SS pipe and type 304 SS flange.	1,100	4	~1,350
4	. . do	2-in, schedule 160, type 310 SS pipe and flange.	1,100	4	~1,350
5	Thermowell in reactor 1	Concentric 3/8- and 1/8-in, schedule 40, type 316 SS pipes.	3,100	All	~1,075
6	Inlet thermowell to steam cooler 2	1/2-in, schedule 40, type 304 SS pipe. . .	730	1	750- 840
7	Steam-jacketed spool between steam cooler 1 and sulfur knockout trap, sulfur-trap end.	1-1/2-in, schedule 40, type 316 SS pipe and flange.	3,100	All	750- 840
8	Steam-jacketed spool between steam cooler 2 and sulfur trap, center tee.	1-1/2-in, schedule 40, type 316 SS pipe and type 304 SS cast tee.	3,100	All	570- 750
9	Water cooler outlet spool, water cooler end.	1-1/2-in, schedule 40, type 304 SS pipe and type 316 SS flange.	3,100	All	~150
10	Water cooler outlet spool, first tee	1-1/2-in, schedule 40, type 304 SS pipe and type 316 SS cast tee.	3,100	All	~150

SS Stainless steel.

[1]Startup procedure: Preheat with airflow to 300° F, switch to steam and heat to 900° to 1,000° F, then switch to sulfur and heat to 1,350° F. The procedure was reversed to shut down.

[2]Operational modes:

Mode 1: All reactants—sulfur, natural gas, and steam—were superheated in separate coils. Sulfur and natural gas were contacted in reactor 1 and then hydrolyzed with steam in reactor 2.

Mode 2: Reactor 2 and steam cooler 2 were bypassed.

Mode 3: Natural gas and steam were fed to the natural gas superheater coil and contacted with superheated sulfur in reactor 1. Reactor 2 and steam cooler 2 were bypassed.

Mode 4: All reactants were superheated in the sulfur superheater coil, and the chemical reaction was completed in reactor 1. Reactor 2 and steam cooler 2 were bypassed.

Specimen 2 was cut from the pipe approximately 18 in from the sulfur superheater end of the spool. General corrosion with shallow pitting centered on grain boundaries produced a tightly adherent scale up to 0.4 in thick. Intergranular sulfide formation to depths of 5 to 10 mils was observed. Sensitization at the operating temperature was indicated by extensive carbide precipitation in the pipe metal. Carbide diminished toward the interior, and a dark gray intergranular phase, identified as sigma (FeCr), became prevalent. The corrosion rate of *specimen 2*, based on remaining wall thickness of the pipe, was about 3 in/yr, similar to that observed for the original sulfur superheater coil.

The pipe in *specimen 2* had a grain size of about ASTM 3,[2] whereas the cast flange of the original sulfur superheater outlet spool was finer grained (ASTM 7). Sulfidation of the flange produced shallow pitting and extensive grain-boundary penetration. Sigma-phase was very prevalent in the flange metal. The weld metal and heat-affected zones between pipe and flange were attacked by shallow pitting not unlike that in the pipe and flange metals.

A loose, black sulfide scale was formed on both pipe and flange of the second sulfur superheater outlet spool (*specimen 3*) during the 1,100 h in service, but corrosion was much less than in its predecessor. Based on a final wall thickness of 0.32 in, the rate of corrosion was 0.2 in/yr. Intergranular attack extended an additional 20 mils, and a rate of 0.4 in/yr is more realistic. The weld metal, which is similar in composition to type 310 stainless steel, and the heat-affected zone in the type 310 stainless steel pipe contained large intergranular precipitates of sigma-phase but very little chromium carbide. The weld metal suffered some intergranular cracking to depths of 2 to 5 mils. In this application, the type 304 stainless steel flange performed as well as the other type 310 stainless steel flanges in the system.

A loose, black scale about 0.1 in thick was observed in pipe and flange of *specimen 4*. Both sulfides and oxides were present in the scale. Corrosion produced an irregular surface of broad, shallow pits on pipe and flange. The pipe was coarse grained (ASTM 3), with sigma-phase present in grain boundaries. The cast flange was finer grained (ASTM 7) and also contained much intergranular sigma-phase. Grain boundaries were clearly the initiation points for subsequent pit formation. Numerous shallow cracks 2 to 3 mils deep were observed in the weld metal, and the heat-affected zone in the flange had been preferentially attacked. The corrosion rate for the flange was 0.8 in/yr, based on 1,100 h exposure, compared with 0.6 in/yr for the pipe.

Considerable corrosion of the thermowell of *specimen 5* had occurred to reduce the original wall thickness of the outer pipe (0.091 in) to zero over a length of 21 in. No scale remained on the pipe. Metallographic examination of the pipes 14 in from the flange revealed each to be free from precipitate phases. Corrosion had been severe but uniform.

The thermowell of *specimen 6*, a 1/2-in schedule 40 pipe, tapered 0.005 in. in 12 in. for a corrosion rate of 0.01 in/yr based on 730 h exposure. The alloy seems ideal for this particular application, but the temperature unfortunately

[2]American Society for Metals. Atlas of Microstructures of Industrial Alloys. Metals Handbook, v. 7, 8th ed., 1972, p. 4.

is not known with certainty. The best estimate is less than 840° F but greater than 750° F.

Both pipe and flange of *specimen 7* were covered with a loose, black scale less than 0.1 in thick. It is interesting to note that nickel sulfide was detected by X-ray analysis of the scale that formed at 750° to 840° F (by best estimate). No measurable decrease was observed in wall thickness of the pipe. Corrosion of the 1-1/2-in schedule 40 pipe appeared to be uniform.

The cast flange, although similar in composition to the pipe, suffered extensive intergranular sulfidation. Weld metal between pipe and flange and heat-affected zones was not attacked.

A loose, black scale less than 0.1 in thick covered the surface of both the pipes and the tee of *specimen 8*. Corrosion produced broad, shallow pitting that was more pronounced in the pipes than in the tee. The original tool marks were visible in the tee.

Corrosion products were not observed on the pipe and flange of *specimen 9*. However, the inner surface of the 1-1/2-in schedule 40 pipe was covered with a thin (0.1-in) layer of sulfur. An accumulation of sulfur about 0.5 in thick was present at the bottom of the pipe. Flange, pipe, and weld metal were covered with pits up to 0.05 in. in diam and 0.2 in deep. Intergranular cracking 2 to 5 mils deep was observed in the heat-affected zone of the type 304 stainless steel pipe.

Numerous small, deep pits (0.05 in. in diam by 0.02 in deep) were observed in the cast tee of *specimen 10*. The welds were severely attacked, and the heat-affected zone in the pipe was pitted to depths of 0.05 in. Pitting appeared to be random, and intergranular attack was not observed.

Weakly acidic aqueous phases, condensed from the vapor reinforced with chloride ion from the municipal water supply, were the apparent cause of pitting corrosion of types 304 and 316 stainless steel in the water cooler.

Summary

On the basis of the failures experienced during operation and the evidence gained in this study, it is clear that 300-series stainless steels are not adequate in the carburizing-sulfidizing atmospheres of the H_2S generator at 1,100° to 1,350° F. Corrosion in the sulfur superheater was very likely increased by thermal cycling and the change to oxidizing conditions during shutdown and restarting of the H_2S generator. The presence of water vapor in the superheater was probably beneficial during mode 4 operation. The observation of extensive carbide formation within the stainless steel operating at temperatures of 1,350° F indicates severe sensitization and/or carburization. Sulfur attack, which was often intergranular, was clearly aided by carbide formation.

The austenitic stainless steels performed adequately in the steam cooler 1 inlet thermowell and the connecting spool between sulfur knockout trap and steam cooler 2, where temperatures were below 840° F. However, the same alloys were severely attacked by pitting corrosion in the final water cooler outlet spool, where the temperature probably did not exceed 200° F.

DEMONSTRATION PLANT AT GEORGE F. WEATON POWER STATION

Background

The Bureau's citrate process for controlling SO_2 emissions in powerplant and industrial stack gases shares with all other aqueous scrubbing processes the problems of corrosion. The severity of this problem became apparent after the postoperative analysis of the pilot plant at the Bunker Hill smelter. Materials-related research was subsequently begun in 1977, prior to constructing the demonstration plant. Plant design, materials of construction, and anticipated operating procedures were scrutinized for potential problems, and a program of corrosion testing was begun to characterize materials in conditions simulating in-plant conditions.

Laboratory Corrosion Tests Simulating In-Plant Conditions

Corrosion testing was begun at the Bureau's Albany Research Center during the design stage for the demonstration plant and continued through construction and initial operation. Screening tests initially were conducted to provide a rational basis for recommending materials of construction. Later testing was designed to provide alternative materials in the event of failure during operation. Many metals, alloys, vapor-aluminum-diffused alloys, organic coatings, ceramic materials, and castable refractories were evaluated in conditions simulating in-plant exposure in the citrate process. These conditions included the following two gaseous and two aqueous environments:

1. Suflur vapor and sulfur vapor containing steam (dry and wet sulfur vapor), simulating the sulfur superheater of the H_2S generator,
2. H_2S-CO_2-steam, simulating the H_2S generator,
3. Rich citrate solution, simulating the SO_2 absorber, and
4. Lean citrate solution, simulating the sulfur melter and decanter.

Sulfur Vapor and Sulfur Vapor Containing Steam

The H_2S reactor requires inputs of preheated sulfur vapor, steam, and CH_4 at 1,150° to 1,450° F to produce H_2S containing about 16 pct CO_2 and 16 pct water vapor. Sulfur could be injected optionally as the element (dry) or premixed with steam (wet). These environments were the most corrosive conditions in the H_2S generator; therefore, corrosion tests were required in both conditions.

Materials and Specimen Preparation

Materials tested in dry and wet sulfur vapor are conveniently considered in four categories: (1) iron-base and nickel-base alloys, (2) vapor-aluminum-diffused iron-base alloys, (3) reactive and refractory metals, and (4) refractory nonmetals and miscellaneous materials. The nominal compositions of metals and alloys tested are listed in table 31.

Corrosion specimens of alloy materials were sheared from sheet as obtained from commercial vendors or prepared in-house. Specimens were nominally 6 by 0.75 in by sheet thickness. The cut edges were deburred by grinding, but the as-rolled mill finish was not altered. Weights of degreased and dried specimens were determined to ± 1 mg. The uncertainty in the surface area of corrosion specimens of alloy materials is estimated to be less than 3 pct.

Alloys to be treated with aluminum were prepared as described for corrosion specimens and then submitted to Alon Processing Inc., Tarentum, PA, for vapor-aluminum diffusion using their proprietary Alonizing and DuAlonizing processes. Alonizing provides an aluminum-enriched sur-

Table 31.—Nominal composition of alloys evaluated in laboratory and in-plant corrosion tests, weight percent

Alloy	Cr	Ni	Mo	Al	Fe	Co	C max	Si max	Mn max	Cu	Zn	Ti	Cb	Other
Aluminum:														
1100	NS	NS	NS	>99	([1])	NS	NS	([1])	0.05	NS	NS	NS	NS	
2024	0.1	NS	NS	Bal	0.5	NS	NS	0.5	.9	4.9	0.25	NS	NS	1.5 Mg
3003	NS	NS	NS	Bal	.7	NS	NS	.6	1.5	.2	.1	NS	NS	
4043	NS	NS	NS	Bal	.8	NS	NS	6	.05	.3	.1	NS	NS	.05 Mg
5052	.25	NS	NS	Bal	([2])	NS	NS	([2])	.10	.1	.1	NS	NS	2.5 Mg
5086	NS	NS	NS	Bal	NS	NS	NS	NS	.5	NS	NS	NS	NS	4 Mg
6061	.25	NS	NS	Bal	.7	NS	NS	.8	.15	.40	.25	0.15	NS	1 Mg
Allegheny:														
6X	20	24	6.5	NS	Bal	NS	NS	NS	NS	NS	NS	NS	NS	
29-4	29	NS	4	NS	Bal	NS	NS	NS	NS	NS	NS	NS	NS	
Armco 18SR	18	.3	NS	2	Bal	NS	0.04	1	.3	NS	NS	.4	NS	
Carbon steel	NS	NS	NS	NS	Bal	NS	.2	NS	NS	NS	NS	NS	NS	
Carpenter 20Cb-3	20	35	[3]2.4	NS	Bal	NS	.07	1	2	4	NS	NS	([4-5])	
Chrysler CRM-4[6]	NS	NS	NS	6	Bal	NS	NAn	NS	NS	NS	NS	NS	NS	
Durichlor 51	4.5	NS	3	NS	Bal	1	.85	14.5	NS	NS	NS	NS	NS	
E-Brite 26-1	26	NS	1	NS	Bal	NS	.005	.4	NS	NS	NS	NS	NS	
Hastelloy:														
B	1	Bal	28	NS	5.5	2.5	.05	1	1	NS	NS	NS	NS	
C	16	Bal	17	NS	6	2.5	.15	1	1	NS	NS	NS	NS	5 W
C-4	16	Bal	15.5	NS	3	2	.015	.08	1	NS	NS	[7].7	NS	
C-276	15	Bal	16	NS	5.5	2.5	.02	.08	1	NS	NS	NS	NS	4 W
G	22	Bal	6.5	NS	19.5	2.5	.05	1	2	2	NS	NS	[4]2	1 W
Haynes 20-Mod	22	26	5	NS	Bal	NS	NS	NS	NS	NS	NS	NS	NS	
Hoskins 815	22	NS	NS	4.5	Bal	NS	.1	.5	NS	NS	NS	NS	NS	
Incoloy:														
800	20.5	32	NS	.3	46	NS	.1	1	1.5	.3	NS	.3	NS	
825	21.5	41.8	3	.15	30	NS	.05	.5	1	3	NS	.9	NS	
Inconel:														
600	15.8	76	NS	NS	7.2	NS	.15	.5	1	NS	NS	NS	NS	
601	23	60.5	NS	1.35	14.1	NS	.1	.5	1	1	NS	NS	NS	
617	22	54	9	1	1.5	12.5	.07	.5	.5	NS	NS	NS	NS	
625	21.5	61	9	[7].4	[7]5	1	.1	.5	.5	.1	NS	[7].4	[4]3-4	
Jessop JS-700	21	25	4.5	NS	Bal	NS	.04	1	2	NS	NS	NS	[7].4	
MP35N multiphase	20	35	10	NS	NS	35	NS	NS	NS	NS	NS	NS	NS	
Multimet N-155	21	20	3	NS	Bal	20	.15	.5	1.5	NS	NS	NS	1	2.5 W
Nitronic 50	22	22	2	NS	Bal	NS	.06	1	6	NS	NS	NS	.2	.2 V, .3 N
Rolled Alloys:														
RA 330	19	35	NS	NS	43	NS	.08	1.5	2	NS	NS	NS	NS	
RA 333	25	45	3	NS	18	3	.08	1.5	2	NS	NS	NS	NS	3 W
Sandia:														
X-1[8]	24	19.5	NS	NS	Bal	NS	.25	1.5	2	NS	NS	2.9	NS	
X-2[8]	29.1	66.4	6.5	NS	Bal	2.5	.001	1	NS	NS	NS	4.5	NS	
Sandvik:														
3RE60	17	12	[3]2.6	NS	Bal	NS	.03	1	2	NS	NS	NS	NS	
2RK65	19.5	25	[3]4.6	NS	Bal	NS	.02	.45	1.8	1.5	NS	NS	NS	
Stainless steel:														
Type 304	19	9	NS	NS	Bal	NS	.08	1	2	NS	NS	NS	NS	
Type 310	25	20	NS	NS	Bal	NS	.25	1.5	2	NS	NS	NS	NS	
Type 316	17	11	[4]2.8	NS	Bal	NS	.08	1	2	NS	NS	NS	NS	
Type 316L	17	12	[4]3.2	NS	Bal	NS	.03	1	2	NS	NS	NS	NS	
Type 317	19	13	[4]3.6	NS	Bal	NS	.08	1	2	NS	NS	NS	NS	
Type 406	13	NS	NS	4	Bal	NS	.08	1	1	NS	NS	NS	NS	
Type 430	16	NS	NS	NS	Bal	NS	.12	1	1	NS	NS	NS	NS	
Type 446	25	NS	NS	NS	Bal	NS	.35	1	1.5	NS	NS	NS	NS	
Stainless steel and aluminum:														
310 + 9Al[9]	23	18	NS	9	Bal	NS	NS	NS	NS	NS	NS	NS	NS	
316 + 8Al[9]	17	11	2.5	8	Bal	NS	NS	NS	NS	NS	NS	NS	NS	
Titanium:														
Ti Code 12	NS	.8	.3	NS	NS	NS	NS	NS	NS	NS	NS	Bal	NS	
Ti-50A	NS	NS	NS	NS	[6].3	NS	.1	NS	NS	NS	NS	99	NS	[7].25 O
Ti-6Al-4V	NS	NS	NS	6	.3	NS	.08	NS	NS	NS	NS	Bal	NS	4 V
Uniloy 18-2	18.5	NS	2	NS	Bal	NS	.08	NS	1.5	NS	NS	NS	NS	
Zr 705	NS	NS	NS	NS	NS	NS	NS	NS	NS	NS	NS	NS	3	3 Hf Bal Zr

Bal Balance.
NAn Not analyzed.
NS No specification.
[1]Fe + Si = 1 wt pct, max.
[2]Fe + Si = 0.45 wt pct.
[3]Analyzed composition.
[4]Cb + Ta.
[5]8 × C.
[6]Experimental alloy by Chrysler Corp.
[7]Maximum.
[8]Experimental alloy by Sandia Laboratories.
[9]Experimental in-house alloy.

face that is generally very resistant to both sulfidation and oxidation (*42-43*).

A consistent specimen configuration was not possible for the refractory nonmetals and miscellaneous materials, and testing was not complete over the temperature range of 1,150° to 1,450° F.

Graphite, SiC, and $MoSi_2$ (molybdenum disilicide) were tested in rod configuration, 4 in long by 3/16 to 3/8 in. in diam. Specimens of alumina, mullite, and fire clay were cut by an abrasive wheel from various shapes obtained from commercial vendors. Cylinders (1 in long by 0.75 in diam) of the castable refractories were core-drilled from

material prepared and cured according to the manufacturer's directions. The performance of Vycor, high-silica glass and fused quartz was inferred from observation of the apparatus, which was constructed solely of these materials.

Apparatus

Corrosion tests in dry and wet sulfur vapor were conducted in a cylindrical Vycor glass test chamber about 36 in long by 2.25 in OD (fig. 44). Sulfur vapor was provided by an internal, 4-in-deep annular reservoir of sulfur, which was heated by a separate furnace. The reservoir was heated to 824° F (boiling point of sulfur) for tests in dry sulfur vapor, and to 752° F (400 mm vapor pressure) for tests in wet sulfur vapor. The condenser (upper part) of the test chamber was maintained at about 300° F to provide continuous condensing and refluxing of sulfur. Helium saturated with water vapor at 175° to 195° F, and flowing at about 20 cm^3/min, was injected into the chamber through the steam generator for wet sulfur tests. This method provided an atmosphere of about one-third each of sulfur, steam, and helium. A small flow of helium (50 cm^3/min) was maintained across the outlet of the test chamber to prevent air from entering. Specimens were hung on the inner sidewall of the sulfur reservoir by Vycor glass rods. Seven specimens, often of different compositions, could be tested simultaneously. Specimen temperature was measured by a thermocouple inserted into the thermowell through the bottom of the test chamber. The thermowell extended to about the midpoint of the specimens. Temperature variation within the zone occupied by the specimens was held to ±20° F by external shunts on the furnace elements.

Analytical Methods

Corrosion rates were calculated from the initial surface area and the weight loss of descaled specimens. Corrosion products were usually loose and readily removed except for an adherent, thin inner layer, which was removed by vapor honing. A simple correction was made for the metal removed by vapor honing based on the response of a blank specimen and the estimated time that metal surface was exposed to abrasive action. The correction was small—equivalent to 1 to 5 mil/yr in the worst case.

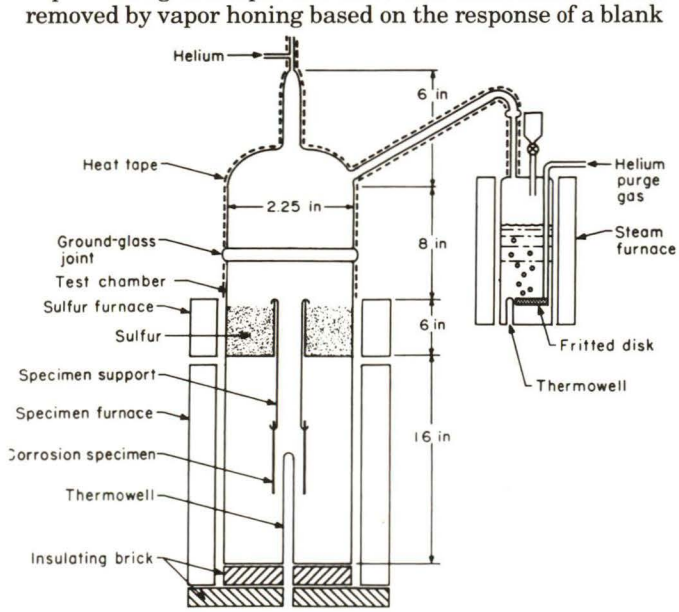


Figure 44.—Apparatus for laboratory corrosion tests in dry and wet sulfur vapor.

X-ray diffraction patterns were recorded for many corrosion products, as discussed later in detail. In some cases, scales could be removed and split into multiple layers, each of which was analyzed front and back. In every case, scales were ground to a fine powder, and the powder diffraction pattern was recorded. A high-angle vertical diffractometer was used with nickel-filtered CuKα radiation, a scintillation detector with solid-state electronics, a pulse height discriminator, and a strip chart recorder. The X-ray tube was a broad-focus, high-energy tube operated at 45 kV and 40 mA. The scan was made at 1° 2θ/min, while the strip chart was run at 1/2 in/min. Phase identification was accomplished with the aid of the Powder Diffraction File of the JCPDS International Centre for Diffraction Data.

Specimens for metallography, scanning electron microscope (SEM) examination, and electron microprobe analysis were carefully removed from the test chamber and immediately submerged in plastic epoxide resin. A small cross section was later cut from near the center by an abrasive cutoff wheel. Conventional metallographic mounting and polishing techniques were used, followed by electrolytic etching at room temperature in 10 pct oxalic acid. Quantitative electron microprobe analyses were made on freshly polished surfaces of metallography specimens. Three elements were analyzed simultaneously by measuring the intensities of the appropriate characteristic radiation. Operating conditions were an accelerating voltage of 15 kV and beam current ranging from 30 to 150 nA.

Results and Discussion

Iron- and Nickel-Base Alloys

Both dry and wet sulfur vapor were extremely corrosive, as shown by the corrosion rates for 10-day tests in table 32. The corrosion resistance of both ferritic and austenitic alloys improved with increasing chromium and aluminum contents. Most alloys were more corroded by dry sulfur vapor than wet sulfur vapor, with the exception of Hastelloy C (a nickel-base alloy), which was more susceptible in the presence of steam. Aluminum was generally more effective than chromium as an alloy addition to both ferritic and austenitic alloys in dry and wet sulfur vapor. The most resistant alloys had the highest alloy content. However, those alloys were also the most erratic in both dry and wet atmospheres.

Corrosion products (scales) were usually nonadherent but provided some protection for both the ferritic and austenitic alloys. For example, the mean corrosion rate for ferritic type 446 stainless steel was 156, 163, and 613 mil/yr in 10-, 5-, and 2-day tests, respectively. Austenitic stainless steels performed in a like manner. The mean rate for type 310 stainless steel in dry sulfur vapor at 1,450° F increased from 343 mil/yr in a 10-day test to 1,115 in a 2-day test. Some test results were very erratic, especially in dry sulfur vapor at intermediate temperatures. This effect was attributed to random spalling or simple disengagement of scales during the test.

Scales formed in wet sulfur vapor were generally thinner and more adherent than scales formed at equivalent temperatures in dry sulfur vapor. The protective nature of scales is manifest in generally lower corrosion rates in wet sulfur vapor on all alloys with the exception of Hastelloy

Table 32.—Corrosion rates of iron- and nickel-base alloys in dry and wet sulfur vapor at 1,150° to 1,450° F, mils per year
(10-day tests)

Alloy	Dry				Wet			
	1,150° F	1,250° F	1,350° F	1,450° F	1,150° F	1,250° F	1,350° F	1,450° F
Allegheny 29-4	[1]59	[2]60- 330	[1]122	296	[1]23	[1]53	[1]6	[1]90
Armco 18SR	32	[2]80-1,000	195	160	[2]7- 120	[2]30-150	[2]70-360	[1]90
Carbon steel	[1]>1,450	NAn	NAn	NAn	[1]>1,100	NAn	NAn	NAn
Chrysler CRM-4	NAn	[1]>250	NAn	NAn	NAn	NAn	NAn	NAn
E-Brite 26-1	[1]62	183	101	240	[1]18	56	[2]5- 58	[1]115
Hastelloy C-276	[1]63	[1]59	[1]182	[1]>182	[1]139	[1]114	[1]203	[1]1,160
Hoskins:								
705	33	[2]80- 470	150	142	6	23	42	65
815	[1]22	58	66	68	[1]7	15	25	[1]53
Ohmaloy 406	17	[2]3-1,000	176	208	12	21	45	48
Stainless steel:								
Type 310	53	117	207	343	38	55	62	[1]73
Type 316	[1]63	100	158	222	68	59	95	[1]83
Type 446	93	156	102	294	35	[1]69	[1]60	NAn
Stainless steel and aluminum:								
Type 310 + 9Al	[1]3	[2]40-1,000	82	67	[1]2	[1]11	53	[1]59
Type 316 + 8Al	[1]17	[1]32	187	[1]46	[1]2	[1]22	58	[1]59

NAn Not analyzed. [1]Result of 1 test. [2]Results were extremely erratic.

C-276, a nickel-base alloy, which was definitely more susceptible to corrosion in wet sulfur vapor.

Nonuniform corrosion in the form of mild pitting and intergranular attack was apparent on all alloys. The additional penetration due to nonuniform corrosion was insignificant in comparison with the overall corrosion rate in both dry and wet sulfur vapor for all alloys except the ferritic iron-base alloys containing chromium and molybdenum (E-Brite 26-1 and Allegheny 29-4). These compositions were susceptible to severe internal sulfidation at temperatures above 1,250° F. The intergranular phase was analyzed by electron microprobe and found to be chromium sulfide (Cr_7S_8).

The alloy of choice for these particularly aggressive environments is Hoskins 815. With adequate corrosion allowance, types 446 and 310 stainless steels could be used with confidence based on their consistent behavior in both wet and dry sulfur vapor.

Vapor-Aluminum-Diffused Iron-Base Alloys

Vapor-aluminum diffusion (Alonizing and DuAlonizing) provides an aluminum-enriched surface layer or layers that vary in thickness and composition with alloy content (*49*). In general, the thickness of the aluminum-enriched layer decreased with increasing alloy content. Ferritic alloys acquired a thicker layer than austenitic alloys. DuAlonizing increased the aluminum per unit area by about a factor of 2, but the depth of the aluminum-enriched layer was increased by a factor of about 3. Actual measurements of aluminum-diffused specimens place coatings in the range of 7 to 10 mils for Alonized alloys and 22 to 33 mils for the DuAlonized alloys.

Aluminum-diffused alloys have good reputations in oxidizing, sulfidizing, and carburizing atmospheres. These alloys were prime candidates for the severely sulfidizing environment of the H_2S generator (*42-43*). Two austenitic alloys, two ferritic alloys, and low-carbon steel in both Alonized and DuAlonized conditions (except for carbon steel and Ohmaloy 406) were exposed to dry and wet sulfur vapor in 10-day tests at 1,150° to 1,450° F. The test results are summarized in table 33.

Corrosion in dry sulfur vapor was observed to be very erratic, especially at the intermediate temperatures. The aluminum-diffused surface has a very low corrosion rate. However, when breached, the more vulnerable substrate alloy corrodes catastrophically. Aluminum appears to exacerbate the corrosion of the substrate alloy in dry sulfur vapor, as evidenced by the observed erratic corrosion rates for all alloys tested in that environment. In contrast, corrosion of aluminum-diffused alloys in wet sulfur vapor was uniform and predictable.

A partial explanation for the erratic and often catastrophic corrosion of aluminum-diffused alloys in dry sulfur vapor is provided by the observed propensity of ferritic alloys to undergo intergranular attack. Cracks provide a convenient conduit for sulfur to the more vulnerable substrate metal and, in that way, provide an explanation for the observed corrosion of aluminum-diffused carbon steel.

It is important at this point to note that all aluminum-diffused iron-base alloys, including the austenitic stainless steels, have a ferritic surface layer containing iron, aluminum, chromium, and molybdenum (if present in the alloy). In austenitic alloys, the nickel is present in a subsurface, two-phase layer as the binary intermediate phase NiAl (*49*). The ferritic outer layer is brittle and often cracks, even before exposure to a corrosive environment. In austenitic alloys, the cracks do not penetrate the two-phase layer before exposure or after exposure to both dry and wet sulfur vapor. Cracking across the two-phase layer on austenitic alloys in dry sulfur vapor was not observed, yet the alloys often experienced catastrophic attack. From those observations, one is forced to conclude that aluminum actually enhances the corrosion rate of the substrate alloy in dry sulfur vapor. This conclusion is supported by the previous observation of erratic catastrophic attack in dry sulfur vapor of some alloys containing aluminum (Ohmaloy 406, Hoskins alloy 750, Armco 18SR, and 310 + 9Al).

From a practical point of view, it is imperative that steam be present during the heating, vaporizing, and superheating of sulfur in the H_2S generator. For that application, DuAlonized type 310 stainless steel is the alloy of choice.

Reactive and Refractory Metals

It is apparent from the corrosion test results in table 34 that the sulfidation resistance of the metals and alloys in this category closely parallels their oxidation resistance. Columbium and tantalum had acceptable and reproducible corrosion rates in dry sulfur vapor but were rapidly con-

Table 33.—Corrosion rates of vapor-aluminum-diffused iron-base alloys in dry and wet sulfur vapor at 1,150° to 1,450° F, mils per year
(10-day tests)

Alloy[1]	Dry				Wet		
	1,150° F	1,250° F	1,350° F	1,450° F	1,250° F	1,350° F	1,450°F
Carbon steel (A)	NAn	2	[2]19-1,100	NAn	NAn	NAn	NAn
E-Brite 26-1 (A)	[2-3]46-1,100	[2-3]31- 274	[3-4]14	[3-4]10	[3]3	[3-4]15	[3-4]26
E-Brite 26-1 (DA)	[3-4]1,100	[2-3]32- 324	[3-4]16	[3-4]9	[3-4]5	[3-4]13	[3-4]26
Ohmaloy 406 (A)	NAn	2	[2]17-1,100	NAn	NAn	NAn	NAn
Stainless steel:							
Type 310 (A)	[4]134	[2]1- 500	[2]27-1,200	[4]19	[4]11	[4]18	[4]28
Type 310 (DA)	[4]22	[2]14- 880	[4]55	[4]26	[4]9	[4]16	[4]24
Type 316 (A)	[4]173	[2]6- 750	[2]12-1,100	[4]13	[4]10	[4]17	[4]28
Type 316 (DA)	[4]38	[2]40-1,240	[4]39	[4]8	[4]2	[4]24	[4]26

NAn Not analyzed.

[1]A = Alonized (treated using a proprietary vapor-aluminum-diffusion process by Alon Processing Inc., Tarentum, PA); DA = DuAlonized (treated using an additional Alon vapor-aluminum-diffusion treatment probably identical to the first).
[2]Results were erratic.
[3]Severe intergranular corrosion noted.
[4]Results of 1 test.

Table 34.—Corrosion rates of reactive and refractory metals in dry and wet sulfur vapor at 1,150° to 1,450° F, mils per year
(10-day tests)

Metal or alloy	Dry				Wet			
	1,150° F	1,250° F	1,350° F	1,450° F	1,150° F	1,250° F	1,350° F	1,450° F
Columbium	18	21	52	28	143	>500	>500	>500
Molybdenum	NAn	456	NAn	NAn	NAn	NAn	NAn	NAn
Tantalum	16	44	16	22	>500	>500	NAn	NAn
Titanium	19	27	32	46	23	[1]77	[1]264	[1]283
Ti-6Al-4V	5	13	13	[2]28-120	12	[1]36	[1]86	[1]144
Tungsten	NAn	348	NAn	NAn	NAn	NAn	NAn	NAn
Zirconium	26	27	[2]38-222	75	>273	NAn	NAn	NAn

NAn Not analyzed.

[1]Result of 1 test.
[2]Results were erratic (cause for this believed to have been an air leak in the test chamber).

sumed in the wet environment. Titanium and its alloys were the best in both dry and wet sulfur vapor, but the corrosion rates in the wet environment were unacceptable above 1,250° F. Zirconium may be useful in dry sulfur vapor but appears to be susceptible to catastrophic attack if water or oxygen is present. Molybdenum and tungsten formed massive sulfide scales in dry sulfur vapor at 1,250° F, and no further testing was done.

Scales that formed on the corrosion specimens in dry sulfur vapor were probably adherent and protective at temperature but tended to disengage on cooling. Only columbium retained its scale at room temperature without some indication of disengagement.

Were it not for catastrophic attack in the wet environment, columbium and tantalum would be the materials of choice for application in sulfur vapor. Titanium and Ti-6Al-4V were the only materials in this category that could be used confidently in sulfur vapor.

Refractory Nonmetals and Miscellaneous Materials

Graphite, $MoSi_2$, and SiC were exposed only to dry sulfur vapor for 10 days at 1,250° and 1,450° F. The observed corrosion rates were as follows, in mils per year:

	1,250° F	1,450° F
Graphite	<1	40
$MoSi_2$	3	45
SiC	<1	<2

The corrosion scale on $MoSi_2$ was MoS_2. No scales were observed on graphite and SiC.

Alumina (Coors AD85) and mullite were evaluated at 1,450° F in both dry and wet sulfur vapor. Corrosion was less than 1 mil/yr in both environments. No evidence of attack was visible when the sectioned and polished specimens were examined under a light microscope.

Immunity of fused quartz (SiO_2) to both dry and wet sulfur vapor at all test temperatures was inferred from the absence of attack on the reactor vessels, which were constructed completely of this material.

Three castable refractory cements (A. P. Green's KS-4, General Refractories Co.'s High-Strength Brik Cast G, and Gunning Refractories Co.'s HYDRA-SEH 4) were evaluated in both dry and wet sulfur vapor. These cements were considered for application in the preconditioner and the two reactor vessels in the H_2S generator. Test specimens were prepared by core-drilling 3/4-in-diam by 1-in-long cylinders from bricks of the materials, which had been prepared and cured according to the manufacturers' recommendations. The ends of the test cylinders were surface-ground to provide parallel faces varying less than 0.005 in across the diameter. Specimens exposed to air, dry sulfur vapor, steam, and wet sulfur vapor for 30 days at 1,450° F were tested for compressive strength.

The mean compressive strengths of four duplicate specimens of the three castable refractory cements in the four environments are compared in figure 45. The data indicate that High-Strength Brik Cast G, which is definitely the strongest material tested in air, dry sulfur vapor, and steam, suffers a significant loss of strength in wet sulfur vapor. That material is probably not suitable for use in the H_2S generator. KS-4 and HYDRA-SEH 4 were satisfactory under all test conditions.

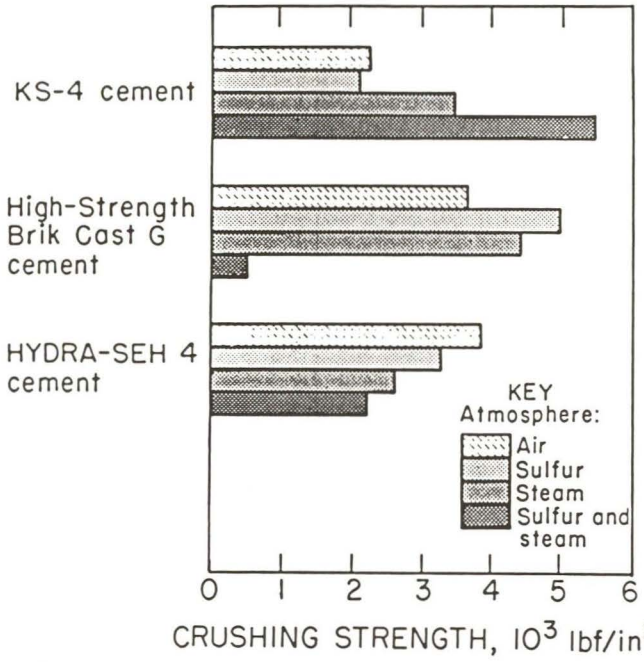


Figure 45.—Crushing strength of castable refractory cements after exposure to air, dry sulfur vapor, steam, and wet sulfur vapor for 30 days at 1,450° F.

H_2S-CO_2-Steam Simulating the H_2S Generator

Corrosion tests at 200° to 1,150° F were conducted on numerous metals and alloys to screen materials for use in the final heat exchanger section of the H_2S generator. The heat exchanger receives reacted gases from the trim reactor at about 1,150° F and discharges the cool gases at about 200° F.

Apparatus and Experimental Procedures

The test reactor of the experimental apparatus was a 4-1/2-in-ID by 60-in-long vitrious silica tube with gastight end seals (fig 46). Gas was introduced through the bottom endseal into a distribution plate having seven milled recesses to index 1-in-OD by 49-in-long Vycor glass tubes in a circular array.. Another plate similarly indexed was placed on top of the Vycor glass tubes to assure that they stood upright and parallel within the reactor. A 1-in-OD closed-end Vycor glass tube (upper end open) occupied the axis of the reactor and extended through the upper endseal to provide access for temperature measurement.

A three-segment heating element wound onto the reactor was powered through three controllers to provide an internal temperature gradient range that could be adjusted from 200° to 500° F at the bottom to 1,150° F at the top. Test temperatures were recorded continuously by six chromel-alumel thermocouples spotwelded at 8-in intervals along a dummy corrosion specimen within the axial closed-end Vycor glass tube.

Premixed H_2S-19.5 pct CO_2, purchased from a commercial vendor, was supplied to the test reactor in two conditions: (1) unaltered and (2) saturated with water vapor at 130° F by bubbling through a 6-in column of water acidified to pH 2 with H_2SO_4. The unaltered gas and the saturated gas, containing about 16 pct CO_2, 16 pct H_2O, and 68 pct H_2S, were piped to the reactor in heated type 316 stainless steel tubing at the rate of about 10 cm^3/min. H_2S was

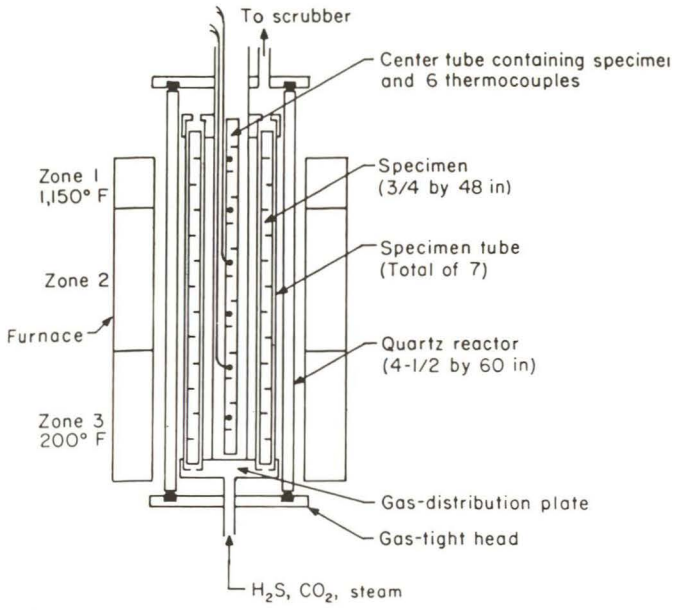


Figure 46.—Apparatus for laboratory corrosion tests in H_2S-CO_2-steam.

removed by a caustic scrubber before the exit gas was discharged to the atmosphere.

Corrosion specimens 3/4 in wide by 48 in long were sheared from 16- to 20-gauge commercial sheet. Saw cuts approximately 1/16 in wide by 1/2 in long were made across each specimen at 2-in intervals for the purpose of impeding heat transfer. Adjacent cuts were begun from opposite sides of the specimen. The cut edges were deburred by filing, and the specimens were degreased with acetone prior to testing. The initial thickness of corrosion specimens at positions corresponding to the desired temperatures was measured by micrometer to ± 0.001 in.

Seven specimens, each occupying a separate Vycor glass tube, were tested simultaneously. Each Vycor glass tube received gas from the gas distribution plate so that an especially active specimen could not deplete the atmosphere for the other specimens.

Following each corrosion test, specimens were removed from the reactor and immediately immersed in plastic epoxide resin to immobilize the corrosion products. Short sections were then removed by a water-cooled abrasive cutoff wheel at predetermined positions for mounting and polishing by standard metallographic procedures. Final cross section was determined by calibrated optical microscope. All specimens were examined for evidence of scale formation, pitting, and intergranular attack. The corrosion rates were calculated from the minimum remaining thickness of unattacked metal. Selected specimens were examined by electron probe microanalyzer, and some scales were analyzed by X-ray diffraction.

Corrosion rates were determined under the following conditions, which simulated continuous and interrupted operation of the H_2S generator supplied with stoichiometric water input (conditions A and B) or excess water input (conditions C and D):

A. About 30 days continuous exposure at constant temperature in an atmosphere of 80.5 pct H_2S-19.5 pct CO_2.

B. Three consecutive 7- or 8-day exposures to 80.5 pct H_2S-19.5 pct CO_2, interrupted by two 8-h cooling-reheating cycles to about 200° F in steam.

C. About 30 days continuous exposure at constant temperature in an atmosphere of 68 pct H_2S-16 pct CO_2-16 pct steam.

D. Three consecutive 7- or 8-day exposures to 68 pct H_2S-16 pct CO_2-16 pct steam interrupted by two 8-h cooling-reheating cycles to about 200° F in steam.

In conditions B and D, steam was admitted to purge the test atmosphere from the reactor before the power was decreased, and steam remained in the reactor until the temperature recovered during reheating. About 8 h was required for each cooling-reheating cycle.

Helium was flushed through the reactor for about 8 h prior to the initial heatup. During final cooling, the test atmosphere was purged from the hot reactor with helium.

During actual operation of the H_2S generator of the demonstration plant, a scheduled shutdown was preceded by purging with steam. The purge was continued on cooling to about 350° F, then N_2 was introduced to displace the steam. The reverse procedure was used during heatup.

Results and Discussion

The majority of the alloys tested were either ferritic iron-base alloys, austenitic iron-base alloys, reactive metals, or aluminum alloys. A convenient grouping is made on that basis. Two experimental iron-base alloys, two specialty nickel-base alloys, and a high-cobalt alloy are included in the austenitic group for discussion purposes only. The nominal composition of the alloys tested, and in some cases the analyzed compositions, were listed previously in table 31.

Ferritic Iron-Base Alloys

Alloys for evaluation were selected to provide a range of single- and multiple-element additions to iron. An experimental alloy obtained from Chrysler Corp. (CRM-4) contains 6 wt pct Al, which is about the maximum concentration available in a wrought alloy. The 400-series stainless steels represent straight chromium additions to iron, and Armco 18SR, Ohmaloy 406, and Hoskins alloy 815 contain both chromium and aluminum. Combined chromium-molybdenum additions are represented by Uniloy 18-2, E-Brite 26-1, and Allegheny 29-4. Corrosion test results are listed in table 35.

Carbon steel was found to be very susceptible to sulfidation in both dry and wet test atmospheres. Corrosion rates were higher and scales were thicker in the dry atmospheres. The thermal cycle in steam apparently increased corrosion in the dry atmospheres but decreased corrosion in the wet atmospheres. Scales were loose at all temperatures and usually completed disengaged above 600° F. On the single specimen in test condition D on which scales were retained, scale thickness was 2.5, 18, and 45 mils at 600°, 800°, and 950° F, respectively. Scales were thicker at 600° F by a factor of 3 in test conditions A and B.

Aluminum as an alloy addition to iron apparently is ineffective at the 6-pct level in CRM-4. The corrosion rate and resultant scale formation for that alloy were not significantly different from the rate and scale formation for

Table 35.—Corrosion rates of ferritic iron-base alloys in H_2S-CO_2-steam, mils per year

Alloy	Test condition[1]	Temperature, ° F				
		600	800	950	[2]1,075	[2]1,150
Allegheny 29-4	B	ND	10	20	33	100 I (1)
Armco 18SR	A	5	7	22	35	78 I (1.5)
	B	2	2	32	51 I (0.5)	90 I (1.5)
	C	2	4	23	38	72 I (1)
	D	<1	3	27	49	63 I (1)
Carbon steel	A	29	ND	ND	ND	ND
	B	41	ND	ND	ND	ND
	C	15	ND	ND	ND	ND
	D	11	56	332	ND	>465 P
Chrysler CRM-4	A	39	ND	ND	ND	ND
	B	35	ND	ND	ND	ND
	D	6	62	ND	ND	ND
E-Brite 26-1	A	2	4	24	39	111 I (1)
	B	2	2	16	36 N	107 I (2)
	C	2	4 N	22 N	36	84 I (1)
	D	<1	1	13	29	75 I (0.5)
Hoskins 815	A	ND	5 N	6 N	3 N	31 I (0.6)
	B	ND	3	10	17	40 I (1)
	C	ND	<1	<1	4 I (0.1)	6 I (0.5)
	D	<1	<1	2	6 I (0.1)	6 I (1)
Ohmaloy 406	A	<1	<1	7	14	46 I (0.5)
	B	<1	1	16	29	36 I (0.6)
	C	<1	3	28 N	34 N	57 N
	D	<1	2 N	29 N	50 N	65 I (0.6)
Stainless steel:						
Type 430	A	5	9	39	63	182
	B	ND	8	50	107	>325 P
	C	2	14	34	82	140
Type 446	C	<1	2	14	28 N	98 I (1)
	D	<1	6	15 N	36 N	107 I (1)
Uniloy 18-2	B	ND	7	42	117	143 I (0.2)
	C	1	8	31	61	115
	D	<1	4	27	85	118 I (1)

I Intergranular corrosion.
N Nonuniform corrosion.
ND Not determined.
P Penetrated.

[1]A = 26 to 30 days at constant temperature in 80.5 pct H_2S-19.5 pct CO_2.
B = 3 7- or 8-day exposures in 80.5 pct H_2S-19.5 pct CO_2, with 2 8-h cooling-reheating cycles to about 200° F in steam.
C = 26 to 32 days at constant temperature in 68 pct H_2S-16 pct CO_2-16 pct steam.
D = 3 7- or 8-day exposures in 68 pct H_2S-16 pct CO_2-16 pct steam, with 2 8-h cooling-reheating cycles to about 200° F in steam.
[2]Numbers in parentheses indicate depth in mils of intergranular penetration.

carbon steel. The dry atmospheres were more aggressive than the wet atmosphere, as inferred from the single test in condition D. Scales were loose and usually disengaged at temperatures above 600° F.

Chromium at the 15-pct (type 430 stainless steel) and 25-pct (type 446 stainless steel) levels in iron decreased corrosion rates considerably in all test atmospheres, but led to nonuniform corrosion and intergranular attack at the higher temperatures. The overall corrosion rate decreased with increasing chromium content, but the tendency for intergranular attack increased with chromium content. Scales decreased in thickness with increasing chromium content as follows, in mils per year (test atmosphere C):

	600° F	1,150° F
Type 430 SS	0.6	42
Type 446 SS	.1	29

Thermal cycling in steam increased the severity of attack.

The extent of nonuniform corrosion of iron-chromium alloys was slight, less than 1 mil penetration, but the nonuniform attack degenerated to intergranular corrosion, which increased in severity with increasing temperature. At 1,150° F, the extent of grain boundary penetration of type 446 stainless steel was only about 1 mil and was, therefore, less significant than the overall penetration (about 8 mils). Additions of chromium and aluminum to iron (Ohmaloy 406, Armco 18SR, and Hoskins alloy 815) act synergistically to decrease general corrosion at all temperatures in all four test atmospheres, but the tendency for intergranular attack at high temperatures remains unchanged. Intergranular penetration was typically 10 to 20 pct of the total penetration.

Scales became more adherent and corrosion rates decreased with increasing chromium content for alloys containing 4 to 6 pct Al (compare CRM-4, Ohmaloy 406 and Hoskins alloy 815). Aluminum additions decreased corrosion rates considerably at constant chromium content (compare type 430 stainless steel with Armco 18SR, and type 446 stainless steel with Hoskins alloy 815). Scales decreased in thickness with increasing total alloy content. Typical thickness values for Armco 18SR in all test conditions and for Hoskins alloy 815 in test condition B were as follows, in mils:

Temp, °F	Armco 18SR	Hoskins 815
600	<0.1	<0.1
800	1.5	.6
900	8	2
1,075	12	4
1,150	20	8

Corrosion and scale formation for Hoskins alloy 815 were significantly decreased by water vapor in the test atmosphere (conditions C and D), with observed scales only 3.5 mils thick at 1,150° F.

Molybdenum as a ternary additive to iron-chromium alloys neither decreased the corrosion rate nor retarded intergranular attack (compare type 430 stainless steel with Uniloy 18-2, and type 446 stainless steel with E-Brite 26-1). Scales were similar in appearance, thickness, and composition to scales formed on iron-chromium alloys except that molybdenum in the iron-chromium-molybdenum alloys was concentrated in the layers of scale adjacent to the metal.

Austenitic Iron-Base Alloys and Miscellaneous Alloys

Alloys for evaluation were selected to provide a wide range of nickel, chromium, and molybdenum compositions in an austenitic matrix. An experimental alloy obtained from the Sandia Laboratory (Sandia X-1) provided an opportunity to determine the effect of titanium in a type 310 stainless steel base material. Inconel alloy 601 is a high-nickel alloy containing aluminum, and MP35N contains high levels of both cobalt and molybdenum. Corrosion rates in H_2S-CO_2-steam are listed in table 36.

The effect of nickel additions to iron-chromium alloys can be determined by comparing ferritic and austenitic alloys having comparable chromium levels. Nickel at the 16- to 20-pct level generally decreased the corrosion rate at higher temperatures but appeared to increase the corrosion rate at lower temperatures. In both cases, the effect is small (compare type 430 stainless steel and Uniloy 18-2 with types 304, 316, and 317 stainless steel). At the 25-pct level and at higher concentrations, nickel is definitely deleterious (compare type 446 stainless steel with type 310 stainless steel, Incoloy alloy 800, and Inconel alloy 601).

Molybdenum additions to the austenitic alloys are apparently ineffective and may be deleterious (compare type 304 stainless steel with types 316 and 317). The average performance of the specialty alloy MP35N was no better than that of type 304 stainless steel over the temperature range studied.

Scales on the austenitic alloys were thicker and less adherent than scales on the ferritic alloys. Scales that formed at 600° F in test condition B were 0.1, 0.2, 0.5, and 1.0 mils thick for types 304, 316, 317, and 310 SS, respectively. Only 1 specimen of the 28 tested for those alloys retained its scale above 1,000° F. That was type 310 stainless steel in test condition A at 1,150° F, for which the scale was 35 mils thick. Only one of four Sandia X-1 specimens retained its scale at 1,150° F, for which the thickness was also 35 mils. Scales on Incoloy alloy 800 were thicker and more adherent. The scales at 600° and 1,150° F in test condition A were 0.5 and 43 mils thick, respectively.

X-ray diffraction analysis of powder specimens of scales from types 304, 316, andd 310 stainless steel indicated the presence of the pyrrhotite and thiospinel structures. FeS and NiS, which are isotypic, have the pyrrhotite structure and constitute the major portion of the total scale.

Reactive Metals

Corrosion test results for titanium, Ti-6Al-4V, and Zr 705, as included in table 36, reveal a marked resistance of titanium and its alloy to sulfidation. They corrode less in the dry atmospheres (A and B) than in the wet atmospheres (C and D), in contrast to the iron- and nickel-base alloys, which show the opposite behavior. Scales on both titanium and its alloy were very thin (7 mils maximum thickness on Ti-6Al-4V in test condition C at 1,150° F).

The chemical-grade zirconium alloy (Zr 705) had adequate resistance up to about 950° F in the single test made in the wet test condition, but corroded very rapidly at higher temperatures. The scale on Zr 705 that formed at 1,150° F in test condition C was the monoclinic form of ZrO_2.

Aluminum Alloys

Aluminum alloys were tested for 30 days in conditions C and D over the temperature range 200° to 900° F. Only

Table 36.—Corrosion rates of austenitic iron-base alloys, nickel- and cobalt-base alloys, and reactive metals in H_2S-CO_2-steam, mils per year

Alloy	Test condition[1]	Temperature, ° F				
		600	800	950	[2]1,075	[2]1,150
Incoloy 800	A	9	11	50	77	166
	B	5	6	29	113	>413 P
	C	3	10	43	49	129 I(0.5)
	D	3	8	39	78	141 N
Inconel 601	C	1	7	62	ND	111
MP35N multiphase	D	<1	19	32	41	149
Sandia X-1	A	2	9	27	45	140
	B	6	10	29	51 N	134 I(1.5)
	C	1	4	21	32	92
	D	2	10	18	32	85 N
Stainless steel:						
Type 304	A	6	7	53	65	140
	B	1	4	48	100	223
	C	1	4	30	51 N	104 N
	D	1	4	50 N	65 N	112 I(0.1)
Type 310	A	4	4	30	49	135 I(0.6)
	B	2	4	27	38	125 I(1)
	C	2	4	25	38 N	100 N
	D	1	3	21	30	102
Type 316L	A	4	7	43	67	153 N
	B	1	4	69	114	138
	C	2	7	46	65	92 N
	D	1	3 N	46 N	76 N	91 I(0.4)
Type 317	A	ND	7	41	60	124
	B	1	2	25 N	79 N	143 N
	C	2	5	31	55	100
	D	1	3	33	72 N	112 N
Titanium	A	<1	4	7	3	22
	B	<1	<1	1	2	14
	C	<1	<1	2	5	15
	D	<1	3	8	10	22
Ti-6Al-4V	A	<1	2	2	2	8
	B	<2	<1	1	<1	4
	C	<1	1	2	3	7
	D	<1	<1	3	3	12
Zr 705	C	<1	1	10	47	>200 P

I Intergranular corrosion. ND Not determined.
N Nonuniform corrosion. P Penetrated.

[1]A = 26 to 30 days at constant temperature in 80.5 pct H_2S-19.5 pct CO_2.
B = 3 7- or 8-day exposures in 80.5 pct H_2S-19.5 pct CO_2, with 2 8-h cooling-reheating cycles to about 200° F in steam.
C = 26 to 32 days at constant temperature in 68 pct H_2S-16 pct CO_2-16 pct steam.
D = 3 7- or 8-day exposures in 68 pct H_2S-16 pct CO_2-16 pct steam, with 2 8-h cooling-reheating cycles to about 200° F in steam.
[2]Numbers in parentheses indicate depth in mils of intergranular penetration.

one test was conducted in each condition; therefore, the results, as shown in table 37, are semiquantitative. Corrosion of all alloys at temperatures less than 600° F was below the limit of detection by micrometer measurement. General corrosion was very slight at temperatures up to 900° F, which was the upper temperature limit, but pitting for some alloys became prominent at much lower temperatures. Most susceptible to pitting attack was alloy 3003, which was penetrated at 900° F. Large blisters, nearly 1/2 in. in diam, formed over the pits on alloy 3003. Pitting with the accompanying blisters was also observed for alloys 5052 and 6061. Alloy 2024 was observed to be the most resistant, with measured corrosion rates less than 5 mil/yr at 900° F in conditions C and D. The weld alloy 4043 was nearly immune to corrosion at all temperatures investigated.

Table 37.—Corrosion rates of aluminum alloys in H_2S-16 pct CO_2-16 pct steam, mils per year

Alloy	Test condition[1]	Temp, ° F[2]		Comments
		800	900	
2024	C	3	5	Dark stain at >600° F, no pitting, no scale.
	D	<3	<5	Stain at >650° F.
3003	C	<1 PT	<1 PT	Pitting, <1 mil, at 750°-900° F, no scale.
	D	<3	30 PT	Blisters, (3/8 in diam) over pits at 950° F.
4043[3]	C	<3	<5	No visible scale.
	D	<3	<5	Stain at >850° F.
5052	C	<1 PT	<1 PT	Pitting, <1 mil, at 450°-750° F; blisters at >800° F; grey scale at 650°-900° F.
	D	<1 PT	<2 PT	Blisters over pits at >650° F.
6061	C	<3	<5	Stain at 500°-900° F, no pitting.
	D	<1 PT	<2 PT	Blisters over pits at >750° F.

PT Pitted.

[1]C = 26 to 32 days at constant temperature in 68 pct H_2S-16 pct CO_2-16 pct steam.
D = 3 7- or 8-day exposures in 68 pct H_2S-16 pct CO_2-16 pct steam, with 2 8-h cooling-reheating cycles to about 200° F in steam.
[2]At 600° F, <1 mil/yr corrosion for all alloys, under test conditions C and D.
[3]Welding alloy applied by metal-inert-gas (MIG) method.

Citrate Solutions Simulating SO_2 Absorption and Solution Regeneration

The citrate process recovers SO_2 from waste gases by scrubbing with an aqueous solution of citric acid and sodium citrate (*52*). Regeneration of the solution containing SO_2 (rich citrate solution) is achieved by reacting it with H_2S to form elemental sulfur. The regenerated solution (lean citrate solution) becomes concentrated in soluble impurities absorbed from the waste gases. These impurities influence the corrosiveness of both rich and lean citrate solutions.

At the time the demonstration plant was being constructed, the only pertinent corrosion data in citrate process environments were those obtained in two previous pilot plant studies (*25*). One pilot plant was jointly built and operated by Arthur G. McKee and Co., Peabody Engineered Systems, and Pfizer, Inc. In this operation, stack gas from a simulated coal-fired utility was scrubbed with a low-chloride-containing citric acid-Na_2CO_3 solution at 80° C. The other pilot plant, built by the Bureau, was jointly operated by the Bureau and the Bunker Hill Co. at its lead smelter in Kellogg, ID (*13*).

Both pilot plant supposedly used citrate solutions containing no chloride, but several alloys (Inconel alloy 825 and types 317, 316, and 304 stainless steel) from in-plant corrosion tests at the Bunker Hill plant showed very slight pitting typical of corrosion in aqueous solutions containing chloride. Because of the possibility of chloride ion buildup in citrate solutions, it was desirable to obtain corrosion data for alloys in citrate solutions containing higher chloride levels. These data could be used to help select candidate alloys for inclusion in in-plant corrosion tests in the demonstration plant and also to serve as a guide in emergencies to replace alloys that failed by corrosion.

Two corrosion environments were simulated in laboratory corrosion tests to measure the corrosion resistance of various metals: (1) rich citrate solution at 1 atm and 120° F, containing SO_2, representing pregnant solution leaving the SO_2 absorber and (2) lean citrate solution at 3 to 4 atm and 260° F, representing stripped solution in the sulfur melter.

The operating conditions and the composition of the citrate solutions used in this laboratory study were essentially the same as those used in the Bunker Hill pilot plant except for the chloride concentration. The citrate solutions used in this study contained 50 g/L chloride, compared with very low, unreported levels in the Bunker Hill operation. The present report describes the results of laboratory corrosion tests on the general and localized corrosion of ferritic stainless steels, austenitic stainless steels, titanium, zirconium, and some highly alloyed iron-chromium-nickel and nickel-base alloys.

Materials, Sample Preparation, and Test Conditions

Corrosion tests were made initially on over 30 alloys in stagnant citrate solutions to enable the selection of about a dozen alloys for subsequent evaluation of localized corrosion (crevice corrosion and pitting) and stress corrosion cracking in recirculating citrate solutions. Generally, only a single set of coupons was tested in stagnant solutions. Sheet coupons were tested in duplicate or triplicate in recirculating solution. Four C-rings for each alloy were tested for stress corrosion cracking in recirculating solution.

Evaluation of sheet coupons was by weight-loss measurements and by visual observation for localized corrosion (pitting and crevice corrosion). Corrosion-tested sheet coupons were rubbed with a rubber stopper, washed in tap water, then ultrasonically cleaned in acetone, rinsed in ethanol, and dried.

Evaluation of stress-corrosion-tested C-rings was primarily by visual examination, including dye penetrant tests and metallography. The surfaces of the C-rings were periodically examined at low magnification for any signs of cracking. At the conclusion of the stress corrosion test, sections from the most highly stressed regions of selected C-rings were metallographically examined for surface cracking and corrosion.

The nominal compositions of the alloys tested were listed previously in table 31. Corrosion test specimens were generally obtained from either 16-gauge (0.06-in-thick) annealed sheet or 1-in-diam annealed tubing. Sheet and tubing of those sizes could not be obtained for all alloys; therefore, sheet thicknesses ranged from 0.02 to 0.1 in, and tubing diameters ranged from 0.38 to 1.06 in OD.

Two types of sheet coupons were used. A plain coupon with one hole was used for general corrosion and corrosion in vapor. The coupon used for crevice corrosion contained a second hole that was fitted with a nylon bolt, washer, and nut to form an artificial crevice. Except for weldments, the surfaces of the 0.75-in by 1.5-in by thickness coupons from sheet were finish-abraded with 180-grit paper, then washed in acetone and rinsed in ethanol before testing. Weldments were washed in acetone and rinsed in ethanol before testing.

C-ring specimens were made in general accord with ASTM G38-73 (*2*). Surface-ground C-rings initially were stressed at 90 pct of their proportional limit before testing. The stress in C-rings was adjusted with a nut and bolt insulated from the C-ring. Type 316 stainless steel nuts and bolts wrapped with plastic shrink-on insulation were used with C-rings exposed to rich citrate solution at 120° F. Hastelloy C-276 nuts and bolts insulated with Teflon fluorocarbon polymer were used with C-rings exposed to lean citrate solution at 260° F.

The nominal compositions of the synthetic citrate solutions are listed in table 38. Reagent-grade chemicals and distilled water were used to synthesize the citrate solutions, with the exception of technical-grade NaOH used in the initial screening tests.

Synthetic flue gas containing 82 pct N_2, 13 pct CO_2, 4.8 pct O_2, and 0.34 pct SO_2 was bubbled continuously through rich citrate solution at 10 to 15 cm^3/min. The pH of rich and lean solutions ranged from 3.6 to 4.2 and 4.4 to 5.3, respectively. Rich solution was maintained at 120° F and 1 atm pressure, whereas the lean solution at 260° F was pressured with air to 4 atm total pressure. Test duration was usually 30 days, with the exception of some tests for up to 180 days in rich solution.

Table 38.—Nominal composition of citrate solutions

Component	Rich solution		Lean solution	
	Conc, *M*	g/L	Conc, *M*	g/L
Citric acid	0.5	96	0.5	96
NaCl	1.4	83	1.4	83
NaOH	1.0	40	1.0	40
$Na_2S_2O_3$	.4	63	.4	63
Na_2SO_4	.5	71	.5	71
SO_2	0.08-.16	5-10	<.003	<.2

Conc Concentration.

Stagnant Rich Citrate Solution at 120° F

A number of tests were made in stagnant solutions to select alloys for subsequent testing in recirculating solution.

Iron- and Nickel-Base Alloys, Titanium, and Zirconium

In initial screening tests, one sheet corrosion coupon from each alloy was exposed to 150 mL of rich citrate solution in a 350-mL Erlenmeyer flask at 120° F. The ferritic stainless steels, including Ohmaloy 406, types 430 and 446 stainless steel, Hoskins alloys 750 and 815, Armco 18SR, Uniloy 18-2, and E-Brite 26-1, were discolored within 3

days and were severely corroded after 16 to 20 days. The pH of solutions containing the ferritic alloys had increased significantly, but the pH of the solutions containing the austenitic alloys remained essentially unchanged. The austenitic stainless steels, titanium, zirconium, iron-chromium-nickel-base alloys, and nickel-chromium-base alloys were sufficiently resistant to warrant further testing.

Twelve alloys were selected for extensive testing to measure the corrosion resistance of as-received alloy sheet and of weldments before and after annealing. Strips from as-received 0.06-in- or 0.12-in-thick sheets were butt-welded together without filler rods by the tungsten arc inert-gas (TIG) method to obtain 75 to 100 pct penetration. The welded strips were sectioned by shearing or abrasive sawing to obtain corrosion test coupons with the weldments centered longitudinally.

Four coupons from each alloy were tested: two as-welded and two after annealing. Weldments were not surface-ground before or after welding. Except for titanium, all weldments were annealed in air and quenched in water. Titanium weldments were annealed in vacuum. The annealing temperatures and the results of these corrosion tests are listed in table 39. All alloys except type 304 stainless steel had general corrosion rates of less than 1 mil/yr. For alloys containing less than 6 pct Mo (types 316L and 317L stainless steel, Incoloy alloy 825, Sandvik 2RK65, and Multimet N-155), there was a general tendency for weldments to be less resistant to corrosion than unwelded coupons. Weldments of these alloys showed a greater tendency for localized corrosion by pitting. Alloys containing 6 pct Mo (Allegheny 6X) and 9 pct Mo (Inconel alloy 625) showed a slight hint of crevice corrosion but only in the as-welded condition. Both Allegheny 6X and Inconel alloy 625 are

Table 39.—Corrosion rates of unwelded coupons, welded coupons, and annealed weldments in stagnant rich citrate solution at 120° F

(90-day tests, pH 4 at start)

Alloy	Molybdenum, wt pct	General corrosion, mil/yr	Crevice corrosion	Corrosion in vapor	
				Crevice	Pitting
Allegheny 6X:					
Unwelded	6	0	None	None	No.
Welded	6	0	..do	Slight	Yes.
Annealed (1,830° F)	6	0	..do	None	No.
Hastelloy:					
C-4:					
Unwelded	16				
Welded	16				
Annealed (1,970° F)	16				
C-276:					
Unwelded	16				
Welded	16	<.1	..do	..do	No.
Annealed (2,100° F)	16				
G:					
Unwelded	6.5				
Welded	6.5				
Annealed (2,150° F)	6.5				
Incoloy 825:					
Unwelded	3	0	Slight	..do	No.
Welded	3	[1]<.1	..do	Moderate	Yes.
Annealed (1,830° F)	3	.8	..do	Slight	Yes.
Inconel 625:					
Unwelded	9	0	None	None	No.
Welded	9	0	..do	Slight	No.
Annealed (2,100° F)	9	0	..do	None	No.
Multimet N-155:					
Unwelded	3	0	..do	..do	No.
Welded	3	0	Slight	..do	No.
Annealed (2,150° F)	3	0	Moderate	Slight	Yes.
Sandvik 2RK65:					
Unwelded	[2]4.5	0	None	..do	No.
Welded	[2]4.5	0	Slight	None	Yes.
Annealed (1,970° F)	[2]4.5	<.1	None	..do	No.
Stainless steel:					
Type 304:					
Unwelded	[2]<.3	[1].4	Severe	Severe	Yes.
Welded	[2]<.3	[1]5.7	Moderate	..do	Yes.[3]
Annealed (1,830° F)	[2]<.3	[1]9.9	Slight	..do	Yes.
Type 316L:					
Unwelded	[2]3.2	0	None	None	No.
Welded	[2]3.2	[1].4	Slight	Moderate	Yes.
Annealed (1,970° F)	[2]3.2	<.1	None	..do	Yes.
Type 317L:					
Unwelded	[2]3.6	0	..do	None	No.
Welded	[2]3.6	<.1	Slight	Slight	Yes.
Annealed (1,970° F)	[2]3.6	0	..do	Severe	Yes.
Titanium:					
Unwelded	0				
Welded	0	<.1	None	None	No.
Annealed (1,380° F)	0				

[1]Pitted and/or crevice corroded.
[2]Analysis of test sheet.
[3]Pitting concentrated at junction of weld bead and heat-affected zone.

suitable for use either welded or unwelded. Hastelloy G, alloys containing more than 9 pct Mo (Hastelloy C-4 and C-276), and titanium were completely resistant to corrosion in all three conditions. Based upon these results in stagnant solution, all of the alloys listed in table 39, except titanium and Multimet N-155, plus Haynes alloy 20 Mod and Allegheny 29-4, were chosen to test alloy compositions representing various levels of molybdenum, chromium, and nickel in recirculating rich citrate solution.

Effect of Chloride Concentration

Thirty-day tests at 120° F were made to determine the effect of chloride concentration on localized corrosion of sheet coupons. Type 316 stainless steel, Incoloy alloy 825, type 317L stainless steel, and Sandvik 2RK65 showed a tendency for localized corrosion in standard rich citrate solution containing 50 g/L chloride but showed little or no tendency for localized corrosion in rich citrate solutions containing less than 25 g/L chloride. The tendency for localized corrosion was slightly increased for alloys containing 2.8 to 4.5 Mo when the chloride content was increased from 25 to 50 g/L.

Aluminum Alloys 5052 and 5086 and High-Silicon Iron Alloy Durichlor 51

Three coupons of each alloy, including a general corrosion coupon (fully immersed), a vapor coupon (semi-immersed), and a crevice coupon (fully immersed), were exposed either to 400 mL of rich citrate solution through which flue gas containing 0.34 pct SO_2 was bubbled at 10 to 15 cm^3/min, or to 400 mL of lean citrate solution containing no flue gas. The citrate solution used for each set of coupons was changed every 10 days.

The aluminum alloys were observed to corrode rapidly and pit severely in rich citrate solutions. The 1/8-in-thick Al 5086 coupon was nearly penetrated in 30 days. Both alloys corroded about the same in the vapor above the solution as in the solution, and there was little if any crevice corrosion. The 10-day-old solutions had been depleted of SO_2, the pH had increased accordingly, but the $S_2O_3^{2-}$ concentrations were unchanged. The corrosion and pitting rate of Al 5086 was more severe in rich citrate soloution than in lean citrate solution. Al 5052 corroded at a much slower rate in lean than rich citrate solutions, but the alloy is not recommended for use in lean citrate because of excessive localized corrosion. After a 10-day exposure, pitting had occurred at the liquid level line on the semi-immersed vapor coupon and along the edge of the washer on the crevice coupon. Pitting increased with exposure time. After 30 days, the pitting was most prominent in the vapor zone and in the crevice.

The high-silicon iron alloy Durichlor 51 (Fe-14.5Si-4.5Cr-1C), was tested in stagnant rich and lean citrate solutions using doughnut-shaped castings provided by the Duriron Co. The doughnuts were about 1-1/4 in. in OD by 1/2 in. in ID by 3/8 in thick. Test results for rich citrate solution showed that the alloy eventually formed a protective layer that reduced the corrosion rate to less than 30 mil/yr. The alloy did not pit in either rich or lean solutions. The observed average corrosion rates of 155, 127, and 60 mil/yr for 3-, 5-, and 19-day exposures were used to derive the hyperbolic equation $R = 25.35 + 217.8/t$, where R is the instantaneous corrosion rate in mil/yr for time exposure, t, in days.

Recirculating Rich Citrate Solution at 120° F

Twelve alloys, as listed in table 40, were tested in recirculating citrate solution saturated with flue gas. A set of three sheet coupons, consisting of a general corrosion coupon (fully immersed), a vapor coupon (semi-immersed), and a crevice coupon (fully immersed), and C-ring specimens were corrosion-tested in horizontal, 2-in-ID Pyrex heat-resistant glass tubes through which citrate solution was recirculated at 12 to 16 cm^3/min. A constant temperature was maintained with a water bath. Approximately 4 L of solution was recirculated with a piston pump located outside the water bath. Initially, the citrate solution was changed every 2 weeks, but later it was changed each month. Analysis of 30-day-old solutions showed that the composition was essentially unchanged.

As shown in table 40, the general corrosion coupons in the unwelded condition had corrosion rates of less than 0.1 mil/yr. The general corrosion rates for weldments of some of the alloys, such as Allegheny 29-4 and types 317L, 316, and 304 stainless steel, were higher owing to localized corrosion. Excluding localized corrosion, there was very little difference in general corrosion resistance among unwelded coupons, as-welded coupons, and annealed weldments. There is also fair agreement between general corrosion rates for unwelded coupons in stagnant (table 39) and recirculating (table 40) rich citrate solution at 120° F.

All of the alloys except Inconel alloy 625 and Allegheny 6X were susceptible to crevice corrosion. Allegheny 29-4 weldments exhibited more pitting than did unwelded material, and there was no significant difference in pitting between as-welded and annealed weldments. The tendency for localized corrosion of alloys was more severe when coupons were partially submerged to permit attack by the vapors. Only Inconel alloy 625 was completely resistant. Some Allegheny 6X weldments exhibited negligible localized corrosion, but all of the remaining alloys showed moderate to severe crevice corrosion or pitting, especially as weldments.

Four C-rings each from Hastelloy C-276, Hastelloy G, Allegheny 6X, Sandvik 2RK65, and types 317L, 316L, and 316 stainless steel were stressed to 90 pct of their proportional limit and exposed for 6 months to recirculating rich citrate solution saturated with flue gas. Each month the changed citrate solution was analyzed, all C-rings were visually examined for stress corrosion cracks at X10 magnification, the outside diameter of all C-rings was measured, and the diameter for one of the four C-rings for each alloy was measured in the as-stressed and unstressed condition to estimate applied stresses.

The SO_2 concentrations in the 30-day-old solutions ranged from 7.5 to 9 g/L, compared with about 10 to 11 g/L in the fresh solutions. The $S_2O_3^{2-}$ and SO_4^{2-} ion concentrations and pH remained essentially unchanged over the 6-month test exposure.

Visual examinations of the C-rings each month showed no stress-corrosion cracking, and cracking was not detected by dye penetrant testing at the end of the 6-month exposure.

The diameters of the as-stressed C-rings remained constant throughout the test. However, there was some stress relaxation, especially during the initial 30-day exposure, as indicated by the change in diameters of the unstressed C-rings. Measurements after the first 30 days indicated that the maximum applied stress for each alloy ranged from 73 to 86 pct of the proportional limits. After 6 months, the maximum applied stress ranged from 71 to 84 pct of the proportional limits.

Table 40.—Comparison of corrosion results for unwelded and welded iron- and nickel-base alloys in recirculating rich citrate solution at 120° F

(30-day tests; solution saturated with flue gas; pH 4; flow rate, 12 to 16 cm^3/min)

Alloy	Submerged coupons			Coupons in vapor		
	General corrosion, mil/yr	Crevice corrosion		Frequency of corrosion[1]	Pits per coupon[2]	Deepest pit, mils
		Frequency[1]	Severity			
Allegheny:						
6X:						
Unwelded	<0.1	0:2	None	0:3	0	0
Welded	<.1	0:2	...do	1:2	0- 2	1
Annealed	<.1	0:2	...do	1:2	0- 1	3
29-4:						
Unwelded	<.1	2:2	Slight	0:3	0	0
Welded	[3].45	2:2	...do	2:2	>20	18
Annealed	.1	2:2	Moderate	2:2	>20	19
Hastelloy:						
C-276: Unwelded	<.1	0:2	None	0:2	0	0
G: Unwelded	<.1	0:2	...do	0:2	0	0
Haynes 20 Mod: Unwelded	<.1	0:2	...do	0:2	0	0
Incoloy 825:						
Unwelded	<.1	1:2	Slight	2:3	0- 1	<1
Welded	<.1	0:2	None	2:2	5- 6	15
Annealed	<.1	1:2	Slight	2:2	5- 6	12
Inconel 625:						
Unwelded	<.1	0:2	...do	0:2	0	0
Welded	<.1	0:2	...do	0:2	0	0
Annealed	<.1	0:2	...do	0:2	0	0
Sandvik 2RK65:						
Unwelded	<.1	0:2	None	0:3	0	0
Welded	<.1	1:2	Slight	2:2	12-20	10
Annealed	<.1	0:2	None	2:2	8-10	12
Stainless steel:						
Type 304:						
Unwelded	<.1	2:2	Moderate	3:3	1- 2	22
Welded	[3]1.8	2:2	...do	2:2	>20	21
Annealed	.15	2:2	Slight	2:2	>20	19
Type 316:						
Unwelded	<.1	2:2	...do	3:3	2- 6	17
Welded	<.1	2:2	...do	2:2	4-15	16
Annealed	<.1	1:2	...do	2:2	7- 8	15
Type 316L:						
Unwelded	<.1	0:2	None	3:3	4- 5	12
Welded	<.1	1:2	Slight	2:2	8-12	18
Annealed	<.1	0:2	None	2:2	5- 6	18
Type 317L:						
Unwelded	<.1	1:2	Slight	3:3	1	5
Welded	.2	0:2	None	2:2	12	22
Annealed	<.1	1:2	Slight	2:2	2- 4	18

[1]Ratio of coupons showing corrosion to total number tested.
[2]Ranges indicate minimum and maximum (number of pits).
[3]High rate due to localized corrosion.

Two C-rings from each alloy were sectioned for metallography to look for corrosion and cracking. Neither corrosion nor surface cracking was noted for any of the alloys.

Visual examination of the type 316 stainless steel screws used to stress the C-rings showed only negligible localized corrosion. Because the C-ring assemblies were washed each month to remove any corrosion deposits, crevice corrosion conditions were minimized. The low level of crevice corrosion over the 6-month exposure suggests that type 316 stainless steel containing about 3 pct Mo might be used safely if kept submerged and reasonably free of crevice corrosion conditions.

Stagnant Lean Citrate Solution at 260° F and 4 Atm

The results for the 30-day tests are shown in table 41, in which the alloys are grouped according to their relative resistance to corrosion.

In group I, the alloys containing more than 6 pct Mo were completely resistant to crevice corrosion. The alloys in group II showed only a very slight tendency for crevice corrosion. The molybdenum content in the group II alloys was 3 pct; however, both alloys also contained 2 to 3 pct W, which might be expected to behave as molybdenum. The alloys in group III, which contained 2 to 4.5 pct Mo, definitely showed some resistance to crevice corrosion and could probably be used under mild crevice corrosion conditions. The alloys containing 3 to 4.5 pct Mo were superior to those containing 2 to 3 pct Mo. The group IV alloys were not resistant to crevice corrosion. Three of these alloys contained no molybdenum, and Uniloy 18-2 (a ferritic alloy containing 2 pct Mo) contained no nickel.

Recirculating Lean Citrate Solution at 260° F and 4 Atm

A schematic drawing of the recirculating system is shown in figure 47. The all-metal system (except for the glass flowmeter) was made of type 316 stainless steel and Hastelloy C-276. Components that operated at 260° F were made of Hastelloy C-276, and the remaining components, operated below 120° F, were made of type 316 stainless steel. Twelve liters of citrate solution was recirculated at 12 to 16 cm^3/min with a piston pump. Citrate solution at 100° to 120° F was reheated to 260° F by a hot-oil heat

Table 41.—Corrosion rates of alloys in stagnant lean citrate solution at 260° F and 4 atm

(30-day tests, pH 4.5 at start)

Alloy	Molybdenum, wt pct	General corrosion, mil/yr	Crevice corrosion
GROUP I[1]			
Allegheny 6X	6.5	0.08	None.
Hastelloy C-4	15.3	.28	
Hastelloy C-276	16	.3	
Hastelloy G	6.5	.07	
MP35N multiphase	10	.07	
Inconel 617	9	.1	
Inconel 625	9	.09	
Titanium	0	.04	
Zr 705	0	.01	
GROUP II[2]			
Multimet N-155	3	[3]0.05	Slight.
Rolled Alloys RA 333	3	.01	Questionable.
GROUP III[4]			
Carpenter 20Cb-3	2-3	<1	Moderate to severe.
Incoloy 825	3	<.3	
Sandvik 2RK65	4.5	<.1	
Stainless steel:			
Type 316	2-3	<5	
Type 316L	2-3	<3	
Type 317L	3-4	<1	
GROUP IV[5]			
Incoloy 800	0	<30	Severe.
Inconel 600	0	<200	
Inconel 601	0	<35	
Uniloy 18-2	2	<45	

[1]Completely resistant to crevice corrosion; low uniform corrosion.
[2]Probably resistant to crevice corrosion; low uniform corrosion.
[3]1 crevice pit.
[4]Slightly resistant to crevice corrosion; low uniform corrosion. Most of weight loss was due to crevice corrosion.
[5]Not resistant to crevice corrosion. Most of weight loss was due to crevice corrosion.

exchanger before entering a box furnace containing a 3-in-ID by 12-in Hastelloy C-276 sample chamber. C-rings were placed on Pyrex heat-resistant glass shelves in the sample chamber. Citrate solution at 260° F leaving the sample chamber was cooled to 120° F in a water-cooled heat exchanger before being returned to the type 316 stainless steel feed tank. The system was pressurized to about 4 atm with compressed air.

The recirculating system frequently became plugged with sulfur, formed by the decomposition of sodium thiosulfate. Because of this plugging, periods of continuous exposure to citrate solution ranged from 2-1/2 to 13 days.

After the second plugging of the system, the initial sodium $S_2O_3^{2-}$ concentration was reduced from 0.4*M* to 0.2*M*, and the initial Na_2SO_4 concentration was reduced from 0.5*M* to zero. These changes decreased the formation of sulfur within the system and decreased the plugging tendency. The change in corrosivity of the solution due to the reduced thiosulfate and sodium sulfate concentrations is believed to be negligible. Analyses of citrate solutions after each exposure segment showed that the pH increased from 4.5 to 4.8, $S_2O_3^{2-}$ decreased to between 15 and 45 pct of the initial concentration, SO_4^{2} increased slightly, and Cl^- remained unchanged.

A stress-corrosion cracking test was made in recirculating lean citrate solution for Hastelloy C-276, Hastelloy G, Allegheny 6X, Ti-50A, Ti Code 12, Sandvik 2RK65, type 317L stainless steel, and type 316L stainless steel. Testing of type 317L and type 316L stainless steel was discontinued after 22 days exposure because of excessive crevice corrosion. The other alloys received a 56-day cumulative exposure to citrate solution in which the pH ranged from 4.5 to 4.8. The maximum applied stresses were not constant throughout the test but ranged from 70 to 90 pct. At the completion of the 56-day exposure, none of the C-rings contained any stress corrosion cracks, as determined by visual examination at low magnification, by dye penetrant tests, and by metallography. There appeared to be slight pitting for the weldments of Ti-50A and Ti Code 12.

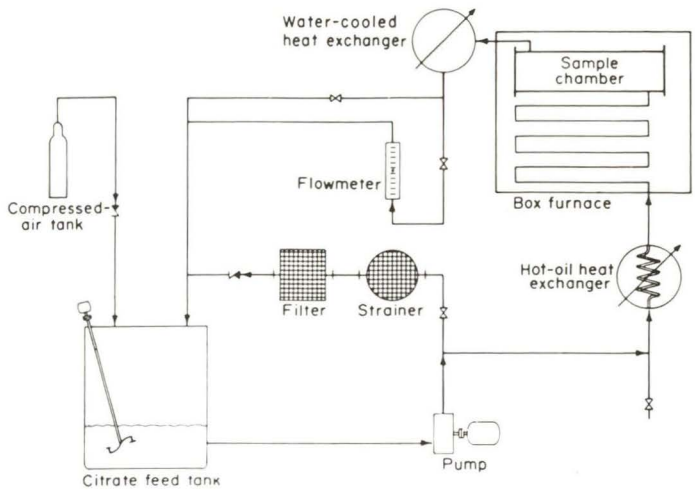


Figure 47.—Schematic drawing of system for corrosion tests in recirculating lean citrate solution at 260° F and 4 atm.

Discussion of Results

Laboratory tests were made to obtain the corrosion resistance of metals and alloys in two aqueous citrate solutions: (1) rich citrate solution at 120° F, simulating conditions in the SO_2 absorber, and (2) lean citrate solution, simulating conditions in the solution regeneration and sulfur recovery circuit. Rich citrate solution was sodium citrate solution with a pH of about 4 containing 35 g/L $S_2O_3^{2-}$, 48 g/L SO_4^{2-}, 50 g/L Cl^-, and 10 g/L SO_2. Lean citrate solution had nearly the same composition as rich citrate but contained only residual amounts of SO_2 with a correspondingly higher pH of 4.5.

The corrosion behavior of alloys tested in this study was typical behavior in acidic, aqueous solutions containing chloride, with respect to chloride content, pH, temperature, and alloy composition. The tendency for localized corrosion was slightly increased for type 316L stainless steel, Incoloy alloy 825, type 317L stainless steel, and Sandvik 2RK65 when the chloride content in stagnant rich citrate solutions was increased from 25 to 50 g/L chloride. This behavior is in general agreement with that reported in the literature (*8, 22, 37*).

The effect of alloy composition on corrosion resistance can be seen by the results in table 42 where the alloys are rated as recommended, conditional, or not acceptable for use in citrate solutions.

Alloys that are recommended, without reservation were completely resistant in solution and in the vapors above the solution. With the exception of titanium and Zr 705, all alloys in this group are iron- or nickel-base alloys that contain more than 15 pct Cr and from 5 to 16 pct Mo.

Alloys with a conditional recommendation, C, are suitable for use in rich citrate solution when submerged. These alloys may, however, show localizsed corrosion in vapors above the solution or in situations where crevices exist. All alloys in this group are iron-chromium-nickel-base alloys containing 4.5 to 5 pct Mo.

Table 42.—Performance ranking of materials in laboratory corrosion tests in citrate solutions

Alloy	Rich citrate solution[1] at 120° F	Lean citrate solution[2] at 260° F
Al 5086	NAc (S)	ND
Allegheny 6X	R	R
Allegheny 29-4	NAc	ND
Armco 18SR	NAc (S)	ND
Carpenter 20Cb-3	NAc	NAc
Chrysler CRM-4	NAc (S)	ND
E-Brite 26-1	NAc (S)	ND
Hastelloy B	NAc (S)	ND
Hastelloy C-4	R	R
Hastelloy C-276	R	R
Hastelloy G	R	R
Haynes 20 Mod	C	C
Incoloy 800	ND	NAc (S)
Incoloy 825	NAc	NAc
Inconel 600	ND	NAc (S)
Inconel 601	ND	NAc (S)
Inconel 617	R	R
Inconel 625	R	R
MP35N multiphase	R	R
Multimet N-155	R	C
Ohmaloy 406	NAc (S)	ND
Rolled Alloys RA 333	R	C
Sandvik 2RK65	C	C
Stainless steel:		
Type 304	NAc (S)	NAc (S)
Type 316	NAc	NAc
Type 316L	NAc	NAc
Type 317L	NAc	NAc
Type 430	NAc (S)	ND
Type 446	NAc (S)	ND
Titanium	R	R
Ti Code 12	ND	R
Uniloy 18-2	NAc (S)	ND
Zr 705	R	R

R Recommended. No observation of localized corrosion.
C Conditional. Slight tendency for localized corrosion.
NAc Not acceptable. Definite to severe (S) tendency for localized corrosion.
ND Not determined.

[1]Saturated with flue gas containing 82 pct N_2, 13 pct CO_2, 4.8 pct O_2, and 0.34 pct SO_2.
[2]No flue gas passed through solution.

Alloys rated not acceptable, NAc, showed moderate to severe tendency for localized corrosion and should be reexamined in field tests in rich citrate solution. These iron-chromium- and iron-chromium-nickel-base alloys, which contain from 2 to 4 pct Mo, showed significantly greater tendencies for localized corrosion as weldments (with slight increases in acidity or chloride concentration) and when partially submerged in solution.

Because type 316 stainless steel is typical of the latter alloys, the corrosion behavior of type 316 stainless steel screws used during the stress corrosion tests was of interest. The small amount of localized corrosion of type 316 stainless steel bolts, nuts, and washers used to stress the C-rings for 6 months showed that type 316 stainless steel may be used with slight risk if kept submerged in rich citrate solution. The susceptibility to crevice corrosion was noted when 17 of 28 bolts inserted in sections of neoprene hose showed crevice corrosion within 30 days. After removal of the neoprene hose, only 4 of 28 showed further evidence of crevice corrosion. Furthermore, C-rings of types 316, 316L, and 317L stainless steel showed no significant localized corrosion during the 6-month stress-corrosion test.

Alloys rated not acceptable, NAc (S), include the alloys that showed a high tendency for general and localized corrosion and are not suitable for use in rich or lean citrate solution. These alloys are mainly ferritic stainless steels that contain no nickel, and little if any molybdenum. Also included in this group is austenitic stainless steel type 304 (which contains nickel but little if any molybdenum) and Hastelloy B (a nickel-base alloy that contains 28 pct Mo but only 1 pct Cr).

IN-PLANT CORROSION TESTING AND ANALYSIS

By P. F. Ellis II[3]

This section summarizes the findings on corrosion coupon exposures at seven locations in the citrate process demonstration plant at the 50-MW George F. Weaton Power Station, Monaca, PA. The following are brief descriptions of exposure times and conditions at each location.

1. Prescrubber liquor cooler: Rack was immersed at the exit to the closed-loop prescrubber liquor heat exchanger at 110° to 125° F for 27 days during acid gas operation and at ambient temperature (32° to 85° F) for an additional 278 days. The rack broke loose and was retrieved from the venturi sump. The heat exchanger was inoperative because of a leak, hence the high temperature at this location.

2. Prescrubber exit: Rack was immersed below demister chevron package in prescrubber exit at 110° to 125° F for 27 days during acid gas operation and at ambient temperature (32° to 85° F) for an additional 278 days.

3. Absorber solution reservoir: Rack was immersed in rich citrate solution in the absorber solution reservoir at about 120° F for 56.5 days during acid gas absorption and at ambient temperature (32° to 85° F) for an additional 123 days.

4. Solution distribution trough: Rack was immersed in lean citrate solution in the primary distribution trough near the top of the scrubber tower at about 120° F for 56.5 days during acid gas absorption and at ambient temperature (32° to 85° F) for an additional 33 days.

5. Vapor space, top of tower: Rack was exposed to scrubbed gas and lean citrate solution mist at about 120° F for 56.5 days during acid gas absorption and to vapor over stagnant liquor at ambient temperature for an additional 33 days.

6. Decanter solution: Rack was immersed in lean citrate solution in the decanter for 6 months at 285° F and an additional 12 months at ambient temperature (32° to 85° F).

7. Sulfur flotation tank slurry: Rack was immersed in lean citrate solution-sulfur slurry in sulfur flotation tank at 145° F for 42.4 days during acid gas absorption and at ambient temperature (32° and 85° F) for an additional 16.5 months.

Two corrosion rates are tabulated in tables 43, 44, and 45. The maximum corrosion rate was calculated by assuming that corrosion occurred only during normal operations with acid gases present and that no corrosion occurred during shutdown periods, even though the coupons remained in contact with potentially corrosive media. The minimum corrosion rate was calculated by assuming that corrosion occurred at a constant rate as long as a potentially corrosive medium was present, whether or not the system was operating.

[3]Staff scientist, Radian Corp., Austin, TX.

The maximum rate includes the corrosion during normal operations plus a superimposed component due to corrosion during shutdown. For this reason, the maximum rate is probably higher than the effective corrosion rate that would be encountered in normal operations. The minimum rate is too low, because much of the total exposure was under shutdown conditions and corrosion would likely be more rapid under normal operations. Thus, the effective corrosion rate during normal operations is expected to be between the two tabulated values. It will probably approach the maximum value as the fraction of downtime decreases.

The weight loss (uniform) corrosion rate data should not be used alone for comparison purposes. As a general rule in coupon tests, especially short-duration tests, materials should be avoided if they show any signs of localized corrosion, either pitting or crevice corrosion. Under no circumstances should pit or crevice corrosion depths be used for design purposes. There are two principal reasons for this. First, pitting in passivated alloys (all materials tested except aluminum are of this type) often accelerates with time. Second, pitting is a statistical function and the probability of finding a deeper pit increases as a power function with increasing area.

Table 43.—Corrosion rates of alloys in prescrubber at George F. Weaton citrate process demonstration plant,[1] mils per year

	Prescrubber liquor cooler		Prescrubber exit	
	Maximum	Minimum	Maximum	Minimum
Al 1100	>216	>19	>216	[2]>19
Allegheny 6X	<.05	<.05	<.05	<.05
Carpenter 20Cb-3	43	[3-5]3.4	38	[4-6]3.3
Hastelloy C-276	.2	<.05	.2	<.05
Hastelloy G	<.05	<.05	<.05	<.05
Haynes 20 Mod	<.05	[6]<.05	1.2	[6].1
Incoloy 825	4.8	[4,6].4	22	[4-6]1.9
Inconel 625	<.05	<.05	<.05	<.05
Jessop JS-700	<.05	<.05	.2	<.05
Nitronic 50	23	[5]2.0	.5	[4-6]<.05
Stainless steel:				
Type 316L	93	[3,5,7]8.2	100	[3,5,7]8.8
Type 317	15.3	1.3	1.4	[3,5].1

[1]Calculated corrosion rates. Maximum rate assumes that all corrosion occurred during 27-day operation with acid gas; minimum rate assumes constant corrosion during entire 305-day exposure to liquor.
[2]Specimen corroded completely.
[3]Few pits.
[4]End grain attack.
[5]Crevice corrosion.
[6]Severe pitting.
[7]Specimen partially corroded away.

Table 44.—Corrosion rates of alloys in absorber at George F. Weaton citrate process demonstration plant,[1] mils per year

Alloy	Absorber solution reservoir		Solution distribution trough		Vapor space, top of tower	
	Maximum	Minimum	Maximum	Minimum	Maximum	Minimum
Al 1100	>103	[2]>32	>103	[2]>65	53	[3-4]33
Allegheny 6X	<.05	<.05	<.05	<.05	<.05	<.05
Carpenter 20Cb-3	.3	[4-5].1	.1	[4]<.05	<.05	[4-5]<.05
Hastelloy C-276	<.05	<.05	<.05	<.05	<.05	<.05
Hastelloy G	<.05	<.05	<.05	<.05	<.05	<.05
Haynes 20 Mod	<.05	<.05	<.05	<.05	<.05	<.05
Incoloy 825	.3	[5-6].1	<.05	[5]<.05	<.05	<.05
Inconel 625	<.05	<.05	<.05	<.05	<.05	<.05
Jessop JS-700	<.05	<.05	<.05	<.05	<.05	<.05
Nitronic 50	<.05	<.05	<.05	<.05	<.05	<.05
Stainless steel:						
Type 316L	.4	[3,4,6].1	<.05	<.05	<.05	<.05
Type 317	<.05	<.05	<.05	<.05	<.05	<.05

[1]Calculated corrosion rates. Maximum rate assumes that all corrosion occurred in 56.5-day exposure to solution during acid gas absorption. Minimum rate assumes constant corrosion during 180-day exposure to liquor in the absorber solution reservoir, or 90-day exposure to liquor in the solution distribution trough, or 90-day exposure to absorber tower vapors.
[2]Specimen corroded completely.
[3]Severe pitting.
[4]Crevice corrosion.
[5]Few pits.
[6]End grain attack.

These results have not been correlated with detailed operating process chemistry conditions at the test locations, and therefore it is not known how well these results will reflect actual in-plant corrosion. In addition, extensive downtime occurred during the tests. The effect of this downtime on test results is unclear and introduces uncertainty about what time basis to use in accessing corrosion rates. For these reasons, considerable caution is required in interpreting and applying these test results.

The uniform corrosion rate was calculated from the weight loss by assuming that all metal was lost evenly from the metal surface. This value has little meaning if significant localized corrosion—pitting or crevice corrosion—occurred. The calculation also assumes that the rate of metal loss was constant (linear) with respect to time. However, higher temperatures and presence of acid gases can be expected to accelerate the corrosion of some of the alloys tested in this study. Corrosion was probably most rapid during normal operations. During extensive shutdown periods, the coupons remained in contact with potentially corrosive media, and some corrosion may have occurred. Very different corrosion rates will be calculated from the same metal loss, depending on whether the time used is the total exposure or only the time of operation with acid gases.

Alloys tested are ranked on the basis of localized corrosion resistance and weight loss in table 46. Conservatively, class B metals should be considered marginal, as they show incipient localized attack. Metals of classes C, D, and E should be avoided.

It is clearly recognized that the principal alloying elements affecting the localized corrosion resistance of stainless steels and nickel-based alloys are chromium and molybdenum. Also, molybdenum is more effective in pro-

Table 45.—Corrosion rates of alloys in decanter and sulfur flotation tank at George F. Weaton citrate process demonstration plant, mils per year

Alloy	Decanter solution[1]		Sulfur flotation tank slurry[2]	
	Maximum	Minimum	Maximum	Minimum
Al 1100	NT	NT	>137	[3]>11
Allegheny 6X	0.1	<0.05	.6	<.05
Carpenter 20Cb-3	[4].2	.1	.3	<.05
Hastelloy C-276	1.1	.4	>.05	<.05
Hastelloy G	.1	<.05	.6	<.05
Haynes 20 Mod	NT	NT	.7	.1
Incoloy 800	[5-7].3	.1	NT	NT
Incoloy 825	.1	<.05	.3	<.05
Inconel 625	.1	<.05	.3	<.05
Jessop JS-700	NT	NT	2	.2
Nitronic 50	<.05	<.05	.3	<.05
Stainless steel:				
Type 316L	NT	NT	1.3	.1
Type 317	.1	<.05	1.2	.1
Titanium	<.05	<.05	NT	NT

NT Not tested.

[1]Calculated corrosion rates. Maximum rate assumes that all corrosion occurred during 6-month exposure to lean citrate solution at 285° F. Minimum rate assumes constant corrosion during the 18-month exposure to solution.

[2]Calculated corrosion rates. Maximum rate assumes that all corrosion occurred during 42.4-day operation at 145° F during acid gas absorption. Minimum rate assumes constant corrosion during the 18-month exposure to sulfur flotation slurry.

[3]Specimen corroded completely.

[4]Severe pitting.

[5]Crevice corrosion.

[6]Few pits.

[7]End grain attack.

Table 46.—Performance ranking of materials tested at George F. Weaton citrate process demonstration plant

	Prescrubber (2 locations)					Absorber (3 locations)					Decanter (1 location)				
Class[1]	A	B	C	D	E	A	B	C	D	E	A	B	C	D	E
Al 1100					X					X					
Allegheny 6X		X				X					X				
Carpenter 20Cb-3				X				X				X			
Hastelloy C-276	X					X					X				
Hastelloy G		X				X					X				
Haynes 20 Mod			X			X									
Incoloy 800														X	
Incoloy 825				X				X			X				
Inconel 625	X										X				
Jessop JS-700		X													
Nitronic 50				X			X				X				
Stainless steel:															
Type 316L					X				X					X	
Type 317				X		X					X				
Titanium											X				

[1]A = No localized corrosion (<2-mil/yr weight-loss corrosion).
B = Localized corrosion detected but <1 mil deep.
C = Localized corrosion >1 but <5 mils deep.
D = Localized corrosion >5 mils deep.
E = Partially or completely corroded away.

moting pitting resistance than chromium, about twice as effective in the ferrous chloride ($FeCl_2$) critical temperature test. The severity of the environments can thus be related to the amount of chromium and molybdenum alloying required for localized corrosion resistance. The prescrubber was the most severe environment. The 22 pct Cr, 6.5 pct Mo content of Hastelloy G was not adequate to resist localized corrosion in this environment. The 22 pct Cr plus 9 pct Mo Inconel alloy 625 was resistant, as was Hastelloy C-276 (16 pct Cr plus 16 pct Mo). All of the other stainless steels and nickel-based alloys tested contained less chromium and molybdenum than did the Hastelloy G, and all suffered localized attack, some catastrophically. Thus, it is suggested that stainless steels or nickel alloys for the prescrubber should contain at least 22 pct Cr and 9 pct Mo. Less chromium can be tolerated with higher molybdenum content.

The absorber was not as severe as the prescrubber, and all of the stainless steels and nickel-base alloys containing at least 19 pct Cr and 3.5 pct Mo resisted localized corrosion, although those close to this alloy composition were probably close to their corrosion resistance limits.

The decanter was surprisingly nonaggressive, given its high operating temperature. Only the stainless steel (type 316L) and nickel-base alloy (Incoloy alloy 800) with less than 3 pct Mo were susceptible to localized corrosion.

Al 1100 failed catastrophically at all test locations. In most cases, the coupons were entirely corroded away.

CONCLUSIONS

The concept of an alternative process for powerplant flue gas desulfurization that does not produce large quantities of waste material and produces a useful sulfur product is an attractive goal. The citrate process remains one of the few processes that meet this goal. The basic principles of the process have been proven in the laboratory and in several pilot plant operations as well as in the full-scale demonstration plant at St. Joe's George F. Weaton Power Station, Monaca, PA.

Test results showed that the Bureau's citrate process is capable of

1. Removing over 90 pct of the SO_2 contained in the flue gas from either a copper smelter, a lead smelter, or a coal-fired powerplant.

2. Producing an elemental sulfur product with a purity of 99.5 pct.

Materials testing in the laboratory, pilot plants, and demonstration plant has shown which materials are acceptable for constructing process pipirg, vessels, and equipment for the citrate process.

Pilot plant and demonstration plant engineering and operating data have assisted the M. W. Kellogg Co. in the design, construction, and startup of an industrial citrate process plant. Today, the Saber Refining Co. successfully operates this citrate process plant to remove SO_2 from flue gas at an oil refinery in Corpus Christi, TX.

REFERENCES

1. Ahlqvist, H. Method of Separating Sulfur From Sulfur Dioxide. U.S. Pat. 1,955,722, Apr. 24, 1934.

2. American Society for Testing and Materials. Standard Recommended Practices for Making and Using the C-Ring Stress-Corrosion Cracking Test Specimen. G38-73 in 1977 Annual Book of ASTM Standards: Part 10, Metals—Mechanical, Fracture, and Corrosion Testing; Fatigue Erosion; Effect of Temperature. Philadelphia, PA, 1977, pp. 757-765.

3. Bacon, R. F., and E. S. Boe. Hydrogen Sulfide Production From Sulfur and Hydrocarbons. Ind. and Eng. Chem., v. 37, May 1945, pp. 469-474.

4. Bacon, R. F., and R. Fanelli. Recovery of Sulfur Dioxide From Gases. U.S. Pat. 2,142,987, Jan. 10, 1939.

5. Beard, H. R. Conductive Cell Apparatus for Continuous Measurement of Sulfur Dioxide Concentrations Between 40 Ppm and 1 Percent. Anal. Chem., v. 44, No. 6, 1972, p. 1104.

6. Beard, H. R., K. R. Farley, S. R. Crane, and W. N. Marchant. Gas Analysis Procedures Applicable to Flue Gas Desulfurization by the Citrate Process. BuMines IC 8793, 1979, 15 pp.

7. Bengtsson, S., and G. Walin. The Flakt-Boliden Desulphurization System. Paper in Flakt Review (A. B. Svenska Flaktfabriken, Stockholm, Sweden), v. 12, No. 2, (Clean Air Issue), 1977, pp. 29-32.

8. Bernhardson, S. O., R. Millstrom, and M. Tynell. Sandvik 2RK65—A High-Alloy Stainless Steel for Sea Water Cooling in Chemical Industry. Steel Res. Cent., Sandvik, Sandviken, Sweden, Lecture 52-59E, Oct. 1977, 24 pp.

9. Bishoff, J. R., and P. Steiner. Coal Converts SO_2 to S. Chem. Eng. (N.Y.), v. 82, Jan. 6, 1975, pp. 74-75.

10. Chalmers, F. S., L. Korosy, and A. Saleem. The Citrate Process To Convert SO_2 to Elemental Sulfur. Pres. at Industrial Fuel Conf., Purdue Univ., West Lafayette, IN, Oct. 3, 1973, 7 pp.; available upon request from W. I. Nissen, BuMines, Salt Lake City, UT.

11. Cigan, J. M. Citrate Process Flue Gas Desulfurization Demonstration Plant (contract SO261008, St. Joe Minerals Corp.). BuMines OFR 67-84, 1983, 153 pp.; NTIS PB 84-176007.

12. Crane, S. R., L. Crocker, and W. I. Nissen. Hydrogen Sulfide Generation by Reaction of Natural Gas, Sulfur, and Steam. BuMines RI 8539, 1981, 54 pp.

13. Crocker, L., D. A. Martin, and W. I. Nissen. Citrate Process Pilot-Plant Operation at the Bunker Hill Company. BuMines RI 8374, 1979, 77 pp.

14. Eckert, J. S. Design Techniques for Sizing Packed Towers. Chem. Eng. Prog., v. 57, No. 9, 1961, pp. 54-58.

15. Farrington, J. F., Jr., and S. Bengtsson. The Flakt-Boliden Process for SO_2 Recovery. Flakt Eng. (Flakt, Inc., Old Greenwich, CT, tech. bull.), v. 3, No. 3, 1979, 4 pp.

16. Fleming, E. P., and T. C. Fitt. Liquid Sulfur Dioxide From Waste Smelter Gases—Use of Dimethylaniline as Absorbent. Ind. and Eng. Chem., v. 42, Nov. 1950, pp. 2253-2258.

17. Folkins, H. O., E. Miller, and H. Hennig. Carbon Disulfide From Natural Gas and Sulfur. Ind. and Eng. Chem., v. 42, Nov.. 1950, pp. 2202-2207.

18. George, D. R., L. Crocker, and J. B. Rosenbaum. The Recovery of Elemental Sulfur From Base Metal Smelters. Min. Eng. (N.Y.), v. 22, No. 1, 1970, pp. 75-77.

19. Girdler Corp. (Louisville, KY). Girdler Compact Package Hydrogen Sulfide Generators. Bull. 961, Sept. 1961, 4 pp.

20. Haines, H. W., Jr. Carbon Disulfide. Ind. and Eng. Chem., v. 55, June 1963, pp. 44-46.

21. Henderson, J. M., and J. B. Pfeiffer. Liquid SO_2 From Copper Converter Gases—The ASARCO Dimethylaniline Process. Paper in Air Pollution Control and Clean Energy, ed. by C. Rai and L. A. Spielman. AIChE Symp. Series, v. 2, No. 156, 1976, pp. 69-73.

22. Hoxie, E. C., and G. W. Tuffnell. A Summary of Inco Corrosion Tests in Power Plant Flue Gas Scrubbing Processes. Paper in Resolving Corrosion Problems in Air Pollution Equipment (Proc.). NACE, 1976, pp. 65-71.

23. Hunt, W. F., T. C. Curran, R. B. Faoro, N. H. Frank, C. Mann, and R. E. Neligan. National Air Quality and Emissions Trends Report 1982. U.S. EPA rep. 450/4-84-002, Mar. 1984, 141 pp.

24. Institut Francais du Petrole, des Carburants et Lubrifiants. Werkwijze ter Bereiding van Elementaire Zwavel door Reactie van Zwavelwaterstof met Zwaveldioxyde (Method of Preparation of Elementary Sulfur by Reaction of Hydrogen Sulfide With Sulfur Dioxide). Netherlands Pat. 6,604,053, Oct. 3, 1966.

25. International Nickel Co. The Corrosion Resistance of Nickel-Containing Alloys in Flue Gas Desulfurization and Other Scrubbing Processes. Corros. Eng. Bull. CB-7, 1980, 76 pp.

26. Johnstone, H. F. Recovery of Sulfur Dioxide From Waste Gases. Ind. and Eng. Chem., v. 27, May 1935, pp. 587-593.

27. Johnstone, H. F., and D. B. Keyes. Recovery of Sulfur Dioxide From Waste Gases. Ind. and Eng. Chem., v. 27, June 1935, pp. 659-665.

28. Johnstone, H. F., J. J. Read, and H. C. Blankmeyer. Recovery of Sulfur Dioxide From Waste Gases. Ind. and Eng. Chem., v. 30, Jan. 1938, pp. 101-109.

29. Keller, J. L. Removal of Sulfur Dioxide From Gases Containing the Same. U.S. Pat. 2,739,543, Jan. 3, 1956.

30. Korosy, L., H. L. Gewanter, F. S. Chalmers, and S. Vasan. Chemistry of SO_2 Absorption and Conversion to Sulfur by the Citrate Process. Pres. at 167th Am. Chem. Soc. Nat. Meet., Los Angeles, CA, Apr. 5, 1974, 15 pp.; available upon request from W. I. Nissen, BuMines, Salt Lake City, UT.

31. _____. Sulfur Dioxide Absorption and Conversion to Sulfur by the Citrate Process. Ch. 16 in Sulfur Removal and Recovery From Industrial Processes, ed. by J. B. Pfeiffer. ACS, 1975, pp. 192-211.

32. Leahy, M. Process of Removing Sulfur Compounds From Gas. U.S. Pat. 1,995,545, Mar. 26, 1935.

33. Lepsoe, R. Chemistry of Sulfur Dioxide Reduction. Ind. and Eng. Chem., v. 32, July 1940, pp. 910-918.

34. Lien, R. H. Stripping SO_2-Loaded Citrate Solutions With Pressurized Steam. BuMines RI 8734, 1982, 8 pp.

35. Lien, R. H., D. A. Martin, and W. I. Nissen. Description and Economic Evaluation of Flue Gas Desulfurization by the Modified Citrate Process. BuMines RI 8638, 1982, 26 pp.

36. _____. Flue Gas Desulfurization by the Modified Citrate Process. BuMines RI 8403, 1979, 19 pp.

37. Lizlov, E. A. Laboratory Corrosion of Stainless Steel for SO_2 Scrubber Service. Mater. Perform., v. 17, Mar. 1978, pp. 36-37.

38. Madenburg, R. S., and R. A. Kurey. Citrate Process Demonstration Plant, A Progress Report. Paper in Proceedings of Symposium on Flue Gas Desulfurization, Hollywood, FL, Nov. 1977. U.S. EPA rep. 600/7-78-058b, v. 2, Mar. 1978, pp. 707-735.

39. Mann, E. L. Power Plant Flue Gas Desulfurization by the Wellman-Lord SO_2 Process. Part 1—The Dean H. Mitchell Station. Paper in Proceedings of Symposium on Flue Gas Desulfurization, Atlanta, GA, Nov. 1974. U.S. EPA rep. 650/2-74-126b, v. 2, Dec. 1974, pp. 739-744.

40. Marchant, W. N., S. L. May, B. W. Moore, and W. W. Simpson. The Chemical Reactions of Sulfur in the Citrate Process for Flue Gas Desulfurization. BuMines RI 8540, 1981, 23 pp.

41. Marchant, W. N., S. L. May, W. W. Simpson, J. K. Winter, and H. R. Beard. Analytical Chemistry of the Citrate Process for Flue Gas Desulfurization. BuMines IC 8819, 1980, 20 pp.

42. McGill, W. A., and M. J. Weinbaum. Aluminum Diffused Steels Resist High Temperatures in Hydrocarbon Environments. Met. Prog., v. 115, No. 2, 1979, pp. 26-31.

43. _____. The Selection, Application, and Fabrication of Alonized Systems in the Refinery Environment. Paper in 1975 Proceedings API Refining Dept., 40th Midyear Meeting (Chicago, IL, May 12-15, 1975). API, v. 54, 1975, pp. 125-159.

44. McKinney, W. A., W. I. Nissen, L. Crocker, and D. A. Martin. Status of the Citrate Process for SO_2 Emission Control. Paper in Technology and Use of Lignite, comp. by W. R. Kube and G. H. Gronhoud (Proc. Symp. spons. by U.S. ERDA and Univ. ND, Grand

Forks, ND, May 14-15, 1975). Grand Forks Energy Res. Cent. (ERDA) Inf. Circ. 75/2, 1975, pp. 148-172; NTIS CONF-750586.

45. McKinney, W. A., W. I. Nissen, and J. B. Rosenbaum. Design and Testing of a Pilot Plant for SO_2 Removal From Smelter Gas (Pres. at AIME Annu. Meet., Dallas, TX, Feb. 23-28, 1974). Metall. Soc. AIME preprint A-74-85, 1974, 12 pp.

46. Nissen, W. I., L. Crocker, and D. A. Martin. Lead Smelter Flue Gas Desulfurization by the Citrate Process. Ch. in World Mining and Metals Technology, ed. by A. Weiss. Port City Press, Baltimore, MD, v. 2, 1976, pp. 825-854.

47. Nissen, W. I., D. A. Elkins, and W. A. McKinney. Citrate Process for Flue Gas Desulfurization, A Status Report. Paper in Proceedings of Symposium on Flue Gas Desulphurization, New Orleans, LA, Mar. 1976. U.S. EPA rep. 600/2-76-136b, v. 2, May 1976, pp. 843-864.

48. Nissen, W. I., R. S. Madenberg. Citrate Process Demonstration Plant Design. BuMines IC 8806, 1979, 16 pp.

49. Oden, L. L., M. P. Krug, and R. A. McCune. Analysis of Vapor-Aluminum-Diffused Stainless Steels. BuMines RI 8629, 1982, 12 pp.

50. Rochelle, G. T., and M. M. Gibson. Thermal Degradation of Sodium Citrate Solutions Containing SO_2 and Thiosulfate. Ind. and Eng. Chem. Proc. Des. and Dev., v. 21, No. 4, Oct. 1982, pp. 569-574.

51. Rosenbaum, J. B., D. R. George, and L. Crocker. The Citrate Process for Removing SO_2 and Recovering Sulfur From Waste Gases. Pres. at AIME Environ. Quality Conf., Washington, DC, June 7-9, 1971, 26 pp.; available upon request from W. I. Nissen BuMines, Salt Lake City, UT.

52. Rosenbaum, J. B., W. A. McKinney, H. R. Beard, L. Crocker, and W. I. Nissen. Sulfur Dioxide Emission Control by Hydrogen Sulfide Reaction in Aqueous Solution. The Citrate System. BuMines RI 7774, 1973, 31 pp.

53. Stull, D. R. Thermodynamics of Carbon Disulfide Production. Ind. and Eng. Chem., v. 41, Sept. 1949, pp. 1968-1973.

54. Thacker, C. M. What's Ahead for Carbon Disulfide. Hydrocarbon Process., v. 49, Apr. 1970, pp. 124-128.

55. Thacker, C. M., and E. Miller. Carbon Disulfide Production. Ind. and Eng. Chem., v. 36, Jan. 1944, pp. 182-184.

56. Timmerman, R. W., A. G. Draeger, and J. W. Getz. Carbon Disulfide and Hydrogen Sulfide by the Reaction of Sulfur and a Hydrocarbon Gas. U.S. Pat. 2,857,250, Oct. 21, 1958.

57. Urban, P. Production of Sulfur. U.S. Pat. 3,149,920, Sept. 22, 1964.

58. Vasan, S. The Citrex Process for SO_2 Removal. Chem. Eng. Prog., v. 71, No. 5, 1975, pp. 61-65.

59. Wackenroder, H. W. F. Liebigs. Anal. Chem., v. 60, 1846, p. 189.

U.S. DEPARTMENT OF LABOR MSHA
00043986